ANALYSIS OF THE EFFECT OF UP-SCALING AND SOIL EROSION ASSESSMENT AT REGIONAL SCALE BY USING PESERA MODEL:

A CASE STUDY OF LOMSAK DISTRICT, PHETCHABUN, THAILAND

Bharat Babu Shrestha
February, 2009

Analysis of the effect of up-scaling and soil erosion assessment at regional scale by using PESERA model:

A case study of Lomsak District, Phetchabun, Thailand

by

Bharat Babu Shrestha

Thesis submitted to the International Institute for Geo-information Science and Earth Observation in partial fulfilment of the requirements for the degree of Master of Science in Geo-information Science and Earth Observation, Specialisation: Natural Resources Management

Thesis Assessment Board

Prof. Dr. V. Jetten (Chairman)
Department of Earth Systems Analysis, ITC, The Netherlands

Dr. T. Veldkamp (External examinar)
Wageningen University, The Netherlands

Dr. D. P. Shrestha (1st Supervisor)
Department of Earth Systems Analysis, ITC, The Netherlands

Dr. A. Farshad (2nd Supervisor)
Department of Earth Systems Analysis, ITC, The Netherlands

INTERNATIONAL INSTITUTE FOR GEO-INFORMATION SCIENCE AND EARTH OBSERVATION
ENSCHEDE, THE NETHERLANDS

Disclaimer

Abstract

Erosion assessment at regional scale in heterogeneous and fragmented land use/land cover situation of Lomsak district of Thailand is an urgent need to address the increasing erosion problem. Therefore PESERA, a physically based and spatially distributed regional scale model was used to assess soil erosion in Lomsak district of Thailand. The study has also focussed to see the effect of up-scaling of grid cells of land use/land cover on erosion prediction. The model was run by using 128 data layers related to climate, soil, land cover and topography factors. Climate parameter maps were prepared by interpolating climate data considering the situation of climatic variation with altitude. Soil parameter maps were generated by ordinary kriging interpolation method on the basis of analyzed soil data collected randomly from the study area. For preparing land use/land cover map Aster image of Feb. 4, 2006 was classified by supervised classification with nearest neighbour algorithm. Monthly canopy cover maps prepared from both the crop calendar and NDVI data were used separately for their comparative study. DEM as a topographic parameter was prepared by interpolating from contour maps of 20m interval. Model was run using 250m, 500m and 1000m resolution data to see the effect of up-scaling. The model result shows that the rate of soil erosion spatially varies from < 1.0 ton/ha/year to 19.2 ton/ha/year. There is not much difference in average annual soil erosion rate between model results whether crop calendar (1.17 ton/ha/year) or NDVI (1.13 ton/ha/year) data is used. The soil erosion rate has also varied with the seasonal and land use/land cover variation. The highest erosion rate occurs during month of June and followed by August and October having second and third highest erosion rate respectively. Agriculture land generates more soil erosion than natural land. Maize field has highest erosion rate while dense forest and grass land have the least erosion rate. Erosion assessment at various land use scenarios shows that the conversion of land use from degraded forest and grass land to agriculture has resulted substantial increase in erosion rate. Erodibility is the most sensitive model parameter among the selected parameter used for sensitivity analysis. There is not difference in average annual soil erosion rates of the whole study area whether 250m, or 500m data is used, however, there is significant difference in total erosion with respect to various land use classes as there is change in areas of land use/land cover classes while up scaling the grid cells of land use/land cover map.

Key words: PESERA model, up-scaling, NDVI, crop calendar, canopy cover, land use scenarios, DEMs.

Acknowledgements

I would like to express my sincere gratitude to those people who supported me in various ways to accomplish this research.

My sincere and deepest thanks goes to Dr. Dhruba Pikha Shrestha, for his supervision of my work throughout the research period, constructive comments and feedback. It would not be possible for me to complete this research without his guidance. My sincere thanks also go to my second supervisor Dr. Abbas Farshad who always encouraged and guided me to carry out this research work. I would like to express special thanks to Prof. Dr. Victor Jetten for his valuable comments and suggestions during proposal and mid-term presentation of my research work. I would also like to thank to Dr. Michael Weir, Course Director of NRM Department of ITC for his continuous encouragement and moral support.

I am grateful to all staffs of Land Development Department, Thailand for their supports during my field work and especially to Ms. Rapeephan Wudthiphan for her help in gathering secondary data from Thailand.

I would like to extend many thanks to the Government of The Netherlands for providing me ITC grant to pursue MSc study in ITC.

Warm thanks goes to all of my classmates for their cooperation and creating cheerful and happy environment during the study at ITC. I would like to express my heartfelt thanks to all the Nepalese students who study at ITC for their support and encouragement towards study and creating homely environment. Special thanks goes to Mr. Nav Raj Subedi, Mr.Pramod Sharma and Mr.Gandhi Prasad Subedi for their valuable comments and suggestions during my research work.

Without enough support from my family it was not possible for me to bring this work at this end. Thanks a lot to all of my family members.

Table of contents

List of figures

List of tables

Acronyms & Abbreviations

AML	Arc Micro Language
ASTER	Advanced Space borne Thermal Emission and Reflection Radiometer
CC	Crop Calendar
CVRF	Coefficient of Variance of Rainfall
DEM	Digital Elevation Model
ET	Evapo-transpiration
FAO	Food and Agriculture Organization
ISRIC	International Soil Reference and Information Center
LC	Land Cover
LDD	Land Development Department
LU	Land Use
MODIS	Moderate Resolution Imaging Spectroradiometer
MRT	Modis Reprojection Tools
ME	Mean Error
NDVI	Normalized Difference Vegetation Index
OM	Organic Matter
PESERA	Pan European Soil Erosion Risk Assessment
RF	Rainfall
SD	Standard Deviation
SPAW	Soil Plant Atmosphere Water
SPSS	Statistical Package for Social Sciences
SWSC	Soil Water Storage Capacity
USDA	United States Department of Agriculture
USLE	Universal Soil Loss Equation
WAP	Water Available to Plant
WAP1	Water Available to Plant at depth of 0-30cm
WAP2	Water Available to Plant at depth of 30-100cm

1. Introduction

1.1. Back ground

Soil erosion is one of the most serious environmental problem in the world today, because it seriously threatens agriculture and the natural environment (Pimentel, 1993). It has been reported that 1.2 billion hectares of land (almost 11 percent of the earth's vegetated surface) have been degraded by human activity over the past 45 years (Oldeman et al., 1991).

Soil erosion is a natural phenomenon. However, due to the various anthropogenic activities the process of soil erosion is further accelerated. Accelerated soil erosion by running water is recognized as serious worldwide problem as it contributes to about 56% of the total human induced soil degradation in the world (Oldeman et al., 1991).

The relationship between soil erosion and its driving factors are complicated. The most important factors of water induced soil erosion are erosivity of the rainfall, erodibility of soil and nature and types of land cover (Morgan and Davidson, 1986). Soil erosion affects on land productivity by reducing the availability of water, nutrients and organic matter and restricting the rooting depth. In addition to reducing the soil productivity, soil erosion causes severe off-site effects. The off-site effects of soil erosion comprise sediment deposition on agriculture field, riverbed, lakes and reservoir. Eutrophication due to nutrient load added to lakes and other water bodies is also a serious off site effect (Pimentel, 1993).

Modelling soil erosion is the process of mathematically describing soil particle detachment, transport and deposition on land surfaces. The erosion models can be used as predictive tools for assessing soil loss for conservation planning, project planning, soil erosion inventories, and for regulation (Lal, 1994). There are three types of soil erosion models; empirical, conceptual and physically based. Empirical model like universal soil loss equation is based on defining the most important factors and through the use of observation, experiment and statistical techniques. Physically based model on the other hand is based on mathematical equations to describe the processes involved in the model, taking account of the laws of conservation of mass and energy (Morgan and Davidson, 1986).

Pan European Soil Erosion Risk Assessment (PESERA) is a physically based and spatially distributed model, developed for soil erosion assessment in environmentally sensitive areas relevant to a regional or European scale and defining the soil conservation strategies (Grovers, 2001). The method uses the climate, soil, land cover and topography as an input data and forecast the run-off and soil erosion. In this study, PESERA model was selected to assess the soil erosion in Lomsak district of northern Thailand.

1.2. Problem statement and justification

Lomsak district in Phetchabun province of Thailand is considered as fertile land and thereby intensive agricultural practices is being carried out. Due to the increase in population and growing economic activities, human pressure is being exerted in the natural resources. The forest and marginal lands in the mountainous area is being encroached. Deforestation and agriculture in mountainous areas has resulted soil erosion problem (Patanakanog et al., 2004). The problem of soil erosion is not only confined to farming on steep slope but inappropriate farming practices equally contribute to soil erosion. The consequences of the soil erosion have been observed as decline in crop yields in upland watershed and flood and sedimentation problem in down stream of the study area.

Implementation of soil conservation measures is very important to preserve and/or improve the land productivity, protect development infrastructure and maintain ecological stability. In order to control soil erosion, appropriate soil conservation strategy is required at different spatial scale and this, in turns requires a thorough understanding of processes of erosion (Morgan and Davidson, 1986). Policy makers need to know the area affected by soil erosion and an estimate of magnitude at regional scale in order to formulate appropriate soil conservation measures and mitigation strategies (Gobin et al., 2004). The physically based spatially distributed process model can allow the identification about the source and sink area of water and sediment which are the useful information for designing the soil conservation measures (Jetten et al., 2003). Moreover, conservation planner can use a physically-based model as an interactive conservation design tool, targeting critical seasons or months in which major erosion events occur (Lal, 1994).

A major problem with soil erosion assessment is its variation in the temporal and spatial scale and the extent to which the phenomenon occurs. There are some limitations in soil erosion prediction and the most important limitations are the natural complexity and the spatial heterogeneity of the processes (Bonilla et al., 2007). Factor and model based approaches offer the advantages of repeatability and transparency. However, the results need to be validated against measurements and evaluated by experts so that the regional methods can be adapted to reflect reality (Gobin et al., 2004).

Several erosion assessment studies have been carried out in Thailand, however, most of them are at the field scale level and for small area. Models like Revised Universal Soil Loss Equation and Morgan, Morgan and Finney methods are specified for the small field size and can not be used to assess the soil erosion in large area due to the scale problem (Morgan and Davidson, 1986). Soil erosion assessment at regional or watershed scale and their field validation are indispensable for formulation and implementation of effective soil conservation programs and their monitoring in the study area. Hence, Pan-European Soil Erosion Risk Assessment (PESERA) method was used to assess soil erosion in this study.

According to (Kirkby et al., 2004) the changes in land use/land cover have the major impact on erosion rate. Canopy cover is crucial information for prediction of soil erosion because vegetation canopy cover will give information on rainfall interception factor (Suriyaprasit and Shrestha, 2008). However, the effect of seasonal canopy cover change of different land uses on soil erosion has not been assessed in the study area. Moreover, as the PESERA method has been recently developed to assess the erosion in European scale and it is in testing phase in Asian condition, several parameters have to be generalized and field validation techniques have to be analyzed. In tropical areas like Thailand, land cover types are highly fragmented, irregularly scattered and patchy. The model which is currently being applied at 1 km resolution for the Europe may not give the accurate result in such case. Because heterogeneous nature of land use/land cover can not be accurately represented at low resolution. The assessment of erosion by applying finer resolution data is therefore needed.

1.3. Research objectives

The main objective of the study is to assess water induced soil erosion in Lomsak district, Thailand by using PESERA model. The specific objectives are:

1. To assess soil erosion in different land uses with seasonal/monthly change in canopy cover.
2. To evaluate the effect of various mapping scales and up-scaling effect of land use/land cover data on erosion prediction.
3. To assess the sensitivity of model parameters on the model outcome.
4. To generate erosion scenarios related to changes in land cover/land uses.

1.4. Research questions

1. Which land use/land cover has high rate of soil erosion?
2. Is there an effect of seasonal change in percentage of canopy cover on rate of soil erosion?
3. How sensitive is the model to different individual parameters?
4. What is the effect of change of mapping scale of land use/land cover on model prediction?
5. What is the effect of change in land use scenarios on the rate of soil erosion?

1.5. Research hypothesis

1. Rate of soil erosion significantly vary with different land use/land cover types.
2. Rate of soil erosion significantly vary with change in percentage of canopy cover.
3. Beginning of the monsoon period has more erosion rate than later period.
4. There is a significant effect of up-scaling of land use/land cover mapping on model prediction.
5. There is a significant increase in soil erosion rate due to land use change from forest and grass land to agriculture.

1.6. Thesis structure

Chapter 1 Introduction
This chapter introduces the background, problem statement and justification, research objectives, research questions and research hypothesis of the study.

Chapter 2 literature review
In this chapter information, facts and figures relevant to the study were reviewed from various sources and described.

Chapter 3 Description of the study area
This chapter includes the description about the location, climate, soil, geomorphology and land use/land cover of the study area.

Chapter 4 Methods and techniques
This chapter describes about data sets, materials, equipments and software used in the study. It also describes about the model used to assess soil erosion, data requirements and collection techniques.

Chapter 5 Data processing
This chapter describes about the processing and analysis of the data, preparation of input parameter maps to run the model as per the need to fulfil the defined objectives.

Chapter 6 Result and discussion
In this chapter, the results obtained from chapter 5 were discussed in view with the research objectives and research questions.

Chapter 7 Conclusion and recommendation
On the basis of findings from chapter 6, conclusions were drawn and recommendations were made in this chapter.

2. Literature review

2.1. Soil erosion

Soil erosion is the process of detachment of soil particles from the soil mass and the subsequent transportation and deposition of those sediment particles. It is a natural process and becomes a problem when human activity causes it to occur much faster than under natural conditions. The process of soil erosion can be distinguished from two different but interrelated phenomena; the depletion and soil degradation (Lal, 1990). The soil erosion lessens the soil productivity through physical loss of top soil, plant nutrients and soil moisture. Soil depletion includes the process of removal of the nutrients or the components which contribute to soil fertility without their replacement, and the conditions which support soil fertility are not maintained. In agriculture, depletion can be due to excessively intense cultivation and inadequate soil management. The soil erosion process is less drastic and can easily be maintained through the proper agricultural practices. Soil degradation implies the reduction in vigour of physical, chemical or biological properties of the soil and there by soil becomes less able to support plant and animal growth as there is a decline in levels of available moisture, available nutrients, and biological activity.

The process of soil erosion starts from the rain drop splash erosion. Then the run off wash away the thin and uniform layer of surface soil without development of conspicuous water channels which is called sheet erosion. The sheet erosion is less apparent particularly in early stages. The sheet erosion is followed by the rill erosion characterized with the removal of soil through the cutting of many small but conspicuous shallow channels due to the concentration of overland and finally the gully erosion. The interaction of rain splash and sheet wash is important during erosion process because their combined effect is more efficient when acting together rather than acting separately (Evans, 1989). When rain drop breaks the soil aggregates and brings it into suspension the sheet flow easily transport. Rills and gullies are developed when velocity of water flow increases and flow becomes turbulent. Flow in the rills acts as a transporting agent to carry sediment from rill and interrill sources to the down slopes. If shear stress in rill flow is high enough it can also detach the soil particles (Nearing et al., 1994). Whether rills or gullies will be formed depends on soil factors as well as the velocity and depth of water flow. In comparison to sheet erosion the soil loss due to rill and gully erosion is quite larger (Evans, 1989).

Eroded soil materials often move only short distance before a decrease in runoff velocity causes their deposition. They may remain in the fields where they originated or may be deposited on more level slopes that are remote from the stream system. The ratio of sediment delivered at a given location in the stream system to the gross erosion from the drainage area above that location is the sediment delivery ratio for that drainage area (Renard, 1997). The term “soil loss tolerance” denotes the maximum level of soil erosion that will permit a high level of crop productivity to be sustained economically and indefinitely.

2.2. Factors influencing soil erosion

Scientific planning for soil and water conservation requires knowledge of relations between the factors that cause loss of soil and those that help to reduce such losses. The major factors contributing to soil erosion are; erosivity of eroding agent, the erodibility of the soil, slope of the land and the vegetation cover (Morgan, 1995).

2.2.1. Erosivity of rainfall

The term erosivity refers to the potential ability of rainfall to cause erosion and is the function of physical characteristics of rainfall (Hudson, 1986). In mountainous areas, the amount of rainfall and their intensity are the important erosion factors causing soil erosion partly due to the detaching power of rain drops and partly through their contribution to overland flow (Shrestha, 2000). Rainfall intensity is generally considered to be the most important rainfall characteristic as this causes particularly erosion by overland flow and rills. In addition to rainfall intensity the duration of rainfall also has role on rate of soil erosion. Erosion is related to two types of rain events, the short duration intense storm where the infiltration capacity of the soil is exceeded, and the prolonged storm of the low intensity which saturates the soil (Morgan, 1995). However, in many cases it is difficult to separate the effects of these two types of rainfall events how they are accounting for soil loss. The most suitable expression of the erosivity of rainfall is an index based on the kinetic energy of the rain. Thus the erosivity of a rain storm is a function of its intensity and duration, and of the mass, diameter and velocity of the raindrops (Morgan, 1995).

2.2.2. Soil erodibility

The meaning of the term “soil erodibility” is different from that of the term “soil erosion”. The rate of soil erosion as described in the Universal soil loss equation is influenced more by land slope, rain storm characteristics, cover and management than by inherent properties of the soil. However, some soils erode more rapidly than others even when all other factors are the same. This difference, caused by properties of the soil itself, is referred to as soil erodibility. The susceptibility of soil to erosion is an inherent property of the soil and is influenced by soil characteristics, including texture, structure, permeability, organic matter content, clay minerals and contents of iron and aluminium oxide. Some climatic factors also influence soil erodibility e.g. air and soil temperature and water balance. Soil subjected to extremes of temperature and moisture regime differ in degree of susceptibility to erosion (Lal, 1990).

The mechanical and physical properties of soil which are related to water induced soil erosion, are determined by the cohesive forces between soil particles and the interactions between soil particles with liquid and gaseous form in soil (Lal, 1990). Texture and particle size distribution are primary soil properties that influence on soil erosion. Soil texture determines how easily the soil can be dispersed. The size of the soil particles also determine the threshold force of the erosive agent that requires for detachment and entrainment. The Large particles are resistant to transport because greater force is required to carry away them and that fine particles are resistant to detachment because of their cohesiveness. Richter and Negendank (1977) in (Morgan, 1995) state that soil with 40 to 60 percent silt content are the most erodible. According to Evan (1980) soil erodibility can be examined in terms of clay content indicating that soils with a restricted clay factors, between 9 and 30 percent, are the most susceptible to erosion. The clay content can be taken as an indicator of erodibility because combination of clay particles with organic matter form soil aggregates or clods resulting in to the soil stability determines the resistance of the soil (Morgan, 1995).

Soil structure and its strength are also important soil properties which influence soil erosion by determining the resistance capacity of soil against dispersion and detachment. The aggregation of individual soil particles in to different geometric shapes is called soil structure. The properties related to soil structure which influence on soil erosion are binding of soil particles and resistance to dispersion from water, ability to transfer water through profile, relative proportion of macro pores, and pores stability. According to (Styczen and Hogh-Schmidt, 1986), soil having highest aggregate stability will have the least susceptibility to runoff detachment. Soil structure influences the rate of soil erosion by changing soil property particularly in its water absorption capacity and physical resistance to erosion. However, a soil's erodibility is a function of complex interactions of a substantial number of its physical and chemical properties and often varies within a standard texture class (Renard, 1997).

Soil bulk density and shear strengths are also important soil physical properties which have impact on erosion. The bulk density determine the total pore space in the soil and thereby infiltration capacity of soil. Compacted soils with high bulk density beyond the certain threshold limit are more vulnerable to water induced soil erosion than un-compacted soils. Soils with higher shear strength are more resistance to detachment. The role of shear strength is important in detachment and mass movement with particular relevancy in erosion caused by flowing water (Lal, 1990).

2.2.3. Topography

Surface steepness, slope length and the shape of the profile are the major topographic variables that influences on soil erosion. In general, steep land is more vulnerable to water erosion than the flat land. Both the length and the steepness of the slope substantially affect the rate of soil erosion by water with the reasons that the erosive forces; splash, scour and transport all have a greater effect on steep slope. Raindrop splashes soil particles uniformly in all direction in a flat surface whereas in slope land it splashes more on down slope than up slope and the amount of splash particles is also increase as the steepness increase. The splashed particles move three times farther in down slope than in up slope on a 10 percent surface slope (Thornes, 1989). The erosive power of surface run off is even more affected by increased steepness and length of slope. This is simply because of the fact that the higher the steepness the higher the velocity of runoff and the more the length of slope the more the accumulation of runoff volume which ultimately increases both the entrainment and transportation capacity of runoff. Soil movement on a uniform slope is greater than on a concave slope but less than on a convex slope. Therefore on convex slopes with increasing steepness and slope length the erosion rate will be maximum (Thornes, 1989). The effect of topography at regional scale is quantified as H^2/S, where H is the average height of relief and S the surface area (Hudson, 1986).

2.2.4. Vegetation cover

Under the same climatic, topographic and soil condition the rate soil erosion vary with the varying land use and land cover condition and this variation is due to the effectiveness of plant cover condition (Hudson, 1986). Vegetation acts as a protective layer or buffer between the atmosphere and the soil. The above ground components of plants such as leaves and steams absorb some of the energy of falling raindrops so that less is directed at the soil, while the under ground component; the root system contribute to the mechanical strength of the soil.

The effectiveness of plant cover in reducing erosion by raindrop impact depends upon the height, density and continuity of the canopy. The height of the canopy is important because water drops falling from seven meters may attain over ninety percent of their terminal velocity. Decrease in soil detachment by splash can not be expected for the canopy taller than 1m (Styczen and Hogh-Schmidt, 1986). Moreover, raindrops intercepted by the canopy may coalesce on the leaves to form larger drops which are more erosive due to having more kinetic energy. Therefore the reduction of erosive power of raindrop by the canopy cover can be found in the case of canopy cover close to the ground surface. The effectiveness of the plant cover also depends on whether it is above ground i.e. aerial cover or ground-hugging cover. The ground-hugging cover which has intimate contact with ground surface can bear a substantial fraction of shear stress exerted by runoff water. This can also reduce the likelihood of the formation of rills and thereby contribute to reduce sediment concentration in overland flow (Rose, 1994).

A plant cover dissipates the energy of running water by increasing roughness flow, thereby reducing velocity. The level of roughness with different plant cover types depends upon the morphology and the density of the plant as well as their height in relation to the depth of flow. The greatest reduction in velocity occurs with dense and uniform vegetation cover. Clumpy, tussocky vegetation is less effective as it lead to concentration inflow with localized high velocity between the clumps (Morgan, 1995).

There is complex relationship between the soil loss and change in the extent of plant cover. According to (Elwell, 1981), there is an exponential decrease in soil loss with increasing percentage interception of rainfall energy by the plant canopy. There is a steep fall in sediment yield as cover increases from 0 to 30 percent after this the rate declines more slowly (Thornes, 1986). However, the canopy cover of plants varies during the year with the natural growth processes. In addition to this, factors like soil properties, soil moisture, soil fertility, aspect and the micro climate may result in to the variation of canopy cover within the same species and same growing season. Dense growth of grass may be almost as efficient and quicker to protect the soil against erosion. The effectiveness of agricultural crops to protect soil against erosion depends on their stage of growth and the amount of bear ground expose of the erosion (Morgan, 1995). Therefore maximum erosion control can be achieved by the effect of canopy cover by maintaining maximum canopy cover during period of maximum erosivity.

The basal area of the plants is also important factor on reducing soil erosion as the surface area covered by the basal area of the plant is totally eliminated from the erosion. In dense forest, basal area may covers 20 to 30% of the total surface area (Toy et al., 2002) and thereby reduces the rate of erosion substantially.

2.3. Effect of Soil erosion

Water induced soil erosion has been identified as the most severe hazard that threatens the protection of soil (Jetten, 2003) .The consequences of soil erosion occur both on and offsite.

Onsite effects are particularly important on agricultural land where the loss of soil from a field, the breakdown of soil structure and the decline in organic matter and nutrient result in a reduction of cultivable soil depth and a decline in soil fertility. Erosion also reduces available soil moisture, resulting in more drought-prone conditions. The net effect is a loss of productivity which, at first, restricts what can be grown and results in to increased expenditure on fertilizers to maintain yields, but later threatens food production and leads, ultimately, to land abandonment and change in land use/cover types. It also leads to a decline in the value of the land as it changes from productive farmland to wasteland.

Soil erosion in mountainous areas have direct and obvious impact on low lying areas where loss of life and property and siltation on agricultural lands occur (Shrestha, 2000). The off site effects of soil erosion include the movement of sediment and agricultural pollutants into watercourses. These lead to the silting-up of dams, disruption of the ecosystems of lakes, and contamination of drinking water. In some cases, increased downstream flooding may also occur due to the reduced capacity of water course from eroded materials. Many hydro-electricity and irrigation projects have been ruined as a consequence of erosion. Sediment is also a pollutant in its own right and through the absorption of chemicals on it can increase the levels of nitrogen and phosphorus in water bodies and result in eutrophication.

2.4. Soil erosion risk assessment and erosion modeling

The soil erosion assessment is the specialized form of land resource evaluation to identify the areas of land where the maximum sustained productivity from a given land use is threatened by soil erosion (Morgan, 1995). Soil erosion assessment is very important before planning soil conservation work as predicted rate of soil loss can be compared with acceptable rate of erosion. In addition, it is also useful if the effects on erosion rates of different conservation strategies can be determined. What is required therefore is a method of predicting soil loss under a wide range of conditions (Morgan and Davidson, 1986).

2.4.1. Scales for measuring soil erosion

The technique to evaluate the erosion rate depends on the type of erosion to be monitored and the scale of measurement and the objectives (Lal, 1990). There are three scales of measurement: macro scale, meso scale, and micro scale.

The macro scale involves hundreds to thousands of square kilometres of area and deals with streams and river basins. Some of the geographic, ecological and regional aspects of soil erosion are studied at macro scale. These assessments are necessary to evaluate sediment transport in rivers and streams and to plan development strategies at the regional or national level.

The meso scale involves evaluation of sediments sources at the scale of farm units e.g. a few hectares to a few hundred hectares. Measurement of erosion rates at this scale are needed to evaluate the effects of farming practices, land use system, and topographic factors on runoff and erosion. The effects of agricultural practices on pollution of environment and eutrophication of natural water are also assessed at this scale.

The micro scale involves study of hill slope erosion at a scale of few square meters to a few hundred square meters. The basic process governing soil splash, detachability and transportability, initiation of overland flow and of sediment transport by rill erosion is studied at micro scale.

2.4.2. Soil erosion modelling

Modelling soil erosion is the mathematical description of the soil erosion processes. The processes involved in soil erosion are soil particle detachment, transportation and deposition on land surfaces. The reasons behind the modelling of soil erosion are: (a) erosion models can predict or assess the soil loss which then can be used for conservation planning, project planning, soil erosion inventories, and for regulation; (b) physically based mathematical models can predict spatial and temporal occurrence of soil erosion, thus helping the conservation planner to target efforts to right place at right time to reduce erosion; (c) models can be used as tools for understanding erosion processes and their interactions and for setting research priorities (Nearing et al., 1994). Most of the soil erosion models are built up on the concept of transport capacity. The transport capacity can be defined as the capacity of the flow which can carry maximum amount of sediment without any deposition (Nearing et al., 1994).

Depending up on the objective of the modelling, there are generally three types of soil erosion models; empirical, conceptual and physically based. Empirical model like universal soil loss equation is based on defining the most important factors and through the use of observation, experiment and statistical techniques. The primary focus of empirical model is to predict average soil loss. Physically based model on the other hand is based on mathematical equations to describe the processes involved in the model, taking account of the laws of conservation of mass and energy (Morgan and Davidson, 1986).

Physically-based models represent the essential mechanisms controlling erosion. The importance of physically-based model is that it represents a synthesis of the individual components which affect erosion, including the complex interactions between various factors and their spatial and temporal variability. The research scientist can use the physically-based erosion models to help identify which parts of the system are most important to the over all erosion processes and therefore should be given attention in research and development of erosion prediction and control technology. It has practical implications as conservation planner can use a physically-based model as an interactive conservation design tool, targeting critical seasons or months in which major erosion events occur. The planner can also quickly suggest and evaluate new conservation strategies for individual fields (Nearing et al., 1994).

2.4.3. Model field validation

Before making any decision on the basis of model result, it is important to assess the validity of the model. Generally the model result is validated by comparing the predicted value with the measured value and assessing the closeness of fit by correlation coefficients or an error statistic. If the objective is to predict the erosion loss, the prediction value can be compared with measured value by dividing the predicted by measured value and the resultant ratio can be used to judge whether model result is acceptable. In ideal condition the ratio is 1 which is rarely happens and therefore the acceptable ratio is between 0.75 and 1.5 (Morgan, 1995).

The sediment yield measured at the outlet of catchment can provide a useful perspective on the rate of soil erosion occurring in that catchment. However, it is essential to understand the fact that there are some constraints that must be recognized before using such data in soil erosion studies. Eroded soil materials often move only short distance and only a fraction of sediment eroded with in a catchment reaches the catchment outlet. They may remain in the fields where they originated or may be deposited on the way where slope gradient decline (Walling, 1994). This process can be illustrated by the concept of sediment delivery ratio (SDR). The ratio of sediment delivered at the catchment outlet to the gross erosion within that catchment is called sediment delivery ratio. Another problem in using such measurement is that the sediment transported by river not only carries the eroded soil but also the material derived from a variety of sources. These sources include channel and gully erosion, mass movements and soil excavated by human and livestock activities. Temporal discontinuity while transporting eroded soil material by the runoff is another problem while attempting to use such data. Sediment eroded from one location may be temporarily deposited in another place and again can be transported. Such type of temporary storage and subsequent remobilization of erosion material usually happens during the process of erosion transportation (Walling, 1994). Therefore the sediment measured at the catchment outlet at a given moment reflects the recent history of erosion rather than contemporary erosion in the catchment.

3. Description of the study area

3.1. Location

The study area covers an entire area of Lomsak district, Phetchabun province of Thailand. It is located in the lower Northern part of Thailand, about 400 km far from Bangkok, the capital city of Thailand (Figure 3-1). It has an area of about 1415 square kilometre situating within the geographic coordinates ranging from 16° 32′ 11.65″ to 16° 46′ 33.08″ North and 101° 03′ 2.63″ to 101° 31′ 51.44″ East.

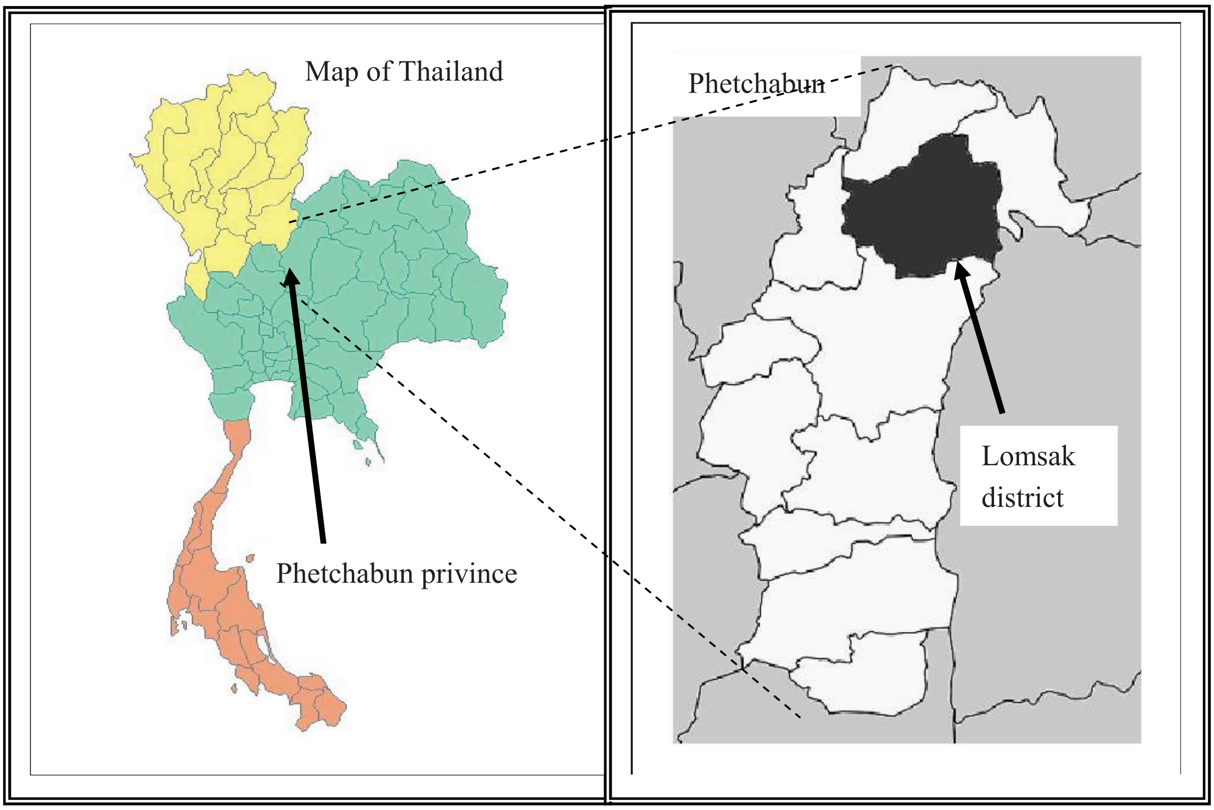

Figure 3-1: Map of study area

3.2. Climate

Thailand has a warm, tropical climate affected by an annual monsoon, with a rainy season from June to October and a dry season the rest of the year. It has average monthly temperature of 26°C with the highest temperatures of 36°C from March to May and the lowest temperature of 15°C in December and January in the northern highland of the country. The average annual rainfall of Lomsak calculated from 35 years rainfall data from year 1973 to 2007 is 1109.19 mm. Most of the rainfall occurs during the month of May to September. The monthly rainfall, temperature and relative humidity of year 2007 of the Lomsak district is shown in table 3-1.

Table 3-1: Monthly climatic data of 2007 of Lomsak district

Month	Rainfall (mm)	Rainy day	Max Temp. (^{0}C)	Min Temp. (^{0}C)	Mean Temp. (^{0}C)	Mean Relative Humidity (%)
Jan	0.00	0	34.80	11.30	23.10	77.19
Feb	2.00	1	37.70	11.30	24.50	80.32
Mar	3.10	2	39.80	18.00	28.90	80.55
Apr	46.30	10	41.20	20.00	30.60	85.13
May	204.00	19	39.50	21.50	30.50	91.93
Jun	109.20	15	36.80	22.00	29.30	91.40
Jul	40.10	16	35.30	21.40	28.40	90.68
Aug	225.70	18	35.70	21.70	27.50	91.84
Sep	131.10	19	35.00	18.80	26.90	94.53
Oct	287.20	11	34.00	18.30	26.20	91.10
Nov	0.90	3	33.80	11.00	24.30	86.40
Dec	0.00	0	34.80	12.50	25.30	85.87
Total	1049.60	114				

(Source: Thai Royal Meteorological Department, Thailand)

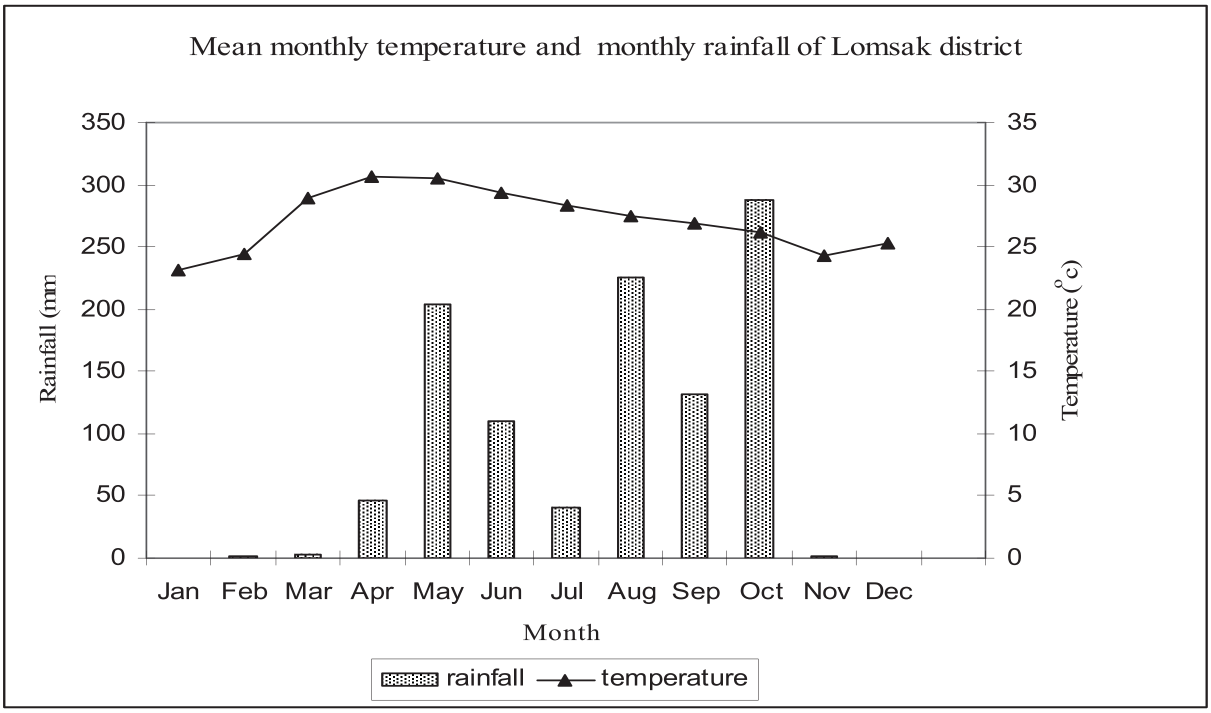

Figure 3-2: Graph of monthly rainfall and temperature of 2007 of Lomsak district

3.3. Land use/land cover

Forest, agriculture, grass land and settlements are the major land use types in the study area. These land use / land cover types are highly fragmented, irregularly scattered and patchy (Figure 3-3). Most of the area is used for agriculture and human settlements. Agriculture lands are categorized as irrigated rice field, mixed agriculture, maize and orchard. Tamarind, mango, litchi and banana are the main fruit trees. Rice and maize are the dominant agricultural crops in the study area. Rice is grown in low land followed by tobacco, cucumber, vegetables and maize during dry season. In mountainous area maize, mung bean and horticulture are commonly grown and farming is done even up to 40° slope without proper soil conservation measures and there by causing soil erosion problem. Many accessible forests area are encroached by the people for cultivation. The forest near by settlements and road seems degraded. In the south-east part of the district forests are preserved as conservation area aiming to protect watershed and biodiversity. In the western mountain the abandoned agriculture area are turning to grass land.

Figure 3-3: Land use/land cover type of study area

3.4. Soil

The soil in the study area is mainly developed from the weathering of sedimentary rocks and can be categorized mainly to silty clay loam and silty clay textural classes (Prachansri, 2007). They are very shallow to moderately deep and well drained. Alluvial soil is found in the lower plain areas. According to the study of Hansakdi (1998), soil in the study area is divided into five classes of USDA soil taxonomy as Entosols, Mollisols, Inceptosols, Alfisols and Ultisols. The soil types are varying according to landscape and landform type. Entisols are dominantly found in mountains and plateau hills whereas the Mollisols scatters over the mountains, piedmont and plateau hills. Inceptisols are most commonly found in all types of landscapes. The Alfisols are found relatively in high topography areas.

3.5. Geomorphology

The area consists of four different types of landscape; valley, piedmont, plateau and mountain. The mountains are located in the west and northeast part of the district and plateaus are in the north eastern and south eastern part. The piedmonts are found both in the west and east and the valley is located at the centre part between the mountains and plateau where the Pa Sak River flows. Each landscape is divided into different relief and landform types. The elevation of the study area varies from 121 to 1495 meters above sea level. The present geomorphic configuration of the Pa Sak and

Huai Nam Phuong river area is the result of several geological processes such as tectonics, denudation and sedimentation.

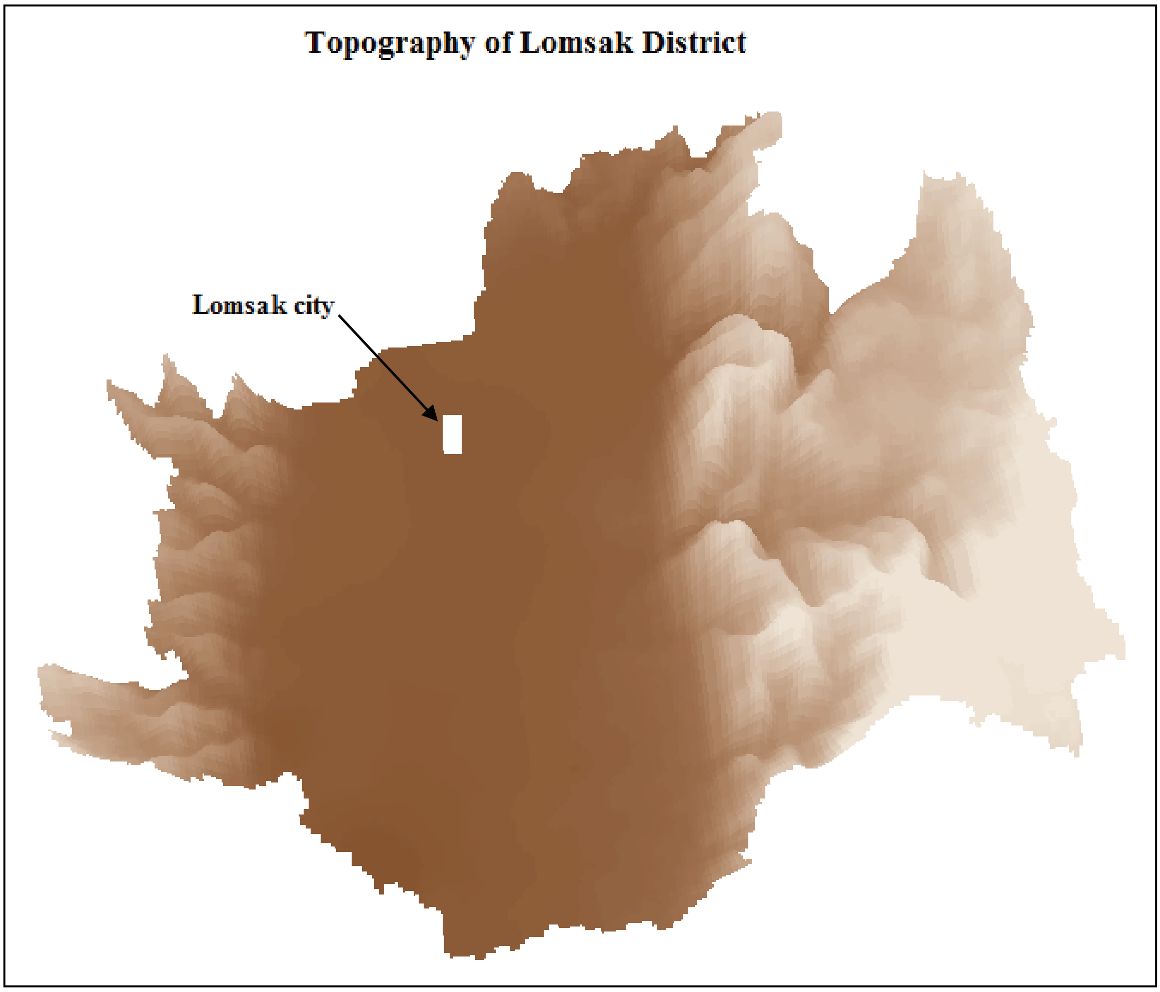

Figure 3-4: Topography and hill shade map of Lomsak district

3.6. Geology

Mountains in the study area form part of the so called Indonesian Orogeny or fold belt. Tectonic movements which occurred in Cretaceous_Tertiary led to the formation of horsts and grabens. The Pa Sak river valley lies in the graben. The study area comprises three major geological formations belonging to Paleozoic, Mesozoic and Cenozoic as described below (Hansakdi, 1998). Geological map of study area is presented in figure 3-5.

3.6.1. Paleozoic group

a.The **Pha Nok Khao** is the oldest one formed in Paleozoic era and exists in the Nam Ko Yei ridge at the western part of the study area. Rocks belonging to this formation are dominantly limestone, gray, massive to thick bedded, chert, black, nodular or thin bedded, with intercalation of thin bedded gray shale.

b.The **Nam Duk** formation is the Middle Permian rocks which are dominantly gray to black shale, yellowish brown and fine grained sandstone, and gray to dark gray, well and thinly bedded limestone. These rocks are mostly existed along the faulted ridge belt in the plateau hills at the eastern part of the study area.

3.6.2. Mesozoic group

These rocks are belonging to Korat group and the most extensive formation in the area. The following formations are the result of a continuous sedimentation during Upper Triassic to Upper Cretaceous.

a. The Huai Hin Lat formation comprising the old Upper Triassic rocks occur on the outer rim of the western mountain landscape area. The rocks are dominantly conglomerate, sandstone, shale, mudstone and argillaceous limestone.

b. The Nam Phong formation comprising the young Upper Triassic rocks are dominantly reddish brown sandstone, brown cross-bedded conglomerate, quartz, quartzite, brown to reddish brown shale and siltstone.

Cenozoic group
This formation was made from alluvial deposits of Quaternary varying in texture from gravel, sand, and silt to clay and occurs along the river in the middle of the valley, in piedmont, and as colluvial deposits.

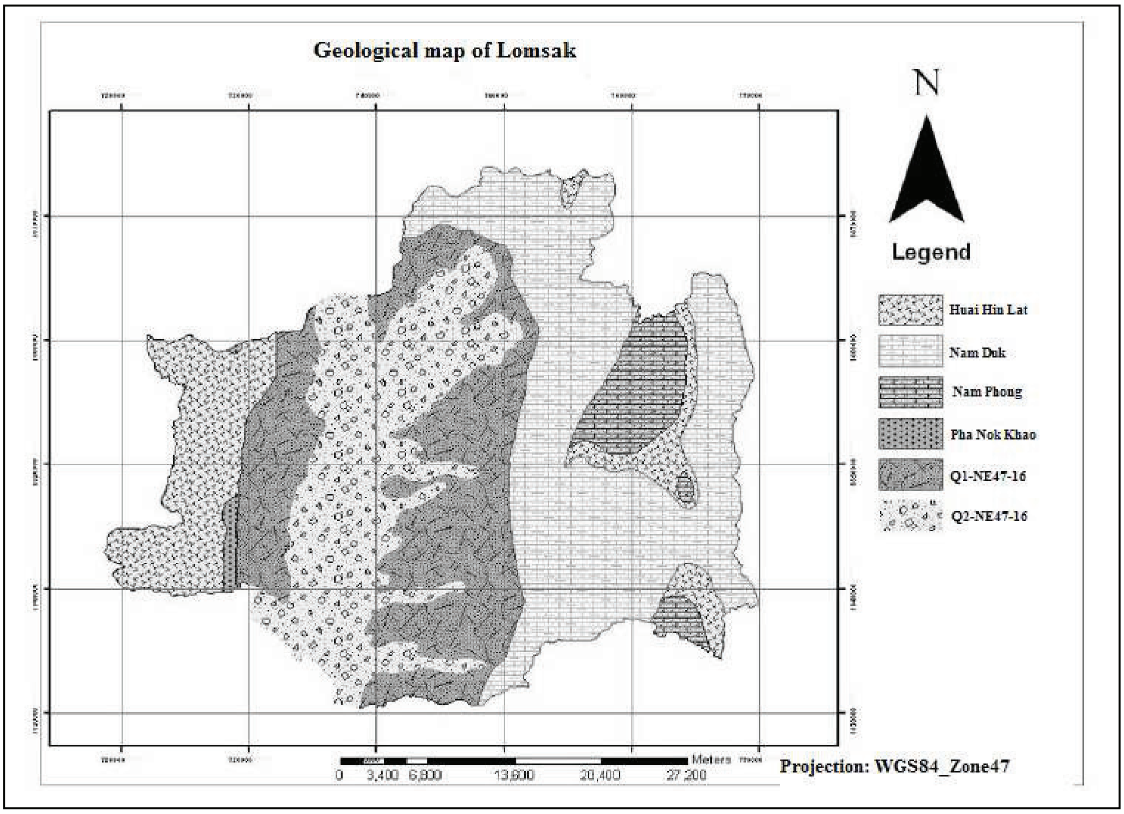

Figure 3-5: Geological map of Lomsak

4. Methods and techniques

4.1. Data sets used

Following data were used in this study.

- ASTER image of April 2006, aerial photo and ground truth data for image classification.
- Land use map of 2007 of study area.
- Monthly NDVI images of 2007 of 250m, 500m and 1km resolution.
- Topographic map of study area.
- Crop calendar and cropping sequence data.
- Soil physical properties viz; soil texture and organic matter.
- Climatic data of 2007 viz; mean monthly rainfall, mean rainfall per rain days, coefficient of variance of monthly rainfall, mean monthly temperature, monthly temperature range and potential evapotranspiration.
- Topographic data in Digital Elevation Model (DEM) format generated from contour map.

4.2. Materials, equipments and softwares used

Garmin GPS instrument, Mobile GIS, Compass, Abneys level, measuring tape, Soil sampling tools and equipments, Camera etc.

Software: MS Word, MS Exel, ArcGIS, Erdas Imagine, SPSS, R-Geo statistical software, Modis Reprojection Tools (MRT), Arc Info workstation, and PESERA-GRID model.

4.3. Methods applied

4.3.1. Erosion study

To assess the erosion risk of study area a Pan-European soil erosion risk assessment (PESERA) model was selected. The model was selected because firstly, it predicts the erosion at regional scale and for mountainous area where data may not be easily available due to inaccessibility problem this model allows the use of remote sensing data. Secondly it provides a quantitative estimate of erosion rate that can be compared with long term averages for tolerable erosion. And third, as land use and climate are explicit within the model sensitivity of changing environment can be estimated by scenario analysis.

4.3.1.1. General description of PESERA model

The Pan-European soil erosion risk assessment PESERA is a physically-base and spatially distributed model developed for soil erosion assessment in environmentally sensitive areas relevant to a regional scale and defining the soil conservation strategies (Kirkby et al., 2003). The model is built in three conceptual steps as follow:

(1) A storage threshold model to convert daily rainfall to daily total overland flow runoff.
(2) A power law to estimate sediment transport from runoff discharge and gradient and interpret sediment transport at the base of the hillside as average erosion loss.
(3) Integration of daily rates over the frequency distribution of drainage.

Storage model

The PESERA model is based on the concept of a storage threshold model to convert daily rainfall to daily overland flow runoff. The runoff can be determined as rainfall minus the runoff threshold where the threshold depends on the factors related to vegetation cover, soil, tillage and soil moisture status. The important soil factors to be used in the model are texture, soil depth and organic matter that determine the threshold storage beneath the vegetation-covered fraction of the soil surface. On bare soil, the susceptibility of the soil to crusting and the duration of crusting determine a lower threshold. The final threshold is estimated by weighted average from vegetated and bare fractions of the surface. As a model input for PESERA model, all the factors are assessed on monthly basis so that the threshold may vary considerably throughout the year (Irvine and Kosmas, 2003).

Power law sediment model

The model uses the power law to estimate sediment transport from runoff discharge and slope gradient. Daily total runoff is linearly scaled up to discharge for each point in as area and daily sediment transport is calculated as follows:

$$\text{Sediment transport} = \text{Erodibility}*(\text{runoff}*\text{distance from divide})^2 *\text{slope gradient} \quad (4.1)$$

Estimating long term average erosion rate

This model involves the integration of daily rates over the frequency distribution of daily rainfall to estimate long term average erosion rate. Daily rainfall data is used because of their availability. The daily runoff and daily erosion for each possible rainfall event is weighted by its frequency in this distribution to estimate the long term averages for each month and summed to give annual soil erosion rate.

4.3.1.2. Erosion prediction using PESERA model

Erosion prediction from the PESERA model is reliant on estimating a stabilized vegetation cover and identifying the generation of overland runoff on a cell by cell basis. PESERA estimates average discharge in a cell by cell basis from infiltration surplus and combines it with a relief factor to simulate both flow detachment and sediment transport. The flow processes in the model are modified by land cover and soil erodibility (Jetten and Favis-Mortlock, 2006).

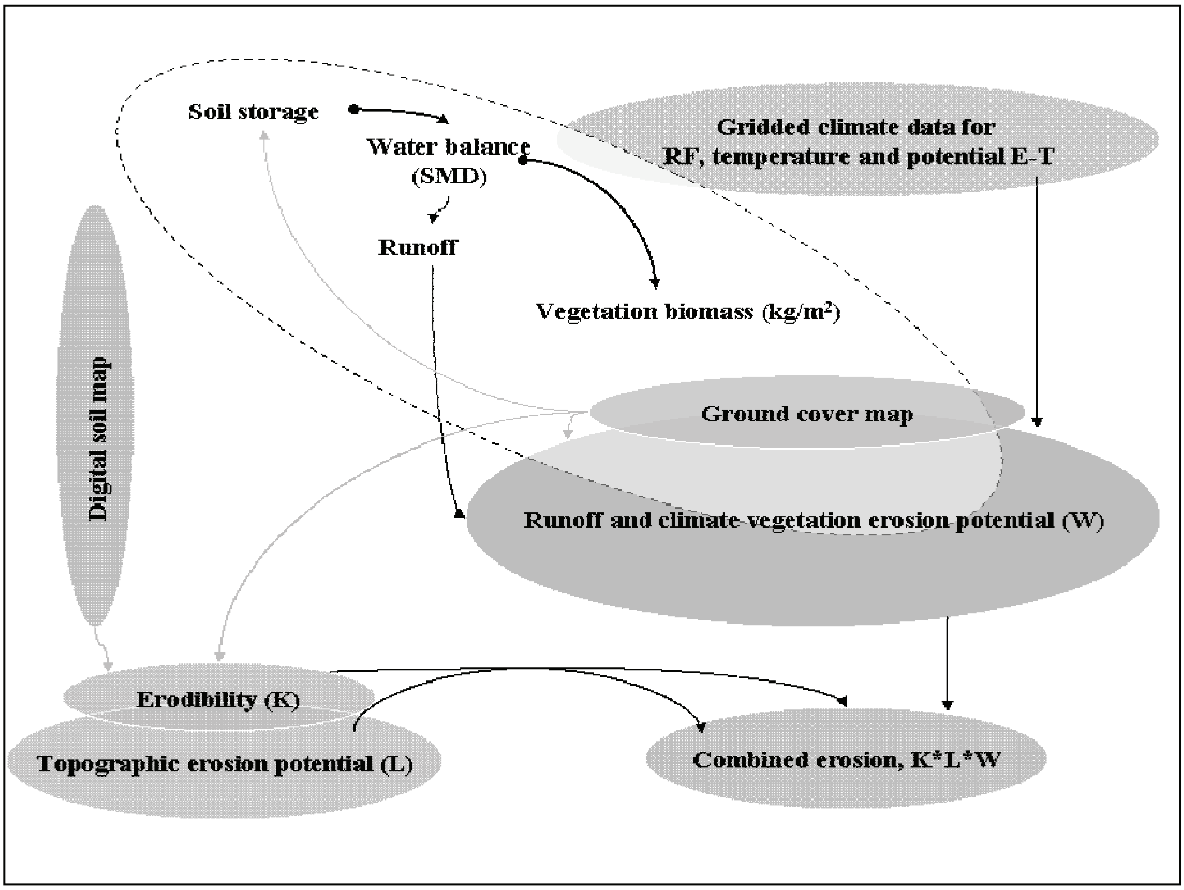

Figure 4-1: Components interaction in PESERA model

(Source: http://eusoils.jrc.it/ESDB_Archive/pesera/pesera_cd/pdf/DL5ModelStrategy.pdf)

The model calculate the rate of soil erosion by integrating three factors; soil erodibility (K), topographic potential (L) and run off and climate/vegetation erosion potential (W) by using following equation (Kirkby et al., 2004), which is illustrated in figure 4-1.

$$E=K*L*W \quad (4.2)$$

Where,
E is amount of soil loss (t/ha/yr),
K is erodibility (mm),
L is topographic erosion potential (m) and
W is run off and climate/vegetation erosion potential (mm), which is calculated by using climate data, vegetation cover water balance and a plant growth model as follow;

$$W= \sum P\,(r-h) \quad \text{for } r>h \quad (4.3)$$

Where,
P is the proportion of run off above the threshold (mm),
r is the overall storms (mm) and
h is the storm exceeds the run off threshold (mm).

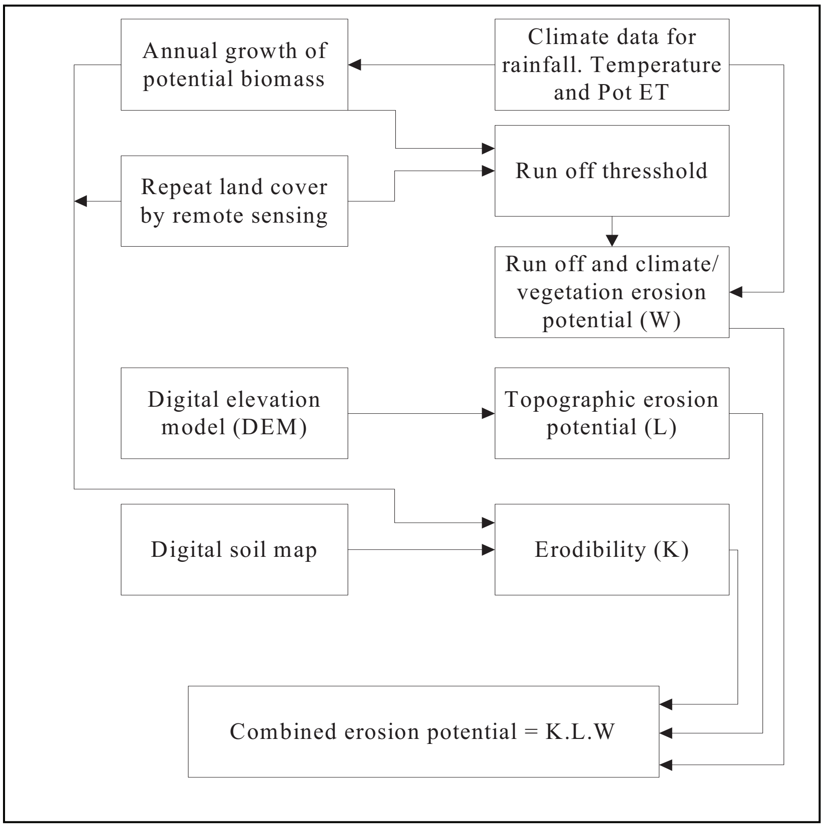

Figure 4-2: Flow chart of PESERA model

(Source: http://eusoils.jrc.it/ESDB_Archive/pesera/pesera_cd/pdf/ThePeseraMap.pdf)

4.3.1.3. Factors used in soil erosion assessment

The PESERA model combines the effect of three factors: topography, climate and soil into a single integrated forecast of runoff and soil erosion. Data for these three factors can be extracted from existing source and combined in a physically based model to create the rational forecasts of soil erosion. The factors of PESERA model are mentioned as follows;

Climate factor

Both the low frequency and high frequency components of climate are important in erosion prediction. The low frequency events determine the seasonal cycle of water balance in the soil, which provides the environment for growth of vegetation. High frequency rainfall events are, on the other hand, important in assessing soil erosion, as these generate the overland flow (Kirkby et al., 2003). The required data of climate factors are based on daily time series data of rainfall, temperature and potential evapo-transpiration (ETo). The parameters for climatic factor of PESERA model required are:

(1) Rainfall data: mean monthly rainfall, mean rainfall per rain day and coefficient of variance of rainfall to provide the distribution of daily rainfall.

(2) Temperature: Mean monthly temperature and monthly temperature range.

(3) Potential evapo-transpiration (ETo) to estimate actual evapo-transpiration, plant production and water balance.

The coefficient of variance of rainfall (CV) can be calculated as;

$$CV=SD/Mean \tag{4.4}$$

Where,
SD is standard deviation of daily rainfall in month,
Mean is mean daily rainfall in the month.

Mean monthly temperature (T_{ave}) used for calculating potential evapo-transpiration is calculated as;

$$T_{ave}=(T_{max}-T_{min})/2 \tag{4.5}$$

Where,
T_{max} is maximum temperature in a month and
T_{min} is minimum temperature in a month.
The potential evapo-transpiration was calculated by using Penman-Monteith equation as mentioned below;

$$ET = \frac{0.408\Delta(R_n-G)+\gamma\frac{900}{T+273}U_2(e_s-e_a)}{\Delta+\gamma(1+0.34U_2)} \tag{4.6}$$

Where,
ET is reference evapo transpiration (mm/day), R_n is net radiation at the crop surface(MJ m^{-2} day^{-1}), G is soil heat flux density (MJ $m^{-2}day^{-1}$), T is mean daily air temperature at 2m height (°C), U_2 is wind speed at 2m height (ms^{-1}), e_s is saturation vapour pressure (KPa), e_a is actual vapour pressure(KPa), e_s-e_a is saturation vapor pressure deficit (KPa), Δ is slope of vapour pressure curve (KPa°C^{-1}), γ is psychometrics constant (KPa°C^{-1}). Data which were not available in the field can be derived from the literature (Allen et al., 1998).

<u>Soil factor</u>

The soil parameter needed for PESERA model are soil erodibility, readily available soil water capacity, crustability and scale depth. These parameter values can be calculated on the basis of soil texture and organic matter as mentioned below;

Erodibility: Soil erodibility is the most important soil property governing soil erosion. It primarily depends on soil texture, with highest values for fine sand and silt soils with low clay contents (Kirkby et al., 2003). It also depends on both vegetation and soil organic matter content. Usually a soil type becomes less erodible with decrease in silt fraction, regardless of whether the corresponding increase is in the sand fraction or the clay fraction. Overall, organic matter content is ranked next to particle-size distribution as an indicator of erodibility. The Wischmeier's formula (eq 4.7) can be used to calculate soil erodibility. The components of this equation are percent of clay, silt and very fine sand and organic matter, soil structure code and permeability class. Erodibility is expressed as ton* per acre per erosion index unit and division of which by the factor 7.59 yield the erodibility (K) value expressed in SI Units (Romkens et al., 1997).

$$\text{Erodibility (K)} = [2.1*M^{1.4}*10^{-4}(12-a)+3.25(b-2)+2.5(c-3)]/100 \qquad (4.7)$$

Where, M = particle size fraction (%silt + %very fine sand)*(100 - %clay), a = %organic matter, b = soil structure code, c = permeability class. (Soil structure code are; very fine granular = 1, fine granular = 2, coarse granular = 3, blocky, platy or massive = 4 and permeability class are; rapid = 1, moderate to rapid = 2, moderate = 3, slow to moderate = 4, slow = 5, very slow = 6).

Soil water available to plant: The amount of soil water that can be used by the plant depends on characteristics of the soil (e.g., texture) and the root depth of the plant and can be estimated as amount of soil water between field capacity (FC) and permanent wilting point (PWP). Field capacity has been defined as water remaining in the soil two to three days after having been wetted with water and after pull down by gravitational force and the point is measured at tension around 33kPa (-0.33 bars). Permanent wilting point has been defined as the largest water content of a soil below which the plant, growing in that soil, wilt and fail to recover (Doorenbos et al., 1984). Permanent wilting point depends on plant variety, but is usually at tension around -1500 kPa (-15 bars).

In developing the PESERA model, only the Soil Water Available to Plant in 1m depth of soil (or to the depth of rooting if less than 1m) has been computed (Gobin et al., 2003). As a model input water available to plant can be calculated for two different root zones; at depth of 0-30 cm and at depth between 30-100 cm. The water available to plant at depth of 0-30 cm is calculated by using eq. 4.8 as mentioned in (Baize, 1993). Likewise, the water available to plant at depth of 30-100 cm can be calculated by using eq. 4.9 as presented by (Parfitt et al., 1985);

$$WAP1 = (FC-PWP)*RD \qquad (4.8)$$

$$WAP2 = 0.5(FC-PWP)*RD \qquad (4.9)$$

Where;
WAP1= water available to plant at depth of 0-30 cm,
WAP2= water available to plant at depth of 30-100 cm,
FC= field capacity (% vol),
PWP= permanent wilting point (%vol), and
RD= effective root depth of plant (mm).

Soil water storage capacity: It is defined as the total amount of water which is stored in the soil with in the plant's root zone (Nyvall, 2002). This provides the maximum storage capacity of the soil before runoff occurs under vegetation. This parameter depends on soil texture, soil organic matter, field capacity, permanent wilting point and effective rooting depth of plants. In this study the soil water storage value was derived by using following equation referred to (Jones et al., 2002).

$$SWSC = SWAP\_AWC + k\,(DRAIN\_PORE\_PROFILE) \qquad (4.10)$$

Where,
SWSC is soil water storage capacity,
SWAP_AWC is soil water available to plants,
k is constant having a value between 0 and 1 and

DRAIN_PORE_PROFILE is the drainable pore space for the soil profile.

The SWAP_AWC is calculated for 1 m. depth. The soil profile is partitioned in to topsoil and subsoil horizons. Assuming the top soil is 30 cm thick, SWAP_AWC is calculated as:

$$SWAP\_AWC = SWAP\_AWC\_TOP + SWAP\_AWC\_SUB \quad (4.11)$$

Where,

$SWAP\_TOP = \sum_{0-30} AWC\_TOP$ and

$SWAP\_SUB = \sum_{30-100} AWC\_SUB$

The DRAIN_PORE_PROFILE is the drainable pore space, as a percentage volume for the profile estimated by integrating the drainable pore space to 1m depth. It was derived on the basis of dominant texture class and packing density of soil by referring value from Table 1 of (Jones et al., 2002). The value of packing density was determined on the basis of top soil texture class as presented in (Gobin et al., 2003).

Crustability: Soil crusting results from rains breaking down soil aggregates into particles that cement into hard layers at the soil surface when drying occurs rapidly. Soil crusting restricts the surface water to infiltrate in to the soil and increase the run off. It sets the lower limit of storage capacity for a crusted soil in unvegetated areas (Kirkby et al., 2004). The crustability depends on soil texture and soil organic matter. The values of crustability varies with the changing of soil textural classes which ranged from coarse to very fine as classified in PESERA user's manual (Irvine and Kosmas, 2003). In this study, the crustability values were derived by using Pedro-transfer rule of European Soil Bureau; SAI/JRC on the basis of the soil texture that were analyzed in the lab. The crustability value varies from 1-5mm in PESERA model.

Scale depth (top model): Top model determines where the saturated land surface areas developed is and the potential to produce saturation overland flow by predicting the movement of the water table. This property is derived on the basis of depth of soil textural classes and the value is ranges from 5 mm for very fine to 30 mm for coarse texture. In this study scale depth was derived on the basis of soil texture which was analyzed in the lab and referring from PESERA Users manual (Irvine and Kosmas, 2003). Texture class was defined on the basis of particle size as shown in table 4-1 and finally the value of scale depth for different textural classes are derived as shown in table 4-2.

Table 4-1: Description of soil texture

Soil texture	Particle size distribution
Coarse	18% < clay and > 65% sand
Medium	18% < clay and 15% < sand < 65%
Medium fine	< 35% clay and < 15% sand
Fine	35% clay < 60%
Very fine	Clay > 60%

(Source: PESERA users' manual)

Table 4-2: Scale depth (TOPMODEL) derived from soil texture

Soil texture		Scale depth (mm)
Coarse	C	30
Fine	F	10
Medium	M	20
Medium fine	MF	15
Organic soils	O	10
Very fine	VF	5

(Source: PESERA users' manual)

Land use/land cover factor

Vegetation exerts an extremely strong effects on both runoff and erosion generation. The cover factor is considered to have a major impact on the runoff threshold when it is associated with soil properties particularly the soil organic matter (Kirkby et al., 2003) and the threshold values range from 10mm for bare soil up to 100 or more for forested areas. The canopy cover values differ depending upon the land use/cover types and on growing stages particularly for agriculture crops. Land cover value in the model ranges from 0% for bare soil up to 100% for dense forest and grass land (Irvine and Kosmas, 2003).

In PESERA vegetation cover can be obtained as a potential cover by using the growth model based on evapo-transpiration and water use efficiency. In alternative to this, it can be obtained from remotely sensed images. The former approach of this model has the advantage of allowing the soil organic mater to be estimated at the same time as vegetation biomass and forecasting the impact of climate and land use changes. In this study the land cover was derived from the remotely sensed land cover data.

PESERA model requires monthly canopy cover maps to produce monthly erosion rate, which is especially important for agricultural crops as canopy cover vary according to growing stages. Monthly canopy cover can be produced by using crop calendar showing planting, growing and harvesting month of major agricultural crops and their respective canopy cover of different growing stages by referring PESERA Users manual (Irvine and Kosmas, 2003).

NDVI maps derived from MODIS image can also be used to prepare canopy cover map and compare it with canopy cover map generated from crop calendar. The NDVI maps were re-projected to WGS84 zone47 projection from sinusoidal projection system by using MODIS re-projection tools (MRT). To derive percentage of canopy cover for each month the negative exponential equation between NDVI and C-factors developed by (van der Knijff et al., 1999) was applied (eq 4.12). The value range of C varies from 0 to 1, which is inverse NDVI value as shown in equation.

$$C = \exp[-\alpha * NDVI/(\beta - NDVI)] \qquad (4.12)$$

Where, α and β are the parameters that determined the shape of the NDVI-C curve.
This equation produces more realistic result than estimated from linear relationship and α value of 2 and β value of 1 give the reasonable results. However; the C-value can not directly be used in

PESERA model as the model requires the canopy cover in percentage ranges from 0-100%. Therefore, C-values were multiplied by 100% and then subtracted from value 100 i.e. (100-C*100%) to be applied as an input in the PESERA model.

Topographic factor

The local relief is the important topographic characteristics that influence on soil erosion. The estimation of the local relief in PESERA is by computing the standard deviation of the elevation of surrounding grid cells (3x3 windows). This can be derived from existing DEM. It is reported that the measure of relief is insensitive to DEM resolution (Kirkby et al., 2004). Therefore, the best resolution of the DEMs which are available should be selected for the model. In this study the DEM was generated from contour map of 20 meter interval using ArcGIS version 9.3 program.

4.3.2. Study of the effect of upscaling (grid cells) on erosion assessment

Land use land covers are the categorical data. While resampling such data nearest neighbour algorithm is generally used. In nearest neighbour method, the value of the pixel of the resampled image is assigned from the value of most dominant nearest pixels of original image (Kerle et al., 2004). Therefore the categorical value of the original image remains preserved. In alternatives to this, bilinear interpolation and cubic convolution method can not preserve the categorical values of the original image because the value of new pixel is assigned from the average value of original pixels in these methods. However, when image is resampled by using nearest neighbour algorithm the area of the classes/categories is expected to be changed. Such changes could occur in the situation where classes are more fragmented and patchy. In such context, the soil erosion assessment model may give different results if the resolution of land use land cover data is varied.

To see the up scale effect of land use/land cover map on model predictions, the classified land use map from Aster image at 15 m resolution was resampled using nearest neighbour algorithm to 250 m, 500m and 1000m resolutions. The land use/land cover input maps at 250m, 500m and 1000m resolutions were used separately as model inputs to see their respective effect on model prediction.

4.3.3. Erosion scenario analysis

Soil erosion is the result of integrating effects of factors such as land use, climate, soil properties and topography. As land use change due to human activities is a continuous process and is expected to change in the future, it is important to examine the potential effect of these changes on soil erosion for conservation planning. PESERA model predicts erosion based on simulating overland flow and estimation of a vegetation cover. Thus PESERA can be used to predict effect of land use land cover changes on soil erosion. For this purpose various land use scenarios can be generated and their effect on soil erosion can be assessed.

4.3.4. Data collection

During field work primary and secondary data needed to run and validate the PESERA model were collected. They are described as follows:

4.3.4.1. Climatic data collection

The required data of climate factors are based on daily time series data of rainfall, temperature and potential evapo-transpiration (ETo). Climate data related to rainfall, temperature and relative humidity of five meteorological stations which are situated in and nearby the study area of year 2007 were obtained from Meteorological Department of Thailand.

4.3.4.2. Soil data collection

Soil data is needed to prepare soil factor related parameter maps for the model. Soil samples were collected randomly representing different landscape and landform units and also representing each land use/land cover types. In order to make sampling design for soil data collection, previous year landform map (Souksakoun, 2008) was used. The landform map and soil sampling design map are presented in figure 4-3 and 4-4 respectively. For running the model previous year's soil data were also used.

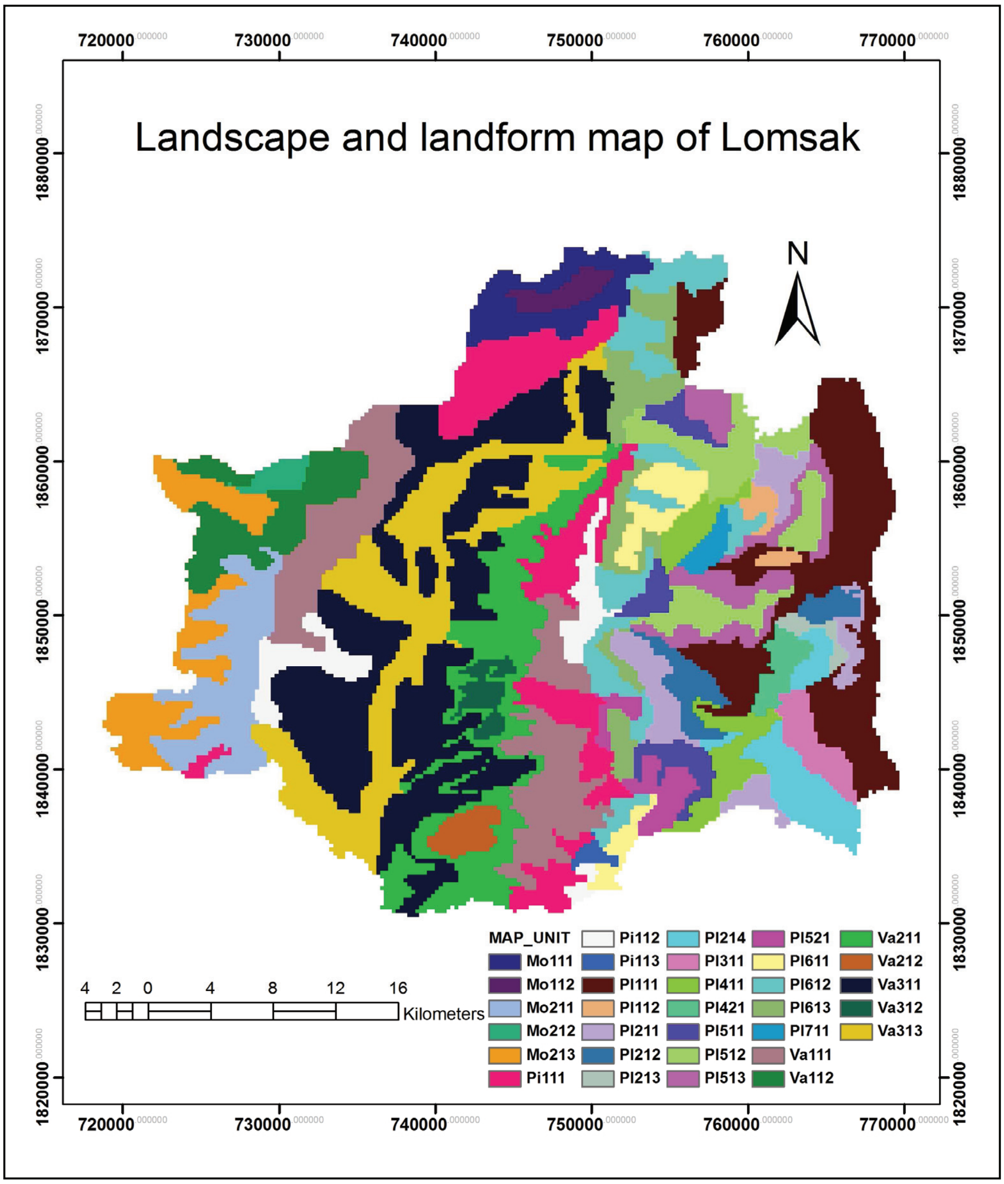

Figure 4-3: Landscape and landform map of study area

Table 4-3: Legend of landscape and landform map in detail

Landscape	Relief	Landform	Map unit
Mountain	hill	Foot slope	MO111
		summit	MO112
	ridge	summit	MO213
Piedmont	fan	apical distal complex	PL111
		apical	PL112
		distal	PL113
Plateau	mesa	undulating	PL111
		rolling	PL112
	hill	summit/shoulder complex	PL211
		shoulder complex	PL212
		back slope	PL213
		summit	Pl214
	incision	side	Pl311
	vale	side bottom	Pl411
		side	PL421
	swale	sidebottom complex	PL511
		bottom	PL512
		side	PL513
		sidebottom	PL521
	escarpment	shoulder	PL611
		talus	PL612
		escarp	PL613
	ridge	summit	PL711
Valley	glacis	level	Va111
		undulating	Va112
	flood plain	tread risen complex	Va211
	terrace	tread	Va212
	flood plain	overflow mantle	Va311
		basin	Va312
		levee	Va313

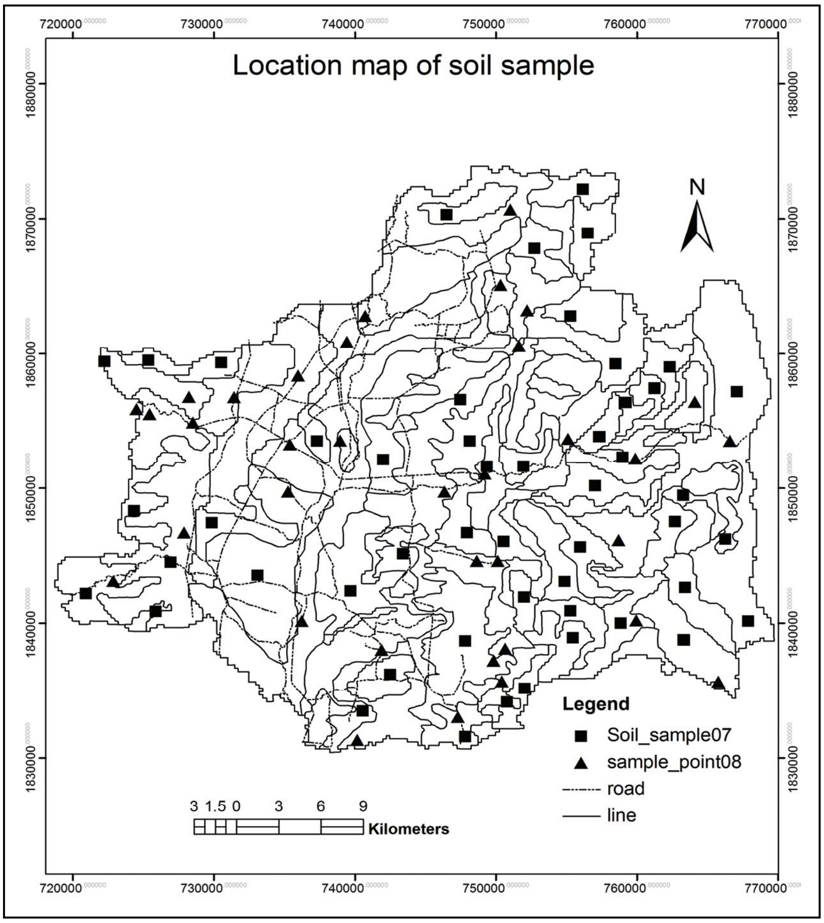

Figure 4-4: Map of soil sample location

4.3.4.3. Data collection for image classification and validation

Training samples were collected for land use/ land cover classification of ASTER image. Separate data set was used for validation of the classification. These data were taken from representing all possible land use/land cover types of the study area (Table 4-4).

Table 4-4: Field data collected for image classification and validation

Land use/land cover	No. of sample collections	
	For image classification	For validation
Paddy	35	19
Mixed agriculture	50	29
Bare land	12	9
Orchard	30	36
Grass land	31	29
Degraded forest	32	52
Dense forest	36	35
Water body	12	8
Urban and residential	34	37

4.3.4.4. Crop calendar data collection

Data like crop types, cropping sequence and patterns were collected from Agriculture Department of Thailand and verified it through discussion with local farmers.

4.3.4.5. Run off and sediment data collection

PESERA model doesn't give the cumulative runoff and sediment of the area. However, it gives an amount of run off and erosion generated on a cell by cell basis (Kirkby et al., 2003). Since there was no erosion plot in the study area, runoff and sediment discharge were measured at the outlet of Namchun River to compare with the accumulated modelled runoff and soil loss from that catchments for field validation. Run off discharge were measured by cross sectional area*velocity method. To measure the cross sectional area of the stream, the stream cross section was divided into different sections and depth of stream at each section was measured. The cross section area of each section was calculated considering each section as trapezoid and the total cross section area of the stream section was calculated by adding cross section area of all sections (Figure 4-5). The run off velocity was measured by using current meter at different sections and average velocity was calculated.

To measure the sediment discharge, sample of 600ml volume of runoff water was collected and sediments were separated by using decantation method. The decanted sediment was air dried, weighted and finally sediment load (grams/litre) was calculated. Total sediment discharge from the catchment outlet was calculated by multiplying sediment load per unit volume of runoff with total run off discharge. Measurement was taken in three days for this study.

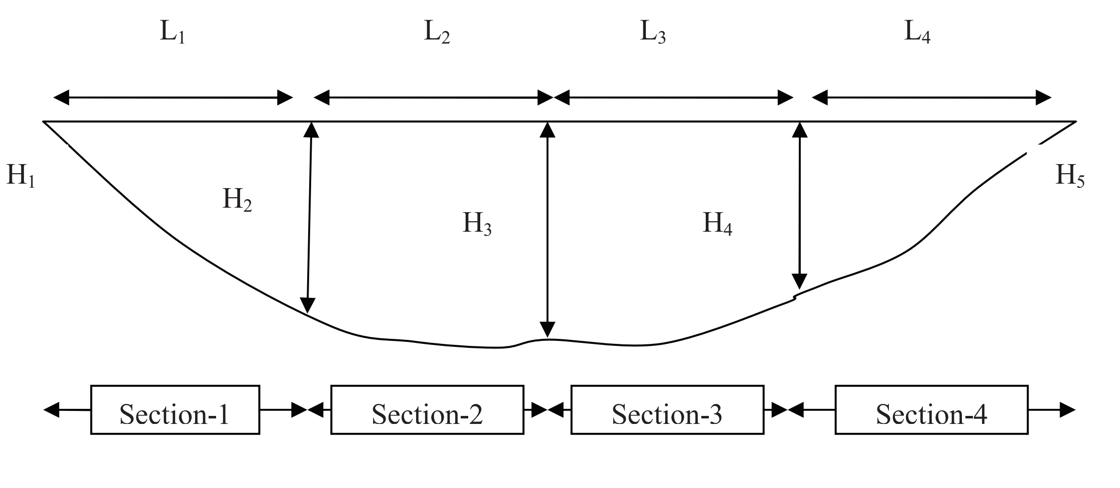

Area of section-1(A_1) = $(H_1+H_2)/2*L_1$
Area of section-2(A_2) = $(H_2+H_3)/2*L_2$
Area of section-3(A_3) = $(H_3+H_4)/2*L_3$
Area of section-4(A_4) = $(H_4+H_5)/2*L_4$
Cross sectional area of stream (A) = $A_1 + A_2 + A_3 + A_4$

Figure 4-5: Calculation of cross sectional area of the stream channel (hypothetical section)

5. Data processing

In this stage data collected from the field were processed and input parameter maps were generated to run the erosion model as per the requirement to fulfil the objectives. The over all methodological procedures are presented in the figure 5-1.

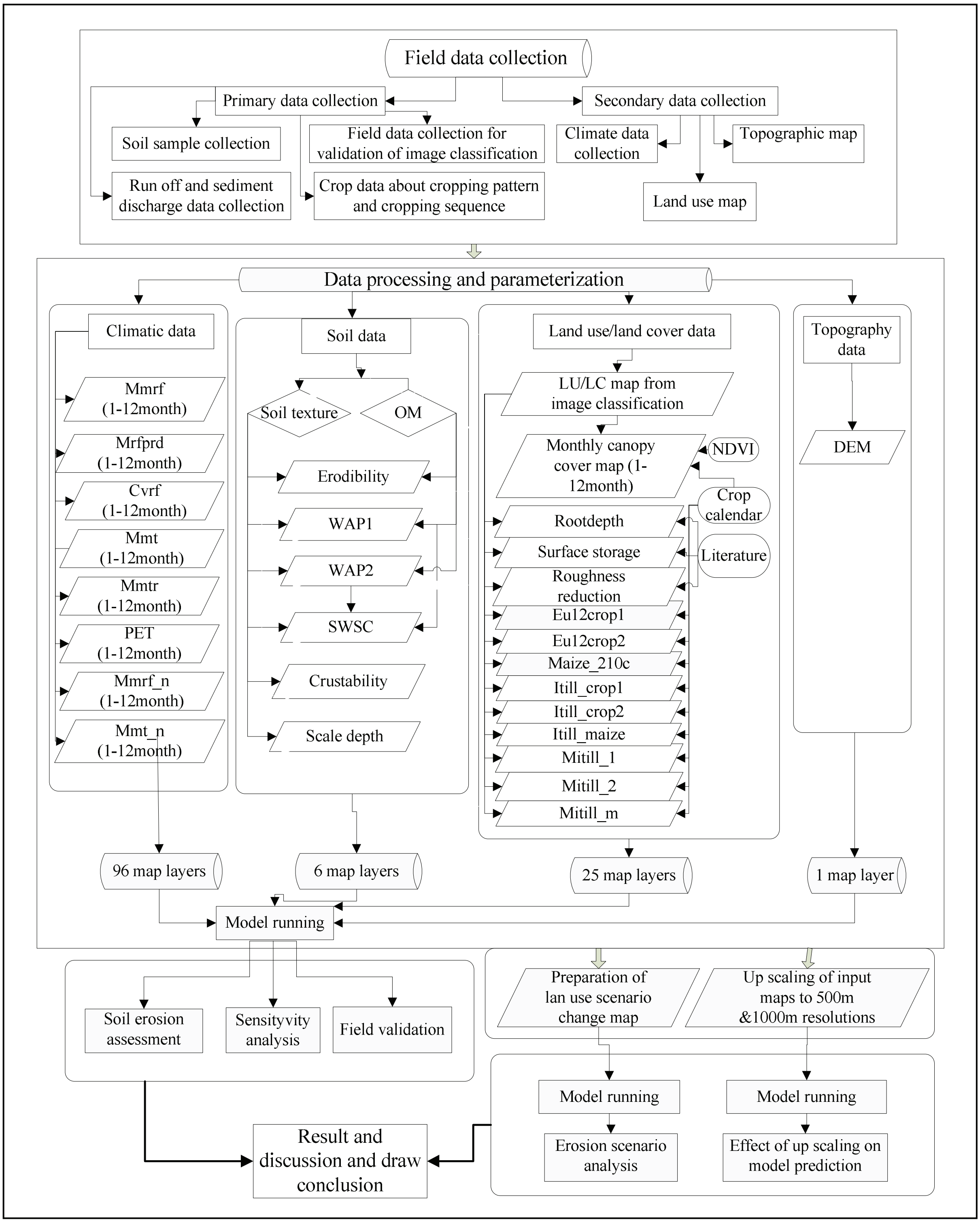

Figure 5-1: Flowchart of overall methodology

5.1. Parameterization of data to run the model

This involves the preparation of input parameters required to run the model. PESERA model requires 128 data layers related to climate, soil, land cover and topography (Table 5-1).

Table 5-1: Input data layers for PESERA model

Model parameter	Unit	Description/Source	Remarks
meanrf1301-13012	mm	Mean monthly rainfall	Climate data (96 layers)
meanrf21-212	mm	Mean monthly rainfall per rain day	
cvrf21-212	-	Coefficient of variation of monthly rainfall per rain day	
Mtmean1-12	°C	Mean monthly temperature	
Mtrange1-12	°C	Monthly temperature range (max-min)	
Meanpet301-3012	mm	Mean monthly PET	
newrf1301-13012	mm	Predicted future rainfall	
newtemp1-12	°C	Predicted future temperature	
Use	-	Land cover type	Land cover data (25 layers)
cov_jan-cov_dec	%	Ground cover	
eu12crop1		Dominant arable crop	
eu12crop2		2nd Dominant arable crop	
maize_210c		Maize crop	
itill_crop1	-	Planting month: dominant arable crop	
itill_crop2	-	Planting month: 2nd dominant arable crop	
itill_maize	-	Planting month: maize	
mitill_1	-	Planting marker: dominant arable crop	
mitill_2	-	Planting marker: 2nd dominant arable crop	
mitill_m	-	Planting marker: maize	
rough0	mm	Initial surface storage	
rough_red	%	Surface rough reduction per month	
rootdepth	mm	Root depth	
crust_0702	mm	Crust storage	Soil data (6 layers)
erod_0702	mm	Sensitivity to erosion	
swsc_eff_2	mm	Effective soil water storage capacity	
p1xswap1	mm	Soil water available to plant at 0-30cm depth	
p2xswap2	mm	Soil water available to plant at 0-100cm depth	
Zm	mm	Scale depth	
std_eudem2	m	Digital elevation model	Topography data

(Source: PESERA users' manual)

All together 96 data layers for climatic factor, 25 data layers for land cover factor, 6 data layers for soil factor and 1 data layer for topography were prepared in 250m resolution as mentioned below.

5.1.1. Climate data

The climatic characteristics required for preparing 96 layers of input map for PESERA model are rainfall, temperature and potential evapo-transpiration. The mean monthly rainfall, mean rainfall per rain day and coefficient of variance of rainfall, mean monthly temperature, monthly temperature range and potential evapo-transpiration were calculated from climatic data of five meteorological stations collected from the meteorological Department of Thailand by using equations mentioned in section 4.3.1.3 in chapter 4.

Using only five stations data, it's not possible to predict climatic variables by interpolation. Beside this, rainfall and temperature can vary according to the altitude in mountainous area. According to (Kuraji et al., 2000), there is an altitudinal variation in rainfall in northern Thailand but with varying degrees depending on season and spatial extent of the rainfall. Therefore, relationship of annual rainfall and monthly rainfall with altitude was calculated separately from linear regression analysis before interpolating the climatic data. The R^2 value for annual rainfall is 0.89 and for the months of June, July and August are 0.93, 0.81 and 0.53 respectively. Most of the months particularly in monsoon seasons have R^2 value more than 0.5 which indicates that there is positive relationship between rainfall and altitude in the study area. Therefore, in order to prepare the climate parameter maps, two meteorological stations, Khaokhor having highest altitude (715m) and Lomsak with lowest altitude (140m) located inside the study area were taken as two reference stations and average altitude between these two stations were calculated. The area having altitude higher than the average altitude was assigned the climatic parameter value from Khaokhor station and the area having lower than the average altitude was assigned the climatic parameter value from Lomsak station. Then climatic parameter maps were interpolated from these values on the basis of altitude from DEM map.

5.1.2. Soil data

In total 38 soil samples collected from the field were taken to ITC soil testing laboratory for particle size and soil organic matter content analysis. For particle size analysis Pipette method was carried out (Figure 5-2) based on the procedure for soil analysis as mentioned in International Soil Reference and Information Center (ISRIC) and FAO (L.P.van Reeuwijk, 2002) . For quality control of the analysis a random duplicate sample was also prepared in each batch. In this study, fractional size of soil particle was defined as: clay (<2μm), silt (2-50μm) and sand (50-2000μm) on the basis of USDA soil textural classification system. The organic matter analysis was carried out by following the Ignition method as mentioned in Soil Science Analysis (Baize, 1993).

In order to see the basic features of location, dispersion and moments of soil variables descriptive statistical analysis was done. Minimum, maximum, mean, coefficient of variance, standard deviation, skewness and kurtosis coefficient for measured variables were calculated. The skewness and kurtosis coefficients are used to describe the shape of the data distribution. Skewness provides the idea about how symmetrically data set are distributed where as the kurtosis provides an idea about how data set ate peaked or flat in relation to normal distribution (Spiegel and Stephens, 1999). The correlation between and among the soil properties were analyzed by using correlation coefficient matrix; this approach provides the idea to measure degree of relationship between the variables.

To test the bias in samples between two data sets i.e. data collected in 2007 and data collected in 2008, bias or mean error of soil parameter was calculated. For this test, soil erodibility parameter was selected. Two separate erodibility maps from two data sets were prepared by using spline interpolation technique. Seventy random points were selected in the same location from both maps and their erodibility values were extracted from respective maps. The value extracted from 2007 map was taken as observed value and value extracted from 2008 map was taken as estimated value. Then, mean error was calculated as mentioned below;

$$\text{Mean error (ME)} = 1/n\Sigma\,(Y_i - Y_i') \qquad (5.1)$$

Where,
Y_i is observed erodibility,
Y_i' is estimated erodibility value and
N is number of samples.

Figure 5-2: Particle size analysis by pipette method at ITC soil laboratory

PESERA model requires six soil parameters. These parameters are erodibility, crustability, effective soil water storage capacity, soil water available to plants at depth of 0 to 300 mm and 300mm to 1000 mm and scale depth. These parameters value were calculated by using equations as mentioned in section 4.3.1.3 in chapter 4. Before calculating soil water available to plant, the value of field capacity and permanent wilting point were derived by using the Soil-Plant-Atmosphere-Water (SPAW) model developed by Saxton (Saxton, 2005), where measured value of % sand, % clay and %organic matter were fed to the model to derive FC and PWP.

The soil parameter maps were generated from ordinary kriging interpolation method by using geo-statistical function on ArcGIS version 9.3 program. Before interpolation, the fitted variogram model, values of partial sill, nugget and range were derived from R-program, the model parameters are given in table 5-2. According to the table, the nugget to sill ratio for all the parameters is less than 75% which means there is good spatial dependency.

Table 5-2: Semivariogram parameters of soil properties

Soil properties	Sill	Range	Nugget	Nugget to sill (%)	Best fitted model
WAP1	185	2400	10	5.41	circular
WAP2	300	2700	100	33.33	circular
SWSC	900	6000	300	33.33	exponential
Erodibility	0.000052	2000	0.00003	57.69	circular
Scale depth	13	2000	5	38.46	circular
Soil crusting	0.25	15000	0.15	60.00	linear

Note: WAP1: water available to plant at depth of 0-30cm, WAP2: water available to plant at depth of 30-100cm, and SWSC: soil water storage capacity.

The best fitted variogram models for the interpolation of the parameters are circular, exponential and linear (Table 5-2). The variogram model for soil water storage capacity and erodability are presented in figure 5-3 and 5-4 respectively. Likewise, the interpolated map of soil water storage capacity (SWSC) is presented in figure 5-5.

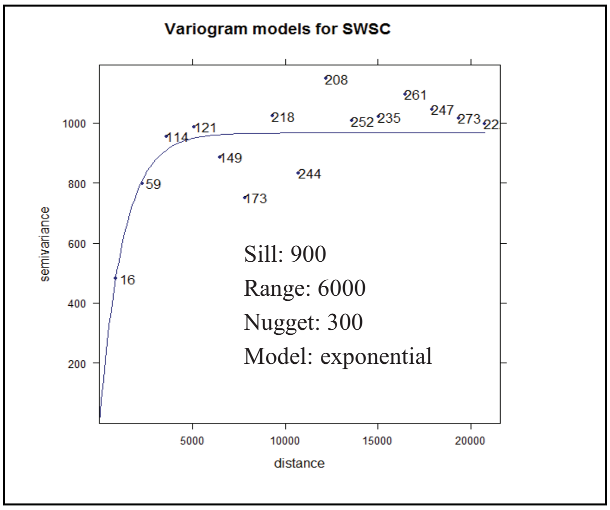

Figure 5-3: Variogram model for SWSC

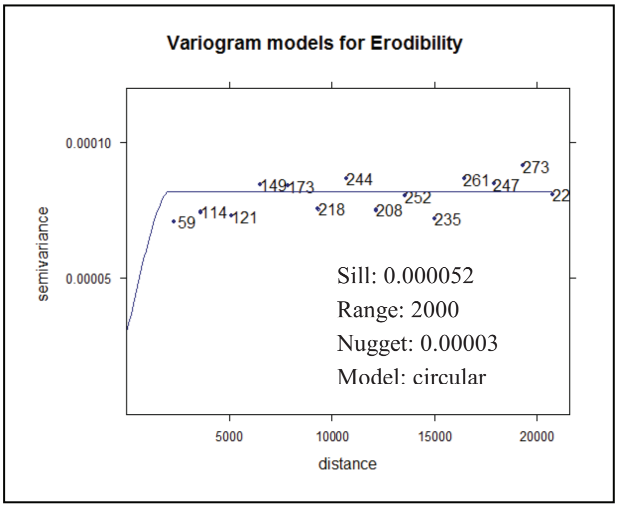

Figure 5-4: Variogram model for erodibility

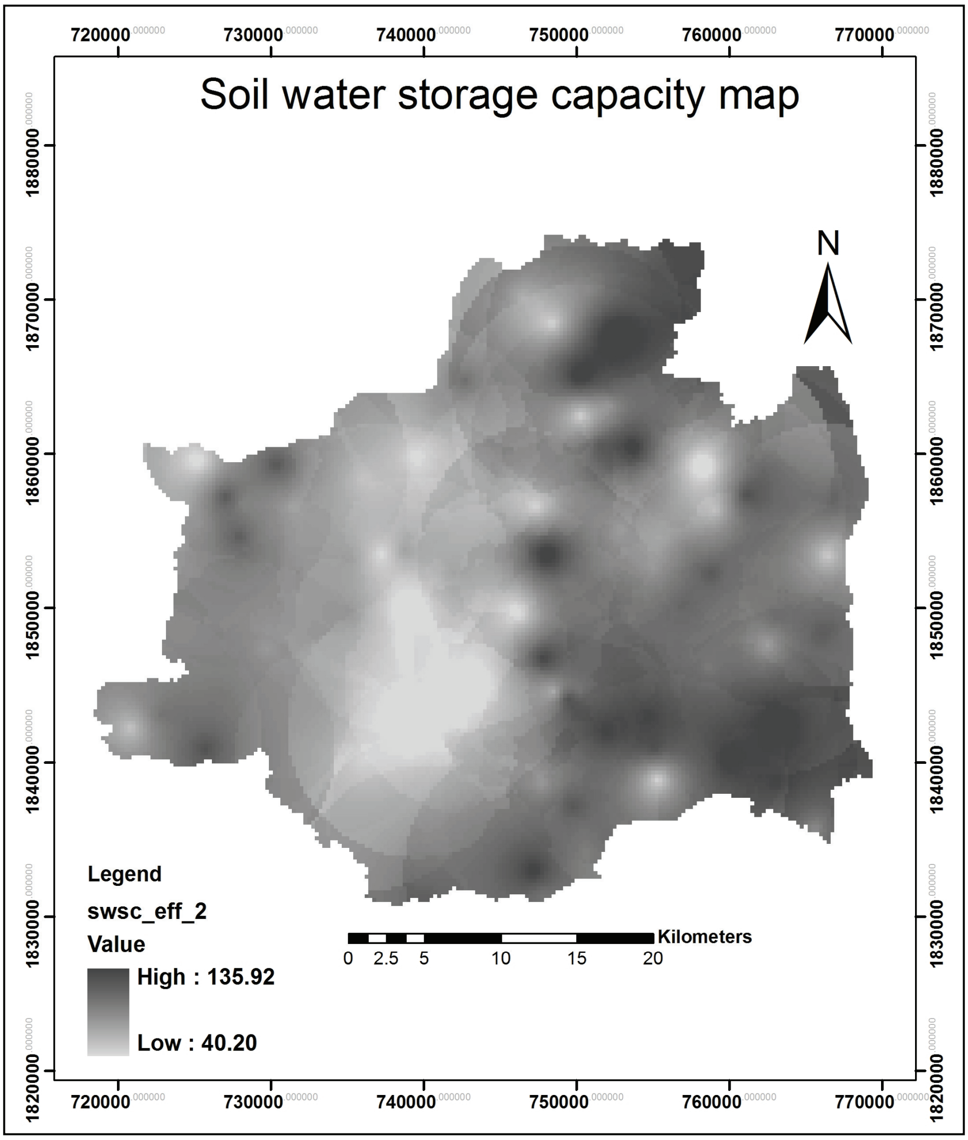

Figure 5-5: Soil water storage capacity (SWSC) map interpolated from Ordinary Kriging

5.1.3. Land cover data

In PESERA model altogether twenty five land use/land cover related data layers are needed. Out of them, the land use map is the basic and the most important. This map was prepared by classifying an Aster image of Feb. 4, 2006. Supervised classification with maximum likelihood algorithm was used. The image was classified in to 9 different classes; paddy, mixed agriculture, bare land, orchard, grass land, degraded forest, urban/residential area, water body and dense forest by using training sample point data taken from the study area. The accuracy of the classification result was validated through accuracy assessment by using separate set of ground truth data. As PESERA model requires detail agricultural cover types, the classified map was converted to polygon map and the agricultural areas were further classified into rice, maize and mixed agriculture through digitization on the basis of land use map of 2007 of the area. The feature space of image classification is presented in figure 5-6.

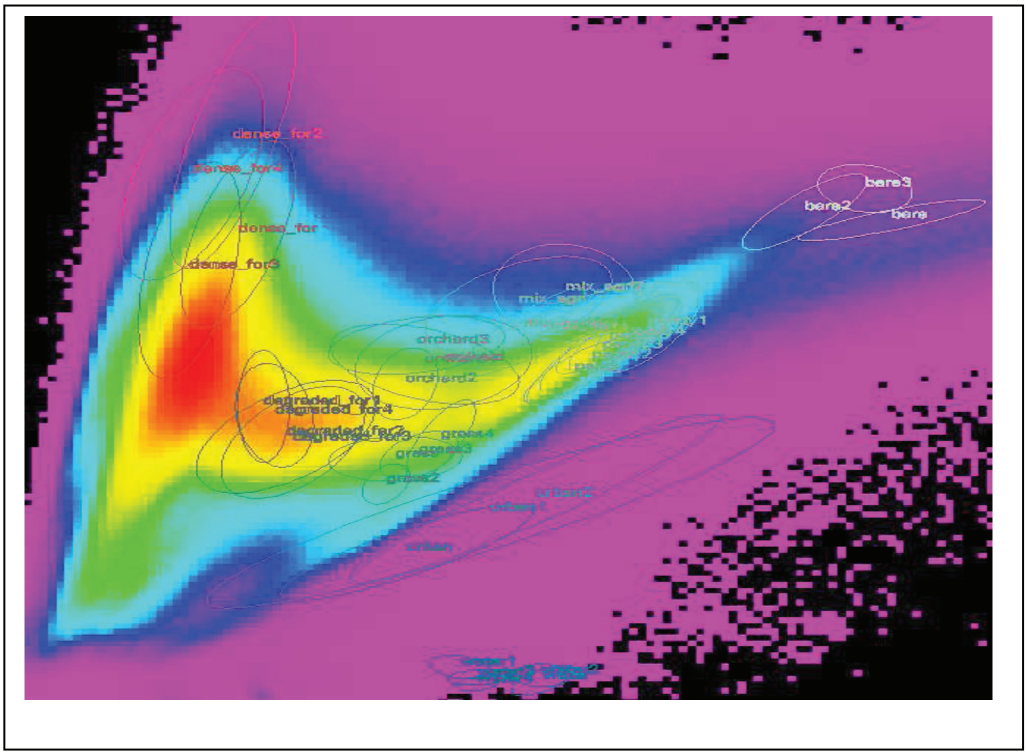

Figure 5-6: Feature space plots of image classification

Since the PESERA model read the land use map on the basis of fixed code the land use/cover types reflected in the land use map were given the code referring according to the Users manual (Irvine and Kosmas, 2003). The land use code value is presented in table 5-3.

Table 5-3: Land use/land cover codes for PESERA model

Code	Land use/cover class
100	urban and residential
210	maize
222	orchard
231	grass land
240	mixed agriculture
310	dense forest
330	bare land
334	degraded forest
400	paddy

The model also requires monthly canopy cover maps to produce monthly erosion rate, which is especially important for agricultural crops as canopy cover vary according to growing stages. To produce monthly canopy cover a crop calendar of study area (Table5-4) showing planting, growing and harvesting month of major agricultural crops was used. The crop calendar was obtained from Land Development Department, Thailand and verified with the local farmers during field work. The canopy cover percentage for different growing stages of different crops were derived by using the Users manual (Irvine and Kosmas, 2003). It is shown in table 5-5. However, the life span of crops in the study area is shorter than in Europe. For example, maize crop in the study area can be harvested after four months while in Europe it is five months. In such case canopy cover percent for planting and harvesting month was assigned as it is by referring from the PESERA users' manual where as for second month average value of second and third month and for third month average value of third and fourth month was assigned.

Table 5-4: Crop calendar of different agricultural crops of the study area

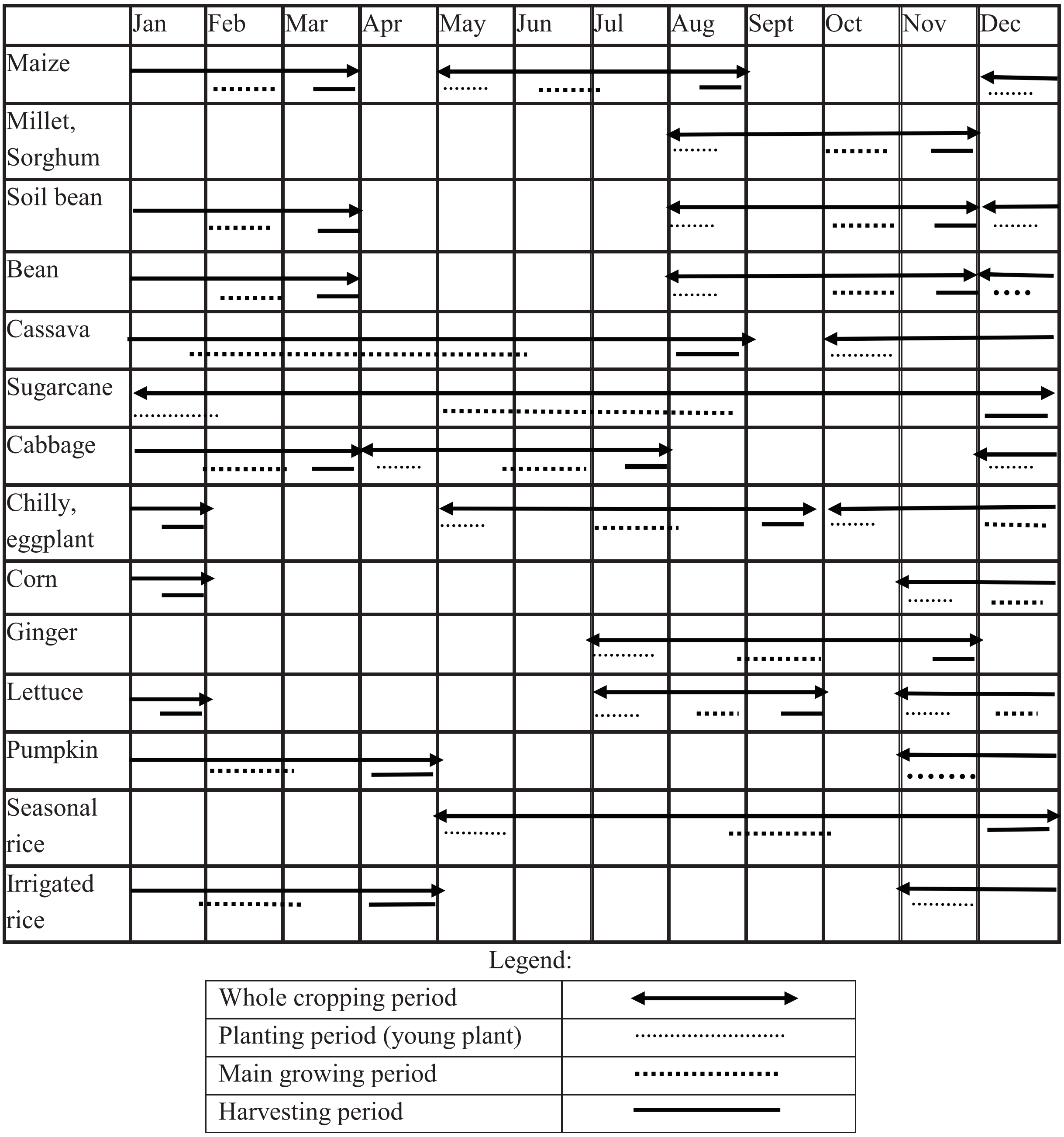

(Source: Land development Department, Thailand.)

Table 5-5: Monthly canopy cover percent for different land use/land cover types

Land use	Code	Jan	Feb	Mar	Apr	May	Jun	Jul	Aug	Sep	Oct	Nov	Dec
Maize	210	77	94	43	0	17	77	94	43	0	0	0	17
Paddy	400	18	81	94	45	8	27	47	78	98	86	59	32
Mixed agriculture	240	50	50	50	60	70	80	90	90	60	50	45	45
Bare land	330	0	0	0	0	0	0	0	0	0	0	0	0
Orchard	222	10	10	15	20	25	30	30	30	30	20	15	15
Grass land	231	100	100	100	100	100	100	100	100	100	100	100	100
Degraded forest	334	30	30	30	30	30	30	30	30	30	30	30	30
Dense forest	310	100	100	100	100	100	100	100	100	100	100	100	100
Urban / residential	100	100	100	100	100	100	100	100	100	100	100	100	100

NDVI map was also used to prepare monthly canopy cover map to compare with the canopy cover map prepared from crop calendar method and to compare the respective model prediction. The methodology was followed as mentioned in section 4.3.1.3 in chapter 4. The monthly canopy cover map prepared from crop calendar and NDVI are presented in figure 5-7 and 5-8 respectively.

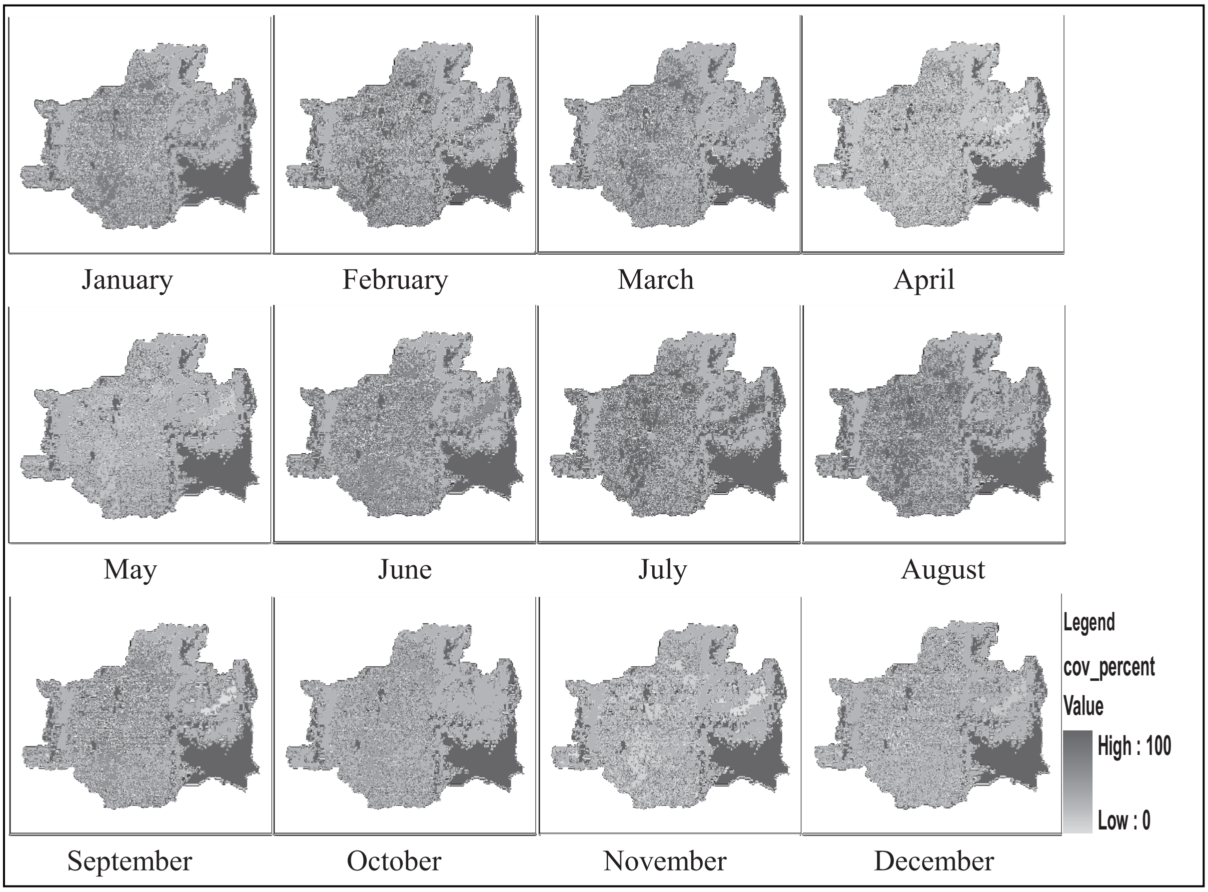

Figure 5-7: Monthly canopy cover map generated from crop calendar

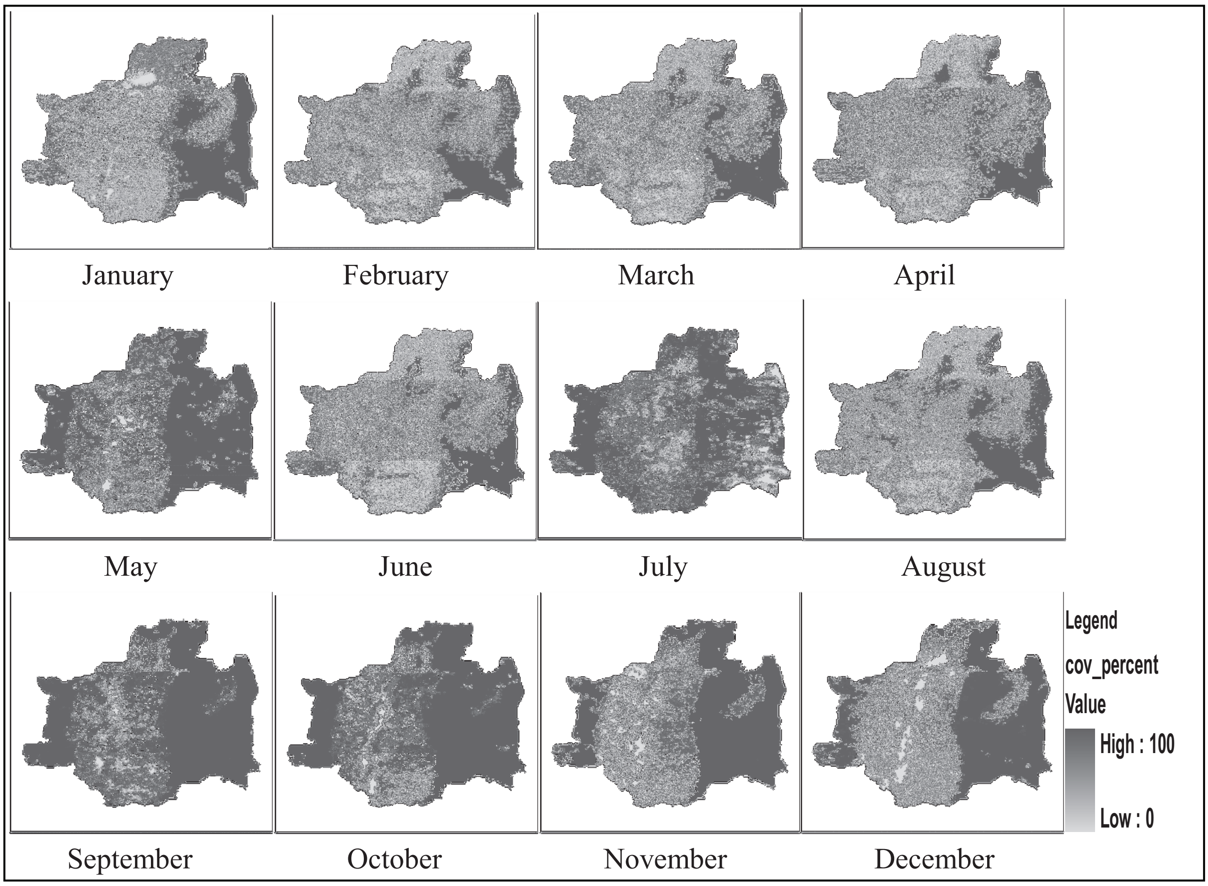

Figure 5-8: Monthly canopy cover map generated from NDVI

As PESERA model requires the first and second dominant crops, paddy and maize were taken as first and second dominant arable crops respectively in this study. In the study area, there were two types paddy cultivation; seasonal and irrigated. Out of these two, the seasonal is more extensively grown and thereby taken as dominant crop. Another one was put in to the mixed agriculture category. The values for the PESERA layer maps of root depth (rootdepth), initial roughness storage (rough0) and surface roughness reduction (rough_red) were derived from the PESERA Users' manual (Irvine and Kosmas, 2003) and the values for tillage dates of agricultural crops (itill_crop1), (itill_maize) and (itill_crop2) were derived from crop calendar. Finally the layer maps were prepared by reclassifying land use map on the basis of these derived values.

5.1.4. Topographic data

The DEM as a topography input parameter map was generated from contour map of 20 meter interval (Figure 5-9).

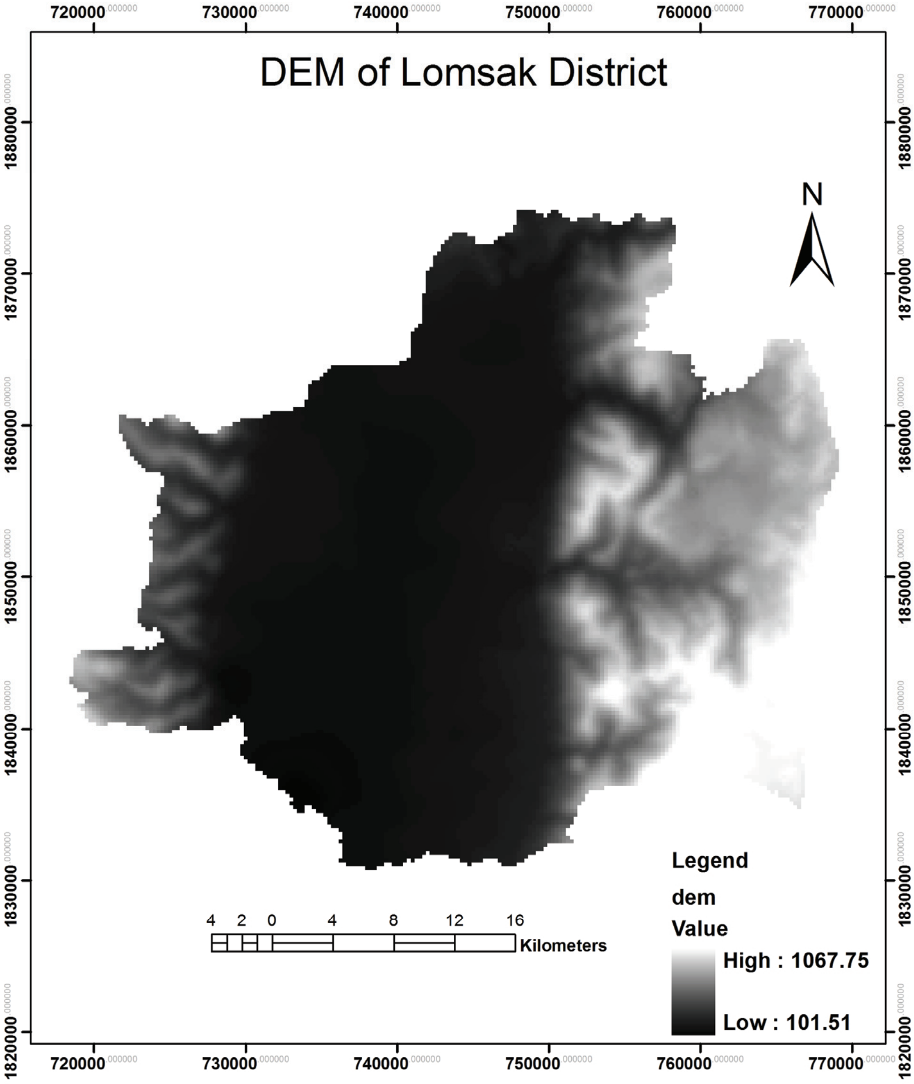

Figure 5-9: Digital Elevation Model (DEM) map interpolated from contour

5.2. Running model to estimate soil erosion potential

The PESERA grid model runs in ArcInfo workstation environment. The PESERA_GRID code has been developed primarily in Fortran90 with Arc Micro Language (AML0 modules, activated using ArcInfo Workstation, to extract data and convert back to Arc Grid format. ESRI ArcGIS software is used to extract data from “grid” to “ascii” and create output “grids”. All the 128 input data layers were generated in ArcGRID format with same projection and coordinates system (WGS1984_UTM47 N) and with the consistent of the description. The number of data layers and their file name are crucial to run the model, and, if any one of the data layers is missing or any file name is wrongly written the, the model does not run. The PESERA grid model is run through five stages (Table 5-6).

Table 5-6: Five stages of running PESERA grid model

S. No.	Stages	Model code
1	GRID to ascii	xgridascii103.aml
2	PREPROCESSING	ftn_input103.exe, ftn_combined_103.exe
3	MODEL EXECUTION	pesera_grid103.exe
4	POST-PROCESSING	to_grid_103.exe
5	ascii to GRID	xasciigrid103.aml

(Source: PESERA Users' manual.)

Before running the model two important tasks need to be done in ArcInfo Workstation/Grid as follows;
Create a work space using the command arc w d:\meteo_grids after the prompt GRID in ArcInfo Workstation and extracting all the input data layers in this folder and

Create a work space by typing arc w d:\temp_ascii after the prompt GRID and extract seven executable files of the PESERA grid model.

Stage 1: GRID to ascii (AML)

The AML file <xgridascii103.aml> was edited to extract localized area data. The study area was set to window as "/*setwindow 718395.68337 1830705.95247 769645.68337 1874455.95247/) northern Thailand". This file extracts the GRID data to ASCII.

Stage 2: GRID data input and pre-processing

GRID data is written to <ftn_input103.dat>. This file eliminates the repetition of data entry generated by executing <ftn_input103.exe>. The following information was required (Table 5-7);

Table 5-7: Variable data for ftn_input103.exe of the study area

Variable required	Description
175, 88 and 44 respectively for 250m, 500m and 1km resolution input maps.	Number of rows in the analysis window (Nrows)
205, 103 and 52 respectively for 250m, 500m and 1km resolution input maps.	Number of columns in the analysis window (Ncols)
250m, 500m and 1000m	Grid resolution (cell size)
718395.68337	Lower left x-coordinate (Xll)
1830705.95247	Lower left y-coordinate (Yll)
For, maize, eu12crop1 or eu12crop2 Enter "1"; "2"; or "3" respectively	Land use scenario
To operate future climate data enter '1' otherwise '0'.	Climate scenario

The grid data (nrows, ncols, cell size, xll and yll) values were derived from header files of the extracted ascii files.

After running <ftn_input103.exe>, the <ftn_combined_103.exe> was run. Programs run from 1 to 128, then 1 to (nrows*ncols).

Stage 3: PESERA_GRID

This is the main stage of running PESERA grid model. In this stage the program runs from 1 to (nrows*ncols).

Stage 4: POST-PROCESSING

In this stage program runs from 1 to nrows and then 1 to 12 months and reassign header and structure.

Stage 5: OUTPUT GRIDS

In this stage the output ASCII files are converted back to GRID format. In order to process this, the work space was set using the command w d:\temp_ascii after the promt Grid in ArcWorkstation and run the code <xasciigrid103.aml>.

Finally the model results were viewed in the ArcMap. The model provides the monthly and annual soil loss (ton/ha/year), runoff (mm) and water deficit (mm). The projection of these result maps was redefined. For this study the monthly and annual soil loss and runoff maps were taken in to account.

5.3. Sensitivity analysis

For sensitivity analysis, monthly rainfall and coefficient of variance of rainfall for the month of August were selected representing the climate parameter. Likewise, the cover percentage of August was selected as representation from land cover parameter. Soil erodibility and soil water storage capacity were also selected representing soil parameters. The parameter value was changed by decreasing and increasing with the rate of 10%, 20% and 30% while keeping other parameter value constant. However, as it is not possible to have canopy cover more than 100%, canopy cover value of cover parameter was changed only by decreasing the value in the same rate.

Soil erodibility is an important soil parameter effecting soil erosion which depends on soil particle size distribution, soil organic matter content soil structure and permeability. Soil particle size distribution is considered to be stable soil property where as soil organic matter is subjected to be change according to vegetation cover and changes in the land use practices. Soil organic matter also influences soil structure and permeability. Therefore the effect of organic matter content on soil erodibility was also calculated by changing organic matter percent by increasing and decreasing with the rate of 10%, 20% and 30%. For this calculation Wischmeier’s formula (eq 4.7) was used.

5.4. Field validation of the model

The model predictions are usually tested by comparing predicted values with measured values. According to (Kirkby et al., 2004), a pan–European calibration of erosion rates is not practicable when there is no acceptable measurements of erosion rates throughout the area and therefore the overall reliability of the model is based on calibration.

- Internal validation is based on a qualitative and quantitative assessment of the physical representation of processes in the model.
- Intermediate validation is based on comparison with spatial distributions that are forecast within the model as intermediate products.
- External calibration is based on comparison with erosion plot, small catchments and reservoir data.

In the study area erosion plot data is not available. Therefore, after running the model, the Namchun catchment boundary was delineated and the erosion and runoff generated from each pixel within the catchment was accumulated. This calculated value was then compared with the measured erosion and runoff value of this catchment.

5.5. Study of the effect of upscaling (grid cells) on erosion assessment

To see the up scale effect of land use/land cover on model prediction, the classified Aster image of 15m resolution was resampled to 250m, 500m and 1000m resolution (Figure 5-10). The nearest neighbour algorithm was used for resampling. Rest of the land use/land cover related input maps were prepared on the basis of these resampled maps following the same procedure as mentioned in section 5.1.3 of chapter 5. Finally the model was run by using upscaled input maps by following the procedure as mentioned in section 5.2 of chapter 5.

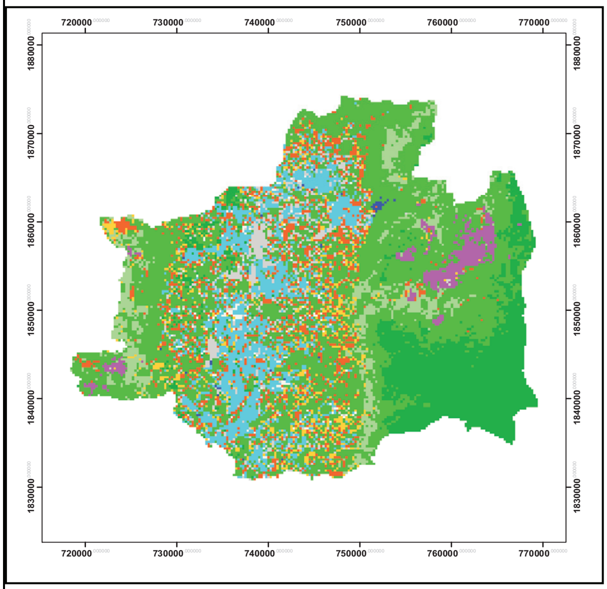

Land use/cover map of 250m resolution

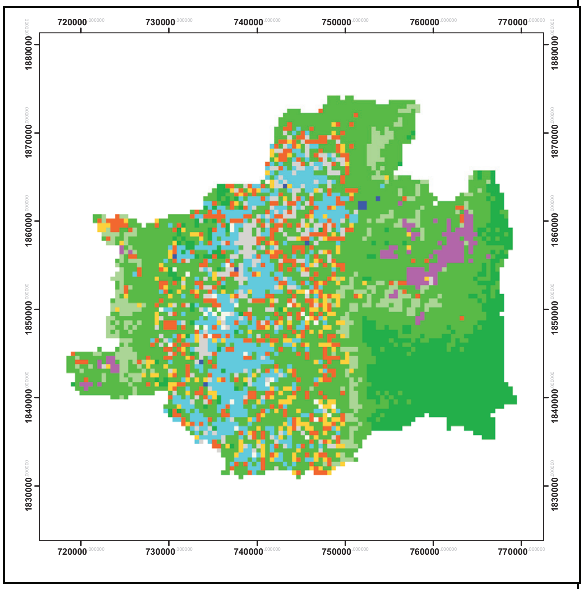

Land use/cover map of 500m resolution

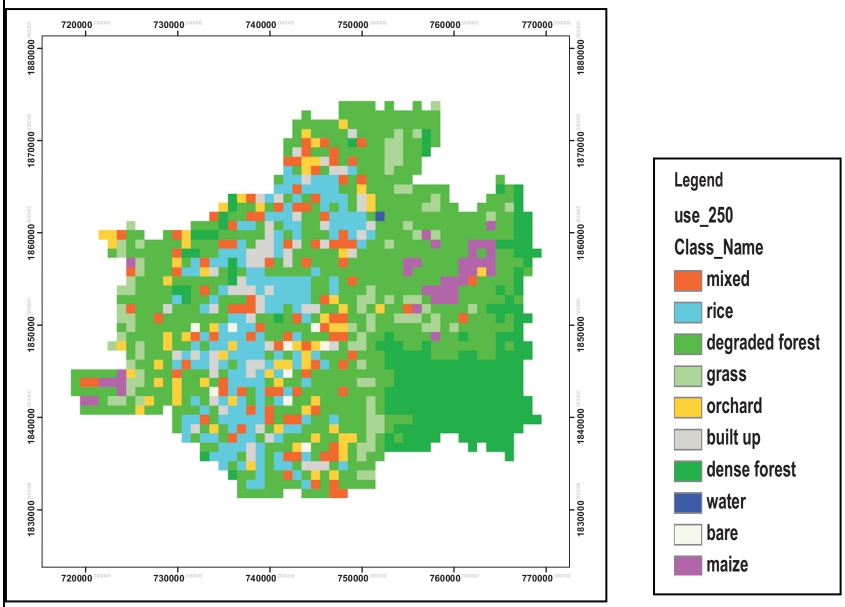

Land use/cover map of 1000m resolution

Figure 5-10: Scaled up land use/land cover map

5.6. Erosion assessment in various land use scenarios

In order to study the effect of various land use change scenarios in the study area five different types of land use scenarios were deliberately created. They are; conversion of existing degraded forest into maize field (scenario-1), conversion of existing grass land into maize field (scenario-2), conversion of existing grass land into orchard (scenario-3), whole area converted to dense forest assuming reforestation works (scenario-4) and whole area converted to maize cultivation (scenario-5). The land use change scenario maps of scenario 1, 2 and 3 are presented in figure 5-11. Rest of the land use/land cover related input maps were prepared on the basis of this changed map following the same procedure as mentioned in section 5.1.3 of chapter 5. The model was run in 250m resolution input parameter maps by following the procedure as mentioned in section 5.2 of chapter 5.

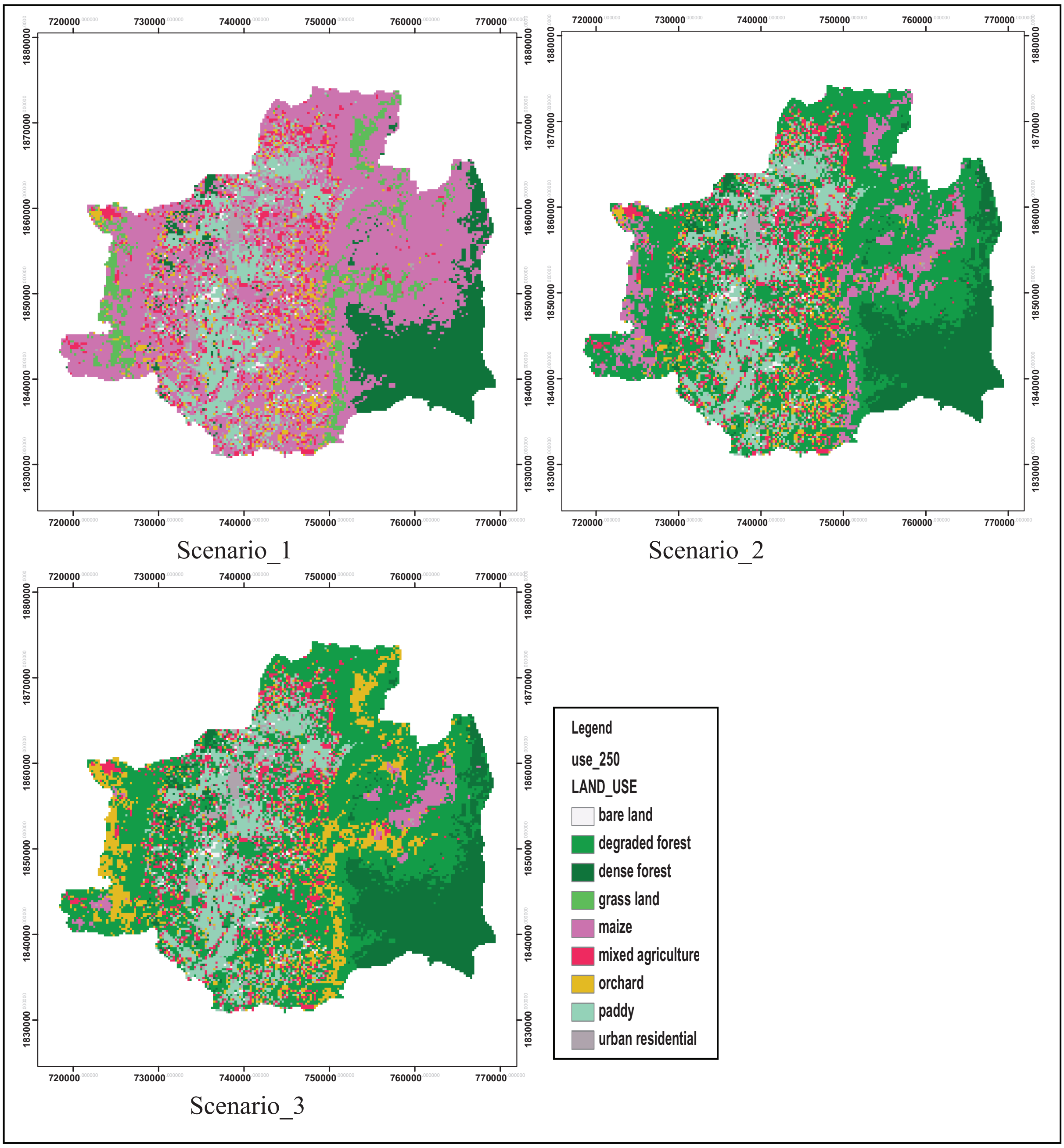

Figure 5-11: Land use change scenario maps

6. Result and discussion

6.1. Land use/land cover classification

The result of land use/land cover classification is shown in figure 6-1. The overall accuracy of the land use classification is 70.87% and the kappa statistics is 0.66 as shown in table 6-1. Accuracy report shows that there is highest accuracy in class dense forest with the value of 91.43%. The reason for this is that the dense forest is located separately in the south east part of the district and it is easy to differentiate the colour reflection of this class in the image. The lowest accuracy was found in built up areas because the built up area actually consists of mixture of different class types like building, road, bare land, grass, trees and water. Therefore there are variable reflection characteristics from built up areas in the image. The lesser accuracy was found in class rice and water body because the rice field is being filled with water and this makes similar reflection from water body and rice field.

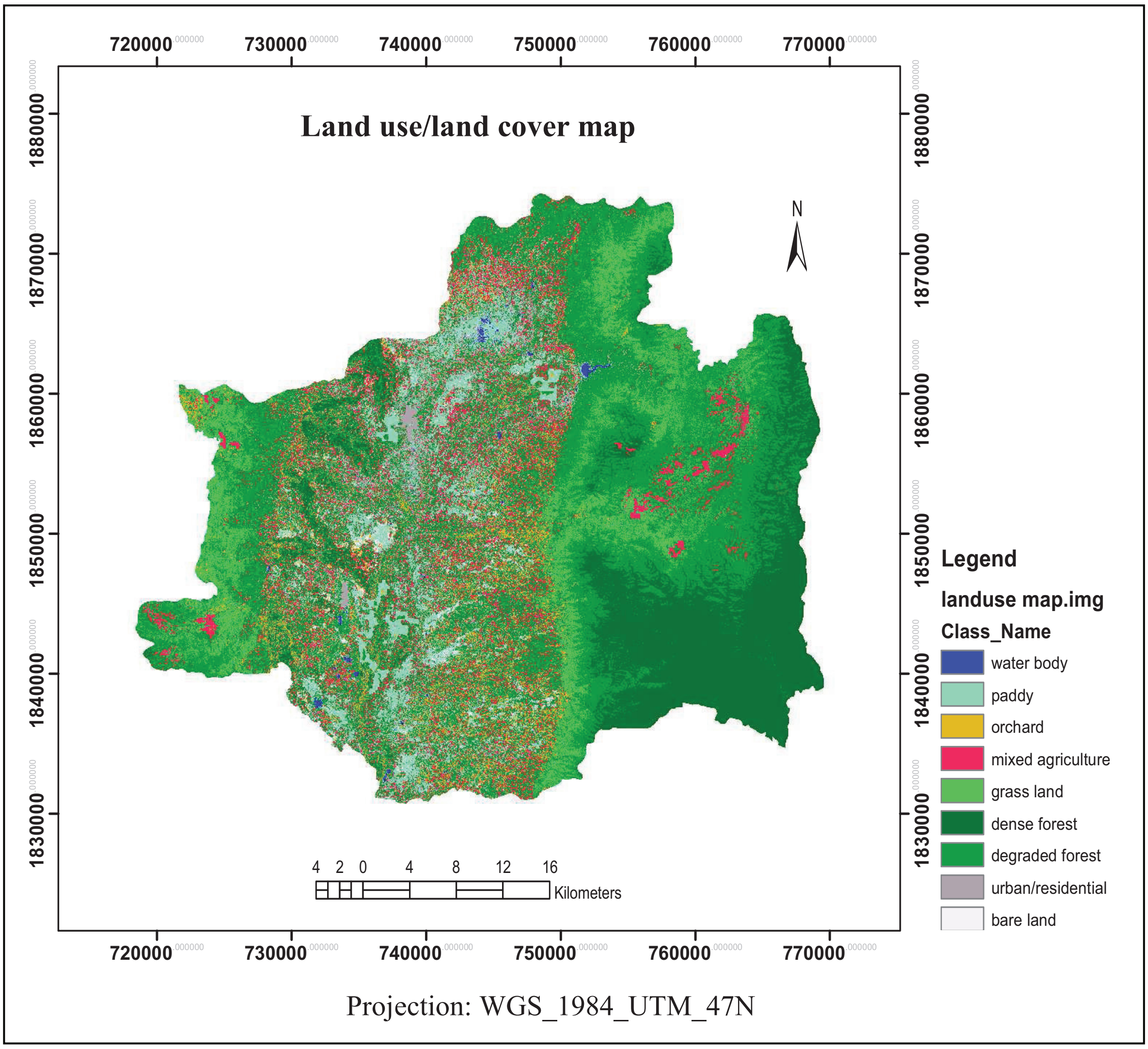

Figure 6-1: Classified land use/land cover map

Table 6-1: Classification accuracy assessment report

ACCURACY TOTALS

Class Name	Reference Totals	Classified Totals	Number Correct	Producers Accuracy	Users Accuracy
rice	19	25	15	78.95%	60.00%
mixed agricultu	29	37	25	86.21%	67.57%
bare	9	11	8	88.89%	72.73%
orchard	36	38	26	72.22%	68.42%
grass	29	24	18	62.07%	75.00%
degraded forest	52	43	34	65.38%	79.07%
dense forest	35	35	32	91.43%	91.43%
water body	8	6	4	50.00%	66.67%
built up	37	31	18	48.65%	58.06%
Totals	254	254	180		

Overall Classification Accuracy = 70.87%

KAPPA (K^) STATISTICS

Overall Kappa Statistics = 0.6652

Conditional Kappa for each Category.

Class Name	Kappa
rice	0.5677
mixed agriculture	0.6339
bare	0.7173
orchard	0.6321
grass	0.7178
degraded forest	0.7368
dense forest	0.9006
water body	0.6558
built up	0.5091

6.2. Effect of different land use practices on soil properties

As soil organic matter content reflects the effect of long-term land use practices and is an important indicator of soil quality and thereby used to calculate soil erodibility and water availability to plant for this study. In the study area the highest amount of organic matter was found in forest areas (Figure 6-2). Both the dense and degraded forest have the organic matter content more than 2% where as it has been decreased to 1.9% in orchard. The least percent of organic matter was found in paddy field with the value of 1.5%. Land use with grass, mixed agriculture and maize also show relatively lesser amount of organic matter content with the value of 1.48%, 1.53% and 1.57% respectively. This result is in the same line with the result of earlier studies.

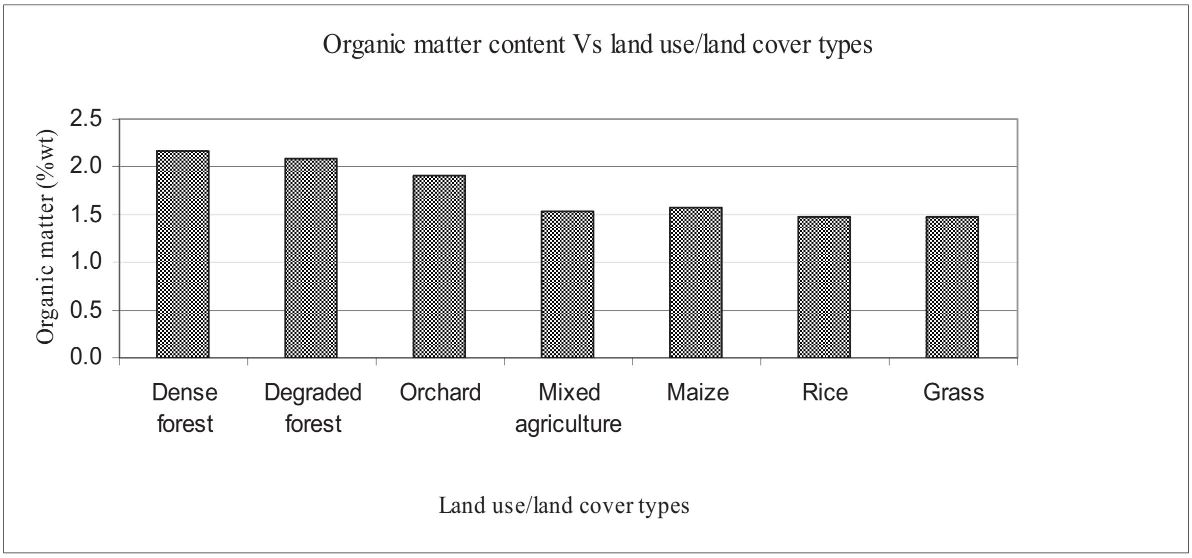

Figure 6-2: Organic matter content vs. land use/land cover types

The soil water storage capacity was found higher in forest and orchard land use classes. The reason for this is that, the forest and orchard trees have higher rooting depth than agricultural crops and there is more organic matter content in comparison to grass and agriculture as well. Like the soil water storage capacity, water available to plant at depth of both 0-30 cm and 30-100cm was found higher in case of forests and orchard. The water available to plant at depth of 30-100cm was found very less in grass and agriculture because of their shallow rooting depth.

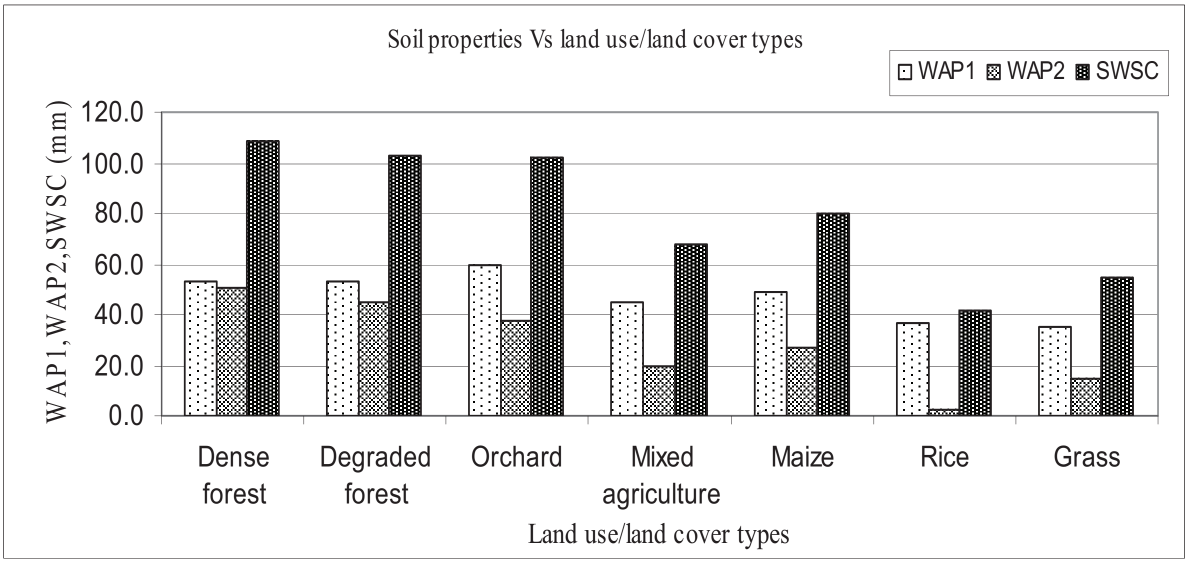

Figure 6-3: Soil properties vs. land use/land cover types

6.3. Comparison of canopy cover maps generated from crop calendar and NDVI

Comparison of canopy cover maps generated from crop calendar (Figure 5-7) and NDVI (Figure 5-8) shows that they are similar in dense forest class through out the year. The two maps show differences in agriculture area, grass land and in degraded forest areas. Moreover, there seems fixed boundary between the land use classes in canopy cover maps derived from crop calendar. This is because while preparing canopy cover map from crop calendar, fixed cover value were assigned for each land use class using the values given in PESERA user's manual. But in reality there is some variation of canopy cover within the same cover class. In contrast to this, as NDVI values are derived from remotely sensed images, the canopy cover maps derived from NDVI vary among different land use/land cover classes and for different seasons. Another reason is that the data sources regarding the crop types, there planting and harvesting dates may not be realistic, as the crop calendar obtained from the field is more generalized. In the study area there is no specific month for planting crops particularly maize, vegetables and other mixed crops which were clearly visible during field work and to depict this reality in crop calendar is quite difficult. Therefore the canopy cover maps prepared from NDVI method seems more realistic than the canopy cover maps prepared from crop calendar.

6.4. Analysis of rainfall and temperature variation against altitude

Analysis of the rainfall data of 2007 from 5 meteorological stations in and around the study area shows that there is variation of monthly rainfall among the five stations (Figure 6-4). The rainfall is concentrated during the period between April to October, while there is no rainfall in the months of January and December. In Khaokhor station, the highest monthly rainfall (239 mm) was received in June, whereas, in Lomsak the highest monthly rainfall (254 mm) was recorded in October. Similarly the highest amount of monthly rainfall is received in May in Phetchabun and in September in Wichanburi station. There is also seasonal and spatial variation in mean monthly rainfall per rain days and coefficient of variance of rainfall as there is variation in monthly rainfall and in number of rain days in a month. There is little but gradual change in mean monthly temperature through out the year in all the stations. The mean monthly temperature vary from 22.6 °C on January at Khaokhor station to 31°C on March at Wichanburi station. There is also small variation in potential evapotranspiration through out the year as there is small and gradual variation of monthly temperature.

Table 6-2: Annual and monthly rainfall (in mm) of five meteorological stations of study area

Stations	Jan	Feb	Mar	Apr	May	Jun	Jul	Aug	Sep	Oct	Nov	Dec	Annual
Wichanburi	0	16	18	214	187	50	69	114	334	134	2	0	1139
Phetchabun	0	38	20	109	233	89	69	212	194	214	1	0	1180
Lomsak	0	2	3	46	204	109	40	226	131	287	1	0	1050
lomkao	0	6	8	65	187	123	86	175	137	254	5	0	1047
Khaokhor	0	35	67	151	236	239	102	235	152	212	1	0	1429

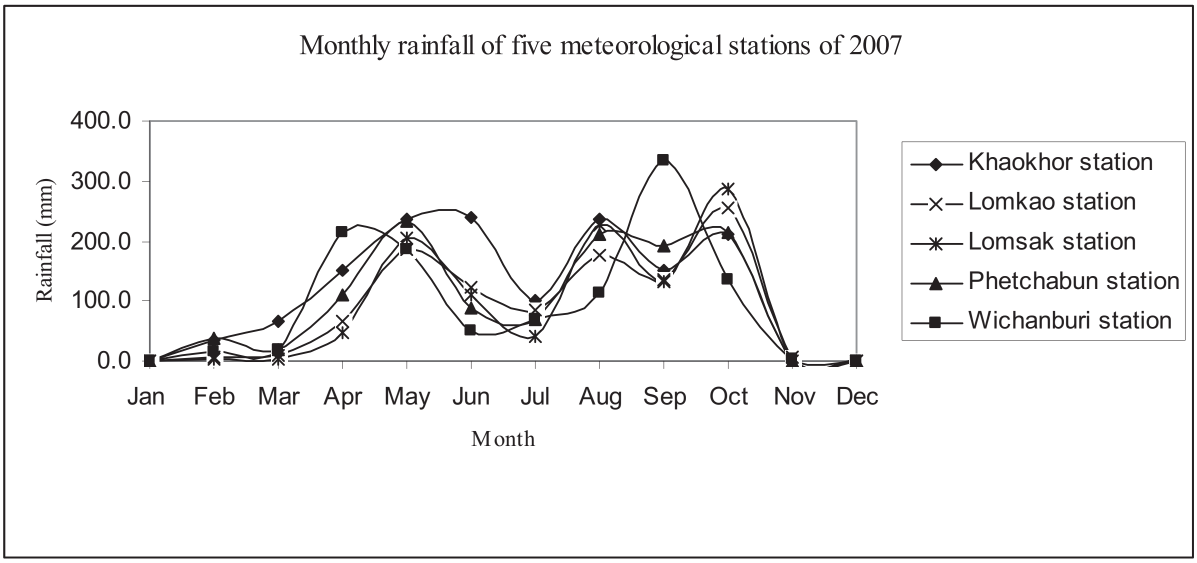

Figure 6-4: Monthly rainfall of five meteorological stations of 2007 in study area

The linear regression analysis of rainfall and altitude of five meteorological stations shows that there is linear relationship between rainfall and altitude. The R^2 value of annual rainfall and altitude is 0.88. Likewise among the relationships between mean monthly rainfall and altitude, particularly the months belonging to monsoon season have R^2 >0.5 (Figure 6-5). This result indicates that it is possible to predict the mean monthly rainfall value on the basis of altitude in the study area.

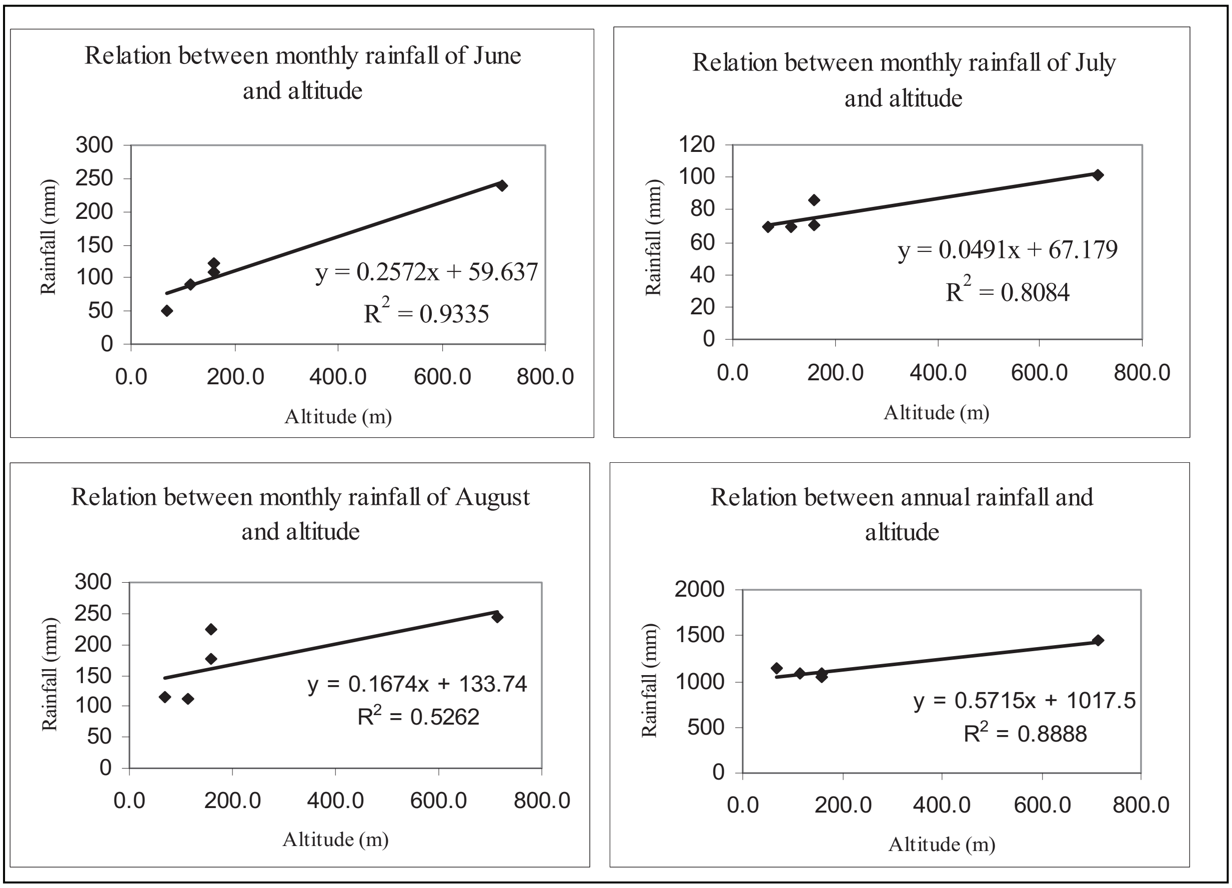

Figure 6-5: Relationship of annual and monthly rainfall with altitude

6.5. Statistical analysis of soil properties

The descriptive statistical analysis of soil properties (Table 6-3) shows that most of the soil properties have normal distribution. The skewness value for most of the properties except silt, clay and crusting are near to zero. As shown in the table, there is spatial variability of the soil properties because most of the soil physical properties have coefficient of variance >15%. The highest spatial variability is found in percent sand and water available to plant at depth of 30-100cm with coefficient of variance >50%. The least variability is found in surface crusting, silt and erodibility with the coefficient of variance < 20%.

Table 6-3: Descriptive statistical analysis of soil physical properties

Soil properties	Range	Min	Max	Mean	Std. Deviation	CV %	Skewness	Kurtosis
Sand (%)	55.76	0.80	56.56	20.09	10.70	53.28	0.58	0.53
Silt (%)	54.52	23.78	78.30	62.55	9.93	15.87	-1.22	1.92
Clay (%)	42.68	6.05	48.73	17.15	6.31	36.79	1.34	5.36
OM (%)	2.54	0.88	3.42	1.86	0.51	27.24	0.37	-0.18
WAP1 (mm)	80.20	15.20	95.40	51.03	13.57	26.60	0.29	1.40
WAP2 (mm)	83.70	0.00	83.70	35.46	19.72	55.62	-0.10	-0.38
SWSC (mm)	133.00	20.30	153.30	90.74	30.28	33.37	-0.19	-0.49
Erodibility (t.h.hr/ha. mj.mm)	0.04	0.03	0.07	0.05	0.01	16.13	0.39	0.23
S Depth	10.00	10.00	20.00	16.26	4.13	25.37	-0.50	-1.35
Crusting	2.81	1.45	4.26	4.17	0.44	10.51	-5.14	26.53
Valid N	103.00							

The correlation coefficient matrix (Table 6-4) shows that there is negative correlation of sand, clay and organic matter with soil erodibility and positive correlation of silt with soil erodibility. This is because the large particle has more resistant to transport and small particle has more resistant to detach due to their higher cohesiveness (Morgan, 1995). Moreover, organic matter improves the soil aggregate stability and thereby reduces the erodibility of the soil. Silt and organic matter have positive correlation with water available to plant and soil water storage capacity where as clay and sand have negative correlation with these soil properties. This is because the water-holding capacity of soil is controlled primarily by soil texture and organic matter. Soil with a higher percentage of silt and organic matter has a higher water-holding capacity because soil with finer particles has large surface area and organic matter percentage improves soil's water-holding capacity. Unlike sand, the silt, clay and organic matter have negative correlation with scale depth and surface crusting. As clay and organic matter content provides the greater strength to the soil, it reduces the soil crustability (Morgan, 1995).

The bias study of the erodibility parameter between two data sets shows that the calculated mean error value is 0.0006, which is near to zero meaning the bias between two data sets is very less.

Table 6-4: Correlation coefficient matrix of soil physical properties

		sand	silt	clay	OM	WAP1	WAP2	SWSC	Erodibility	S D	Crusting
sand	Pearson Correlation	1.00	-.79	-.41	-.022	.12	-.16	-.06	-.15	.22	.09
silt	Pearson Correlation	-.79	1.00	-.19	.10	.10	.20	.18	.27	-.20	-.09
clay	Pearson Correlation	-.41	-.19	1.00	-.19	-.40	-.07	-.22	-.08	-.06	-.02
om	Pearson Correlation	-.02	.10	-.19	1.00	.41	.38	.44	-.24	-.02	-.03
WAP1	Pearson Correlation	.12	.10	-.40	.41	1.00	.60	.83	-.18	-.11	.05
WAP2	Pearson Correlation	-.16	.20	-.07	.38	.57	1.00	.93	-.25	-.21	-.04
SWSC	Pearson Correlation	-.06	.18	-.22	.44	.83	.93	1.00	-.24	-.19	-.01
Erodibility	Pearson Correlation	-.15	.27*	-.08	-.26	-.18	-.25	-.24	1.00	.34	.05
S Depth	Pearson Correlation	.22	-.20	-.06	-.02	-.12	-.21	-.19	.34	1.00	.00
Crusting	Pearson Correlation	.09	-.09	-.02	-.03	.05	-.04	-.01	.05	.00	1.00

Note: OM: organic matter, WAP1: water available to plant at depth of 0-30 cm, WAP2: water available to plant at depth of 30-100 cm, SWSC: Soil Water Storage Capacity, and SD: Scale depth

6.6. Soil erosion study by using PESERA model

6.6.1. Annual soil loss

The model results show that annual soil erosion rate of the study area varies from < 1.0 ton/ha/year to 19.2 ton/ha/year (Figure 6.6). The mean soil loss rate of the study area is 1.13 ton/ha/year with the standard deviation of 1.64. The high erosion rate is mostly marked in mountainous areas and where maize crop is grown.

Soil erosion was assessed separately using canopy cover derived from NDVI and crop calendar data. Both the results show similar soil loss rates (Figure 6.6 and figure 6.7). The mean soil erosion rate is slightly higher in the case of model result obtained by using crop calendar data (1.17 ton/ha/year) than using NDVI data (1.13 ton/ha/year). The reason for this is that, in bare land and in agriculture land use class during fallow period the canopy cover value was assigned zero as referring to PESERA users' manual but in case of NDVI image the value is not zero because of the presence of some vegetation in the field. In the soil loss estimation using crop calendar, relatively large area shows soil loss rates having more than 7.5 ton/ha/yr (Figure 6.6 and figure 6.7).

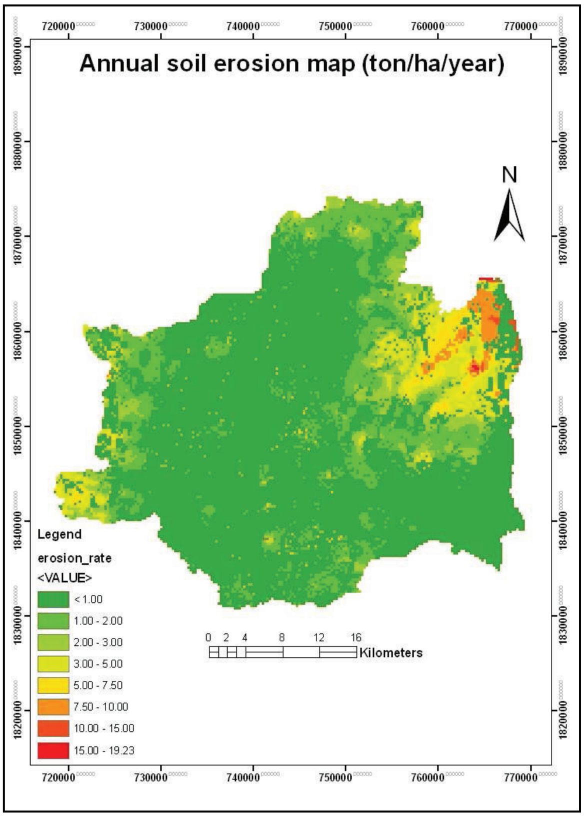

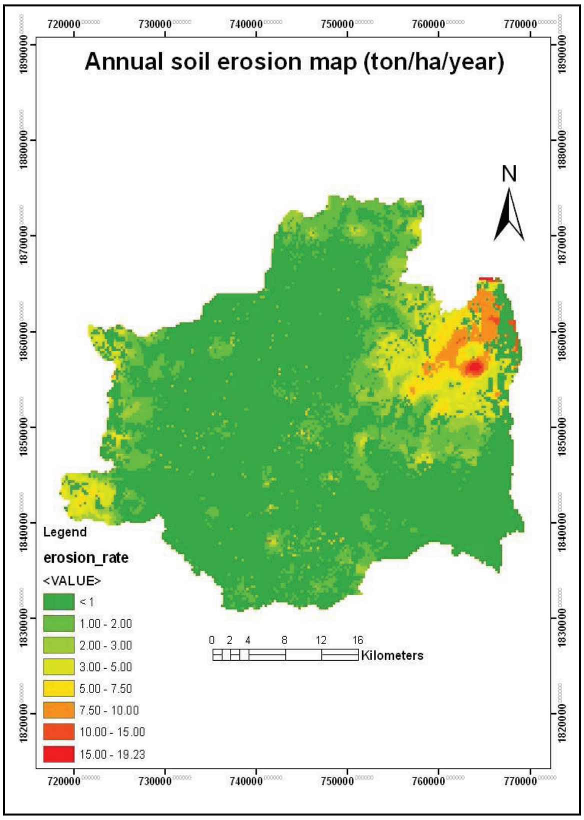

Figure 6-6: Annual soil erosion map by using NDVI **Figure 6-7: Annual soil erosion map by using CC**

6.6.2. Monthly soil loss

The model results derived by using both NDVI and crop calendar data show that there is variation of soil erosion rate throughout the year (Table 6-5). The monthly erosion map derived by using both the crop calendar and NDVI data are presented in figure 6-8 and figure 6-9 respectively. The maps show that there is no soil erosion during January and December because there is no rainfall on these months. There is gradual increase in erosion rate from February and peaked at June with the value of 3.8 (t/ha/month) which then sharply fall on July and again increased to 2.8 (t/ha/month) on August. After August the mean monthly soil erosion rate slightly decrease to 2.3 (t/ha/month) on September which again increases to 2.5(t/ha/month) on October. During November there is no soil erosion because during this month the rainfall is very low. This variation of erosion rate follows the variation in monthly rainfall. As there is highest monthly rainfall in mountainous part of the study area during June thereby causing highest mean monthly erosion rate on this month. Similarly the higher rate of monthly rainfall during month of August, September and October have caused the higher rate of mean monthly erosion during these months. Despite the monsoon season, July has low erosion rate (0.5 ton/ha/month) in comparison to June and August because there is relatively lesser rainfall during this month. The comparison of erosion results obtained by using canopy covers derived from NDVI and crop calendar reveals that there is very little difference between the results obtained from two methods.

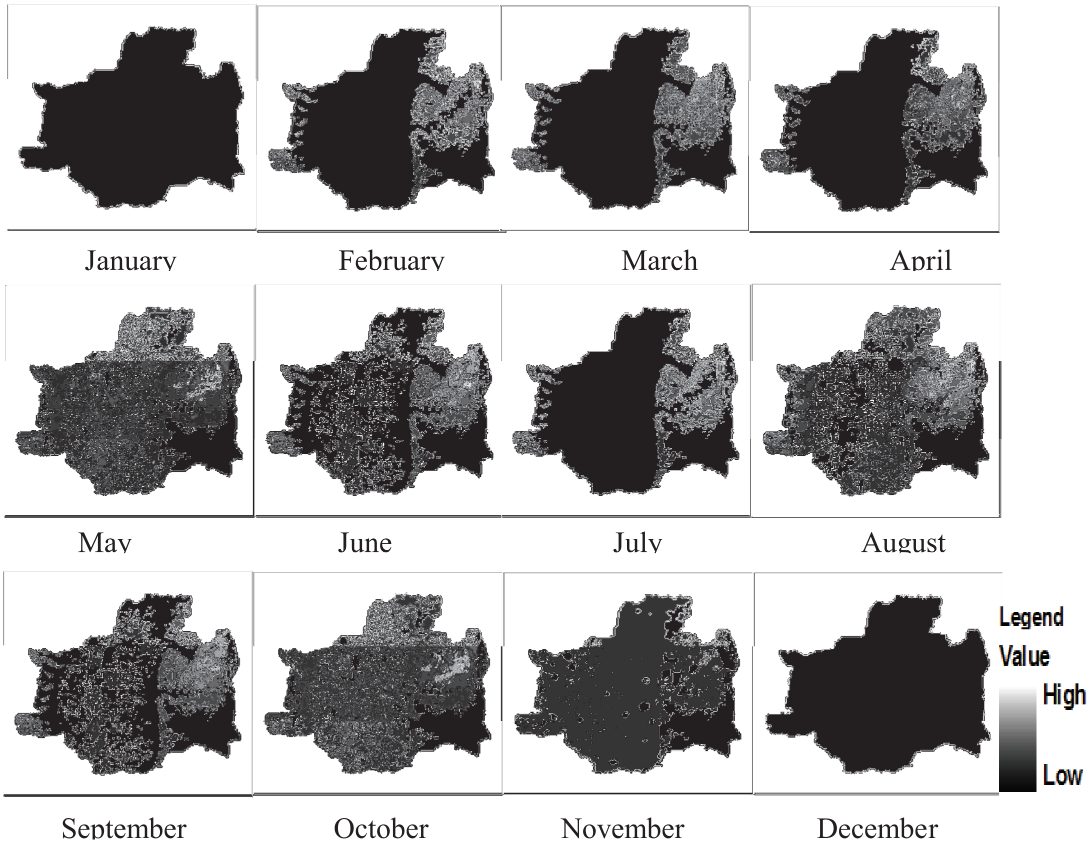

Figure 6-8: Monthly soil erosion map from crop calendar

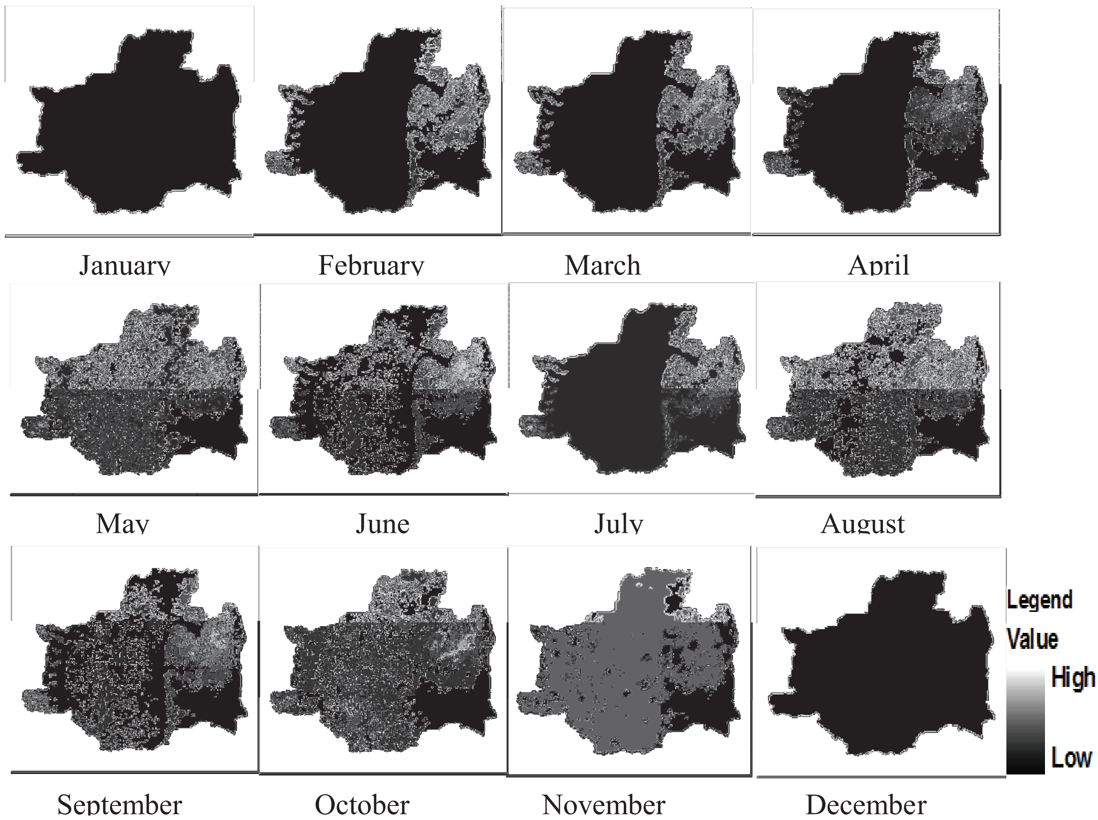

Figure 6-9: Monthly soil erosion map from NDVI

Linear regression was carried out between monthly run off and erosion rates predicted by the model (Figure 6-11). The result indicates that there is good relationship between these two characteristics with the R^2 value of 0.94.

Table 6-5: Monthly soil erosion rate (ton/ha/year) derived from NDVI and crop calendar

Month	NDVI				Crop calendar			
	Minimum	Maximum	Mean	Standard Deviation	Minimum	Maximum	Mean	Standard Deviation
Jan	0.0	0.0	0.0	0.0	0.0	0.0	0.0	0.0
Feb	0.0	3.0	0.1	0.2	0.0	3.0	0.1	0.2
Mar	0.0	15.4	0.4	1.3	0.0	15.4	0.4	1.3
Apr	0.0	31.6	0.8	2.8	0.0	59.0	1.3	4.1
May	0.0	27.2	1.0	1.8	0.0	37.5	1.1	2.4
June	0.0	101.8	3.8	9.1	0.0	101.8	4.0	9.4
July	0.0	17.7	0.5	1.5	0.0	17.7	0.5	1.5
Aug	0.0	56.2	2.8	5.0	0.0	56.2	2.7	5.0
Sep	0.0	12.3	2.3	0.3	0.0	11.9	2.1	0.2
Oct	0.0	70.6	2.5	4.1	0.0	70.6	2.4	3.9
Nov	0.0	0.0	0.0	0.0	0.0	0.0	0.0	0.0
Dec	0.0	0.0	0.0	0.0	0.0	0.0	0.0	0.0

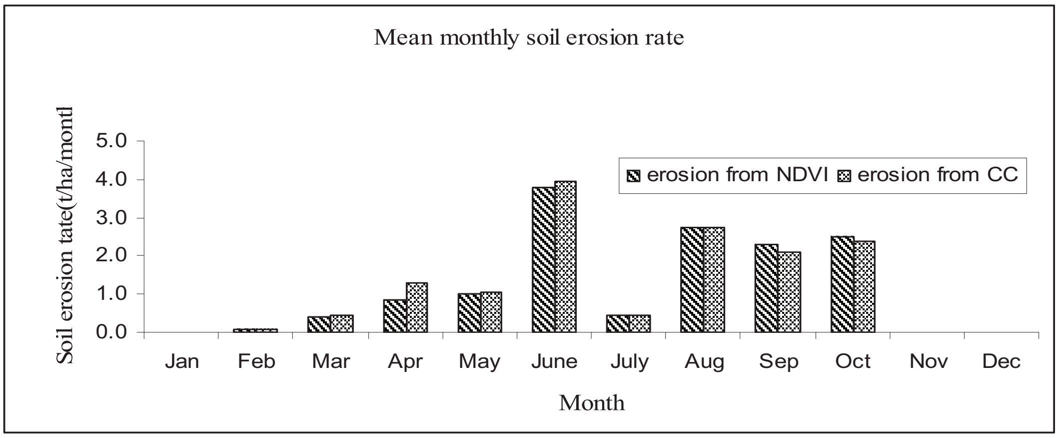

Figure 6-10: Monthly soil erosion rate derived from NDVI and crop calendar

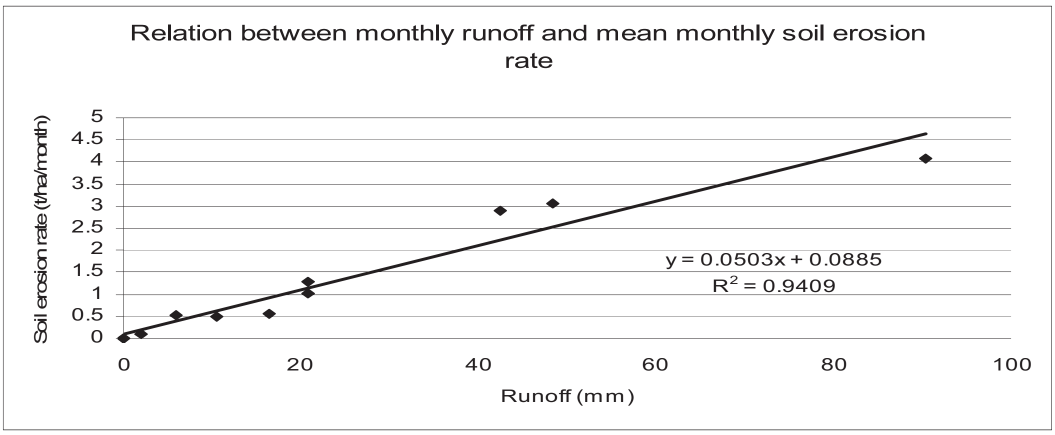

Figure 6-11: Relationship between run off and mean monthly soil erosion rate

6.6.3. Soil loss with respect to land use/land cover types

The erosion risk assessment of the study area shows that there is high variation of erosion among the land use categories (Figure 6-12). Among the land use/land cover categories, maize field has highest average annual soil erosion rate (3.8 t/ha/year) with variation from 1.0 to 18.0 ton/ha/year. Bare land and degraded forest have the second and third highest average annual erosion rate of 2.7 t/ha/year and 1.8 t/ha/year respectively (Table 6-6). In bare land the rate of soil erosion varies from 1.0 to 10.0 ton/ha/year which in degraded forest is varies from 1.0 to 19.0 ton/ha/year. The least rate of soil erosion occurs in dense forest and grass land having rate of <0.1 t/ha/year. Average soil erosion rate decreases with the land cover types in this pattern: maize > bare land > degraded forest > orchard > mixed agriculture > urban > paddy > grass land > dense forest. The result of the study seems in line with the (Sapkota, 2008) and (Souksakoun, 2008).

As soil erosion is the function of land use and its interaction with the climate and topography on soil (Lal, 1990), the rate of soil erosion vary with the land use types. The maize crop which are generally grown in mountainous areas and have less canopy cover percent during rainy season, contributes to high erosion rate among the land cover categories. Vegetation acts as a protective cover to the soil while under ground component; the root system contribute to the mechanical strength of the soil. Such effect of vegetation is higher in natural vegetation and relatively more in perennial crops than in annual. Therefore dense forest and grass land have least amount of soil erosion. Lal (1990) has also reported that forest has less erosion risk than arable and plantation crops. In contrary to this the degraded forest area has higher rate of soil erosion than dense forest. Because, canopy cover percent is lesser in degraded forest and the amount of under-storey vegetation and litter as well as the under ground effect of vegetation to the soil is also less. Despite of being arable crop, the paddy field has less average soil erosion rate (0.1 ton/ha/year) because it is grown in flat terrain. Moreover, as paddy field is covered with few cm layers of water this act as buffering to soil.

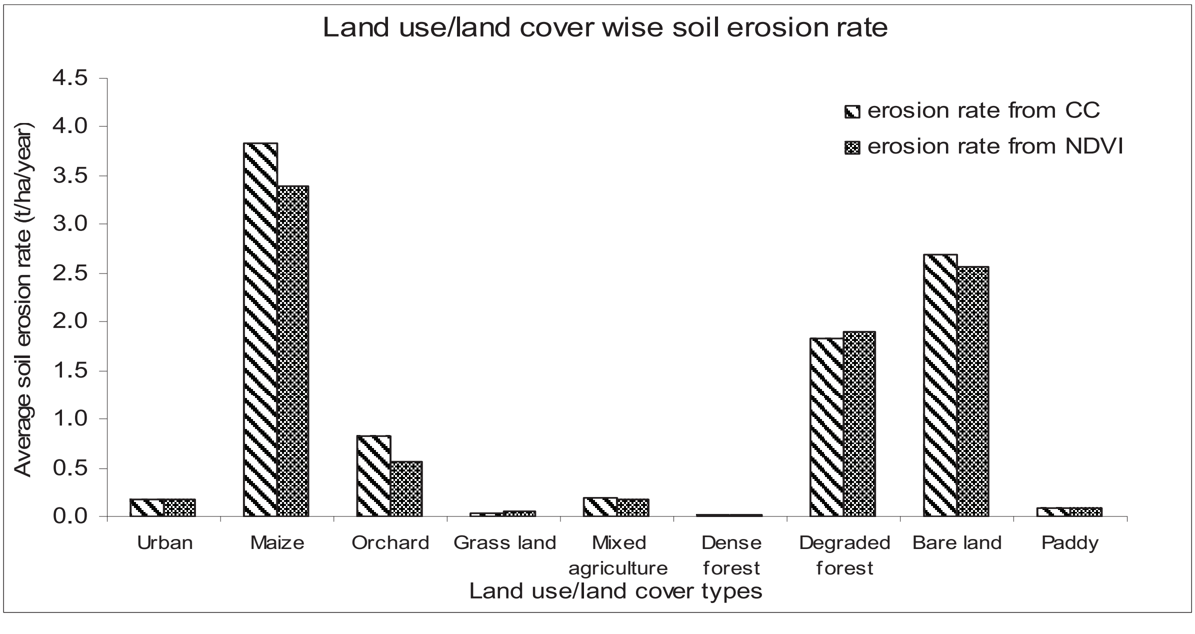

Figure 6-12: Average soil erosion rate with respect to land use/land cover types

Table 6-6: Land use/land cover wise soil erosion rate

Land use/land cover class	Erosion rate (ton/ha/year) using crop calendar data				Erosion rate (ton/ha/year) using NDVI data			
	Min	Max	Mean	SD	Min	Max	Mean	SD
Urban	0.06	2.33	0.17	0.12	0.06	2.87	0.18	0.15
Maize	0.65	17.90	3.83	2.75	0.55	10.04	3.40	1.55
Orchard	0.17	11.23	0.83	0.91	0.14	2.81	0.57	0.33
Grass land	0.00	1.41	0.10	0.10	0.01	1.45	0.10	0.10
Mixed agriculture	0.05	1.39	0.20	0.16	0.04	1.26	0.18	0.12
Dense forest	0.00	0.07	0.10	0.01	0.00	0.28	0.10	0.03
Degraded forest	0.15	19.23	1.83	1.98	0.15	19.23	1.89	1.97
Bare land	0.96	10.61	2.68	1.20	0.93	10.21	2.58	1.15
Paddy	0.03	0.52	0.09	0.03	0.03	0.45	0.09	0.03

Monthly soil erosion rate of land use classes which have higher annual erosion rate is presented in table 6-7. Maize class has the highest erosion rate (11.6 ton/ha) in June because during this month, rainfall is high in mountainous area where maize crop is cultivated. After June, maize field produce higher rate of erosion during October (8.5 ton/ha), September (6.8 ton/ha) and August (4.8 ton/ha) because these months also receive high rainfall and maize field remains fallow during this period. In the case of bare land the highest erosion rate (9.4 ton/ha) is found in October and followed by June and August having second (6.4 ton/ha) and third (5.7 ton/ha) highest erosion rate respectively. This is because of the fact that the rainfall during pre-monsoon and mid-monsoon make the soil saturated resulting in to the high surface runoff and thereby causing more erosion on late-monsoon period. Monthly distribution of erosion rate of degraded forest seems similar to that of maize. Orchard field on the other hand, generate highest erosion rate during October (3.6 ton/ha) and September (3.0 ton/ha) because this is the late monsoon period when runoff generation is more due to the saturation of soil from the rainfall of previous months and at the same time, the orchard has less canopy cover during this season.

Table 6-7: Monthly erosion rate (ton/ha/month) for various land use classes

Month	Maize		Bare land		Degraded forest		Orchard	
	Mean	SD	Mean	SD	Mean	SD	Mean	SD
January	0.0	0.0	0.0	0.0	0.0	0.0	0.0	0.0
February	0.3	0.3	0.1	0.1	0.2	0.3	0.0	0.0
March	1.4	0.6	0.8	0.6	0.5	1.7	0.2	0.1
April	6.6	3.2	2.1	2.0	1.2	3.7	0.4	0.5
May	5.1	3.6	4.8	3.0	1.5	1.1	0.6	0.5
June	11.6	11.1	6.4	2.9	6.6	11.1	1.5	1.2
July	1.2	2.0	1.4	3.5	1.2	2.0	0.6	0.4
August	4.8	2.5	5.7	3.3	4.3	6.0	1.4	2.3
September	6.8	4.5	5.4	3.1	2.8	4.4	2.5	3.0
October	8.5	4.1	9.4	4.6	4.3	5.1	2.9	3.6
November	0.0	0.0	0.0	0.0	0.0	0.0	0.0	0.0
December	0.0	0.0	0.0	0.0	0.0	0.0	0.0	0.0

6.6.4. Analysis of soil erosion with respect to change in canopy cover percentage

The canopy cover of forest remains relatively same throughout the year. However, in agricultural crops there is seasonal change of canopy cover depending on their growing stages. Therefore, to see the effect of change in canopy cover on erosion three land use categories: maize, mixed crops and orchard were selected in this study.

In maize crop it seems that the erosion rate from February to April has been increased (Figure 6-13). Where as, canopy cover of maize has been decreased due to the drying and shedding of leaves during this period. However, there is also gradual increase in rainfall during this period. Therefore during this period it is difficult to conclude whether the increment in erosion rate is due to rainfall change or canopy cover change. But from April to May there is decrease in erosion rate even the rainfall is continuously increasing. This is because the canopy cover has been increased from 0% to 15% during this period. Despite the increment of canopy cover on June, the rate of erosion has also been increased because there is highest rate of rainfall during this month. During July erosion rate has been sharply decreased because canopy cover is high and rainfall is relatively low in this month. In July, growing season of maize is over, leaves start to be dry and thereby causing decrease in canopy cover during this period. After harvesting the maize crop in August it remains fallow during September to November. Therefore the erosion rate has been increased in line with the decrease in cover percent.

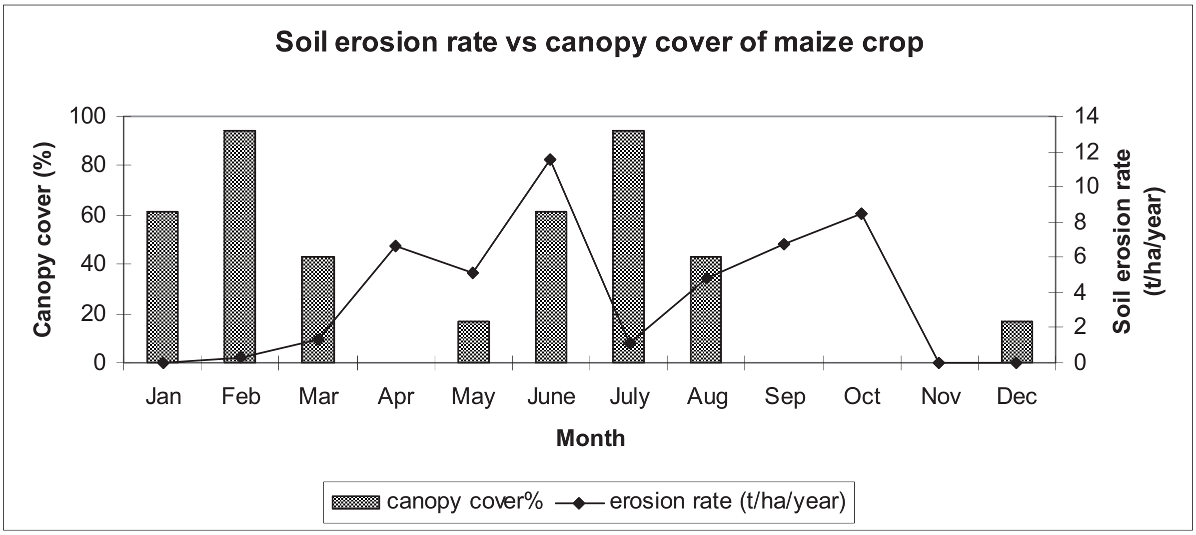

Figure 6-13: Soil erosion rate vs. canopy cover percent of maize crop

As new leaves start to appear from February the cover percent of orchard increases gradually and after June it remains constant for coming four months (Figure 6-14). The erosion rate has also been increased gradually from February to June because monthly rainfall has increased during this period. The erosion rate has followed the same trend of rainfall from June to September. Despite of high canopy cover in September the erosion rate is also high because the continuous high rainfall from previous few months has already saturated the soil and thereby causing higher runoff and erosion in this month. After this, although there is lesser amount of rainfall during October than June and August, the rate of soil erosion seems higher. Because, the canopy cover percent is lesser during October than June and August. This indicates that there is inverse relationship between cover percent and soil erosion rate. Overall, there is gradual change of canopy cover of orchard in line with the pattern of rainfall; it is difficult to see the effect of change in canopy cover on rate of erosion.

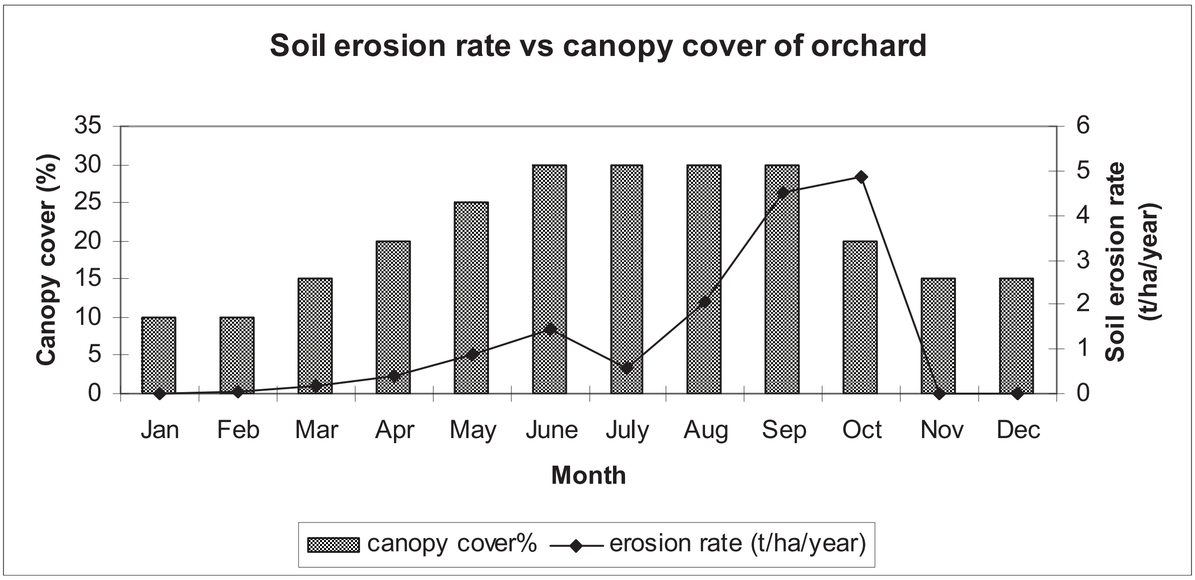

Figure 6-14: Soil erosion rate vs. canopy cover percent of orchard

Like orchard, mixed crop also demonstrates the similar relationship between percent change in canopy cover and its effect on erosion rate (Figure 6.15).

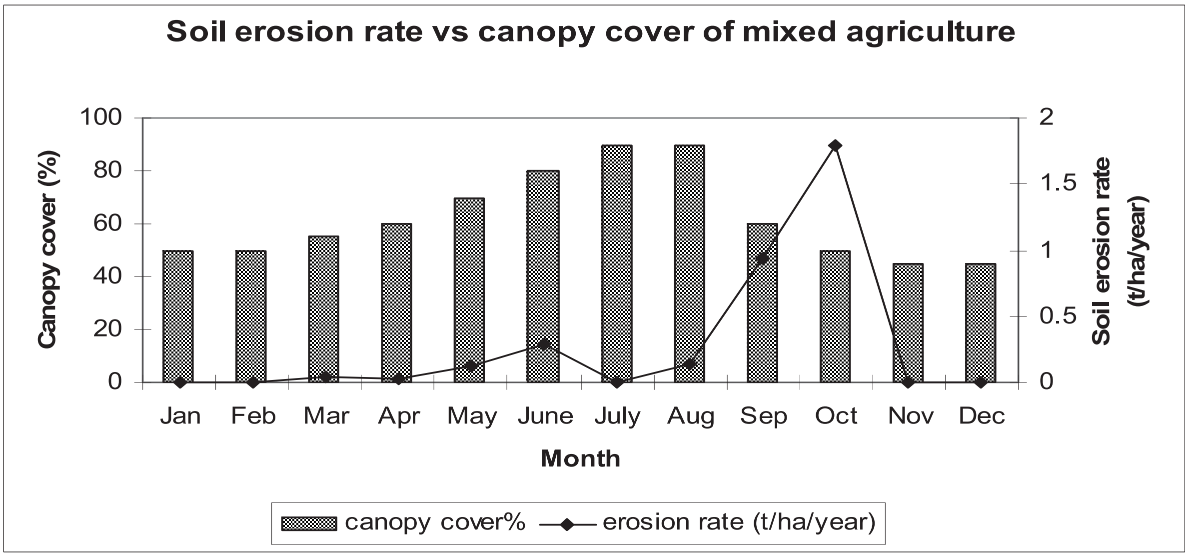

Figure 6-15: Soil erosion rate vs. canopy cover percent of mixed agriculture

6.7. Sensitivity analysis of model parameters

To perform sensitivity analysis, five model parameters were chosen. The chosen parameters were soil erodibility, soil water storage capacity, canopy cover, mean monthly rainfall and coefficient of variance of rainfall. The result of the sensitivity analysis (Table 6.8) shows that erodibility is the most sensitive parameter among the selected parameters as there is highest rate of change in erosion rate with the percent change in input parameters in the same rate. The important aspect of the result is that there is exponential increase in erosion rate due to per unit increase in erodibility value (Figure 6-16). This implies that the erodibility influence the model result most. After erodibility, mean monthly rainfall comes in the second position in the rank of sensitivity class. Among the selected parameters, soil water storage capacity (SWSC) and coefficient of variance of rainfall (cvrf) are moderately sensitive and finally the cover percent is the least sensitive.

As soil erodibility is an important soil parameter effecting soil erosion and depends particularly on soil texture and soil organic matter content, the effect of organic matter content on soil erodibility was calculated by changing organic matter percent by increasing and decreasing with the rate of 10%, 20% and 30%. For this calculation Wischmeier's fomula (eq 4.7) was used. The result shows that there is an inverse but linear relation between organic matter content and soil erodibility (Figure 6-17). The percentage change in erodibility value due to 10%, 20% and 30% decreasing and increasing of organic matter content is 1.51%, 3.01% and 4.52% respectively in both directions.

Table 6-8: Summary of the sensitivity analysis for the PESERA model prediction

Parameter	Percent change in parameter value					
	-30%	-20%	-10%	10%	20%	30%
	Percent change in erosion rate					
Soil parameter						
erodibility	-92.16	-81.81	-57.49	+135.77	+457.75	+1223.67
SWSC	+17.12	+10.39	+6.47	-3.32	-6.04	-8.26
Land cover parameter						
cover percent	+3.83	+2.38	+1.10			
Climate parameter						
mrf	-26.14	-19.44	-17.46	+15.78	+11.22	+39.93
cvrf	-24.85	-27.42	-3.99	+1.22	+0.56	+1.55

Note:
SWSC: soil water storage capacity, mrf: mean monthly rainfall, and cvrf: coefficient of variance of rainfall in a month.

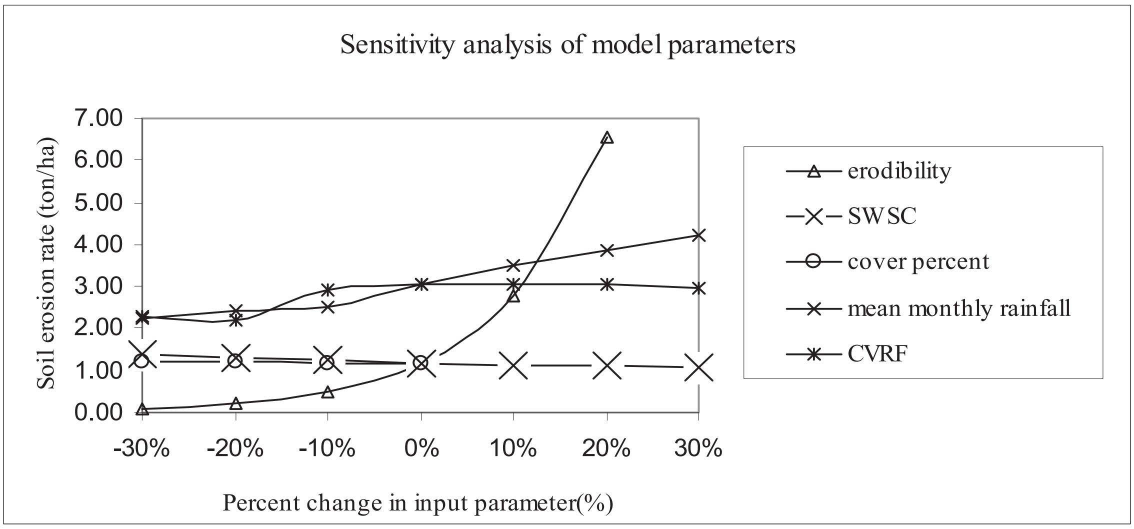

Figure 6-16: Sensitivity analysis of model parameters

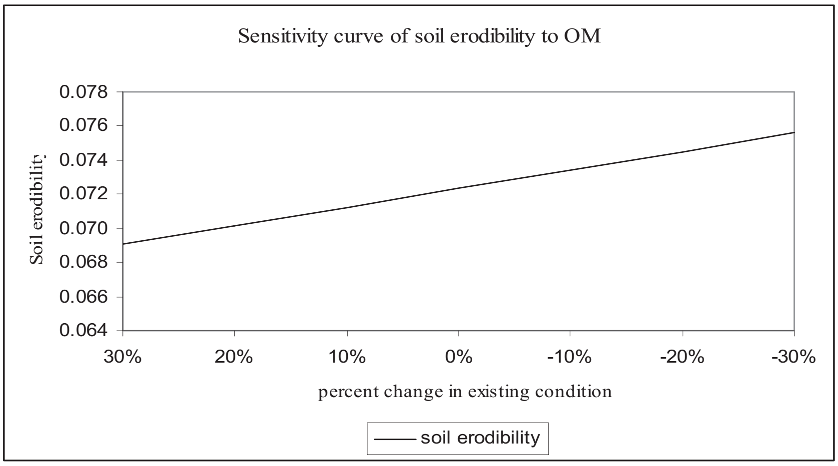

Figure 6-17: Sensitivity curve of soil erodibility to soil OM content

6.8. Validation of model results

PESERA gives daily overland flow by converting daily rainfall. Since field measurements were carried out in September the result of this month was chosen for validating the model result. The daily run off generation from the Namchun catchment (m^3/day) was calculated by multiplying the mean runoff predicted by the model with total area of the Namchun catchment. This value was compared with the measured average daily runoff discharge (m^3/day) at the outlet of Namchun catchment. The average daily run off discharge was calculated by taking the average of discharge from three days measurements. The ratio was calculated by dividing predicted value (1136395 m^3/day) by the measured value (1662933.2 m^3/day) and the ratio is 0.68. This shows that the model is 32% under predicting of runoff discharge than the measured discharge.

Similarly, soil erosion loss from the Namchun catchment on September (ton/month) was calculated by multiplying the total area of catchment with mean monthly soil erosion rate which was predicted by the model. This value was compared with the measured monthly sediment discharge at the Namchun catchment outlet. Average sediment discharge (kg/sec) was calculated by taking average from three days measurement which was then converted to monthly sediment discharge (ton/month) by multiplying value of seconds in month divided by kg per ton. The ratio which was calculated by dividing predicted monthly erosion loss (16331.62 ton/month) by the measured monthly sediment discharge (20565.54 ton/month) is 0.79. This means there is 21% underestimation in model prediction than the measured value. However, the ratio is within the acceptable limit according to Morgan (1995).

There are many reasons behind the underestimation of runoff and erosion by the model in this study. Firstly, there were plenty of landslides, under cutting by roads and river bank cutting which were observed during field work. In addition to these farming was done in the steep slope up to 40° slope and tillage was done by using power tractor along the direction of slope and thereby causing massive erosion in agriculture field. The PESERA model, however does not consider these forms of soil erosion (Kirkby et al., 2004) but it was observed that these are the major causes of soil erosion in the study area. Secondly the Namchun catchment of which the runoff and sediment discharge were measured is situated mostly in the mountainous area. The result of erosion assessment in European areas has shown that PESERA model under predicts the erosion in mountainous areas (Kirkby et al., 2004). Third, the PESERA model also under predicts soil erosion in silty soils (Kirkby et al., 2004) however majority of the soil in the study area is silt loam.

Although there is good correlation between runoff discharge and soil loss in the result of model prediction (section 6.6.2 of chapter 6), the ratio of predicted run off with the measured runoff is lesser than ratio of predicted soil loss with measured sediment discharge. This is because all the eroded soil materials do not reach the outlet of the catchment. They may remain in the place where they originated or may be deposited on the way where slope gradient declines.

As there is no sufficient measured runoff and sediment discharge data for the validation of the model, it is not possible to statistically test the validation.

6.9. Analysis of the effect of up-scaling of land use/cover mapping on erosion assessment

6.9.1. Effect of resampling in surface area covered by various land use/land cover

In order to see the effect of upscaling land use/land cover on model prediction, the classified Aster image of 15 m resolution was resampled to 250m, 500m and 1000m resolution (Figure 6-18). For this purpose the nearest neighbour algorithm was used. The resulting surface area covered by various land use/land cover types for each resolution size is shown in table 6-9 and figure 6-19. Resampling from 250m resolution to 500m resolution resulted in the increased surface area of degraded forest, dense forest, mixed agriculture and urban/residential classes where as, it resulted in the decreased surface area of paddy, maize, grass land, orchard, water body and bare land classes. The highest increase in area is found in degraded forest with the increment of 656 ha followed by mixed agriculture and dense forest having second and third highest increment in areas respectively. The highest decrease in area was found in paddy class with decrease in area by 681 ha. The reason for increasing area of class like forest and decreasing area of classes like grass, maize and bare is that both the degraded forest and dense forest are more extensive while others are scattered and patchy. As the value for new pixels is assigned from the value of nearest most dominant pixel of original map within the 3 by 3 pixel area using nearest neighbour algorithm, the scattered pixels which are surrounded by forest area were converted to the class degraded forest and dense forest.

However, there is nearly opposite trend in change of areas of land cover classes when 250m resolution map was resampled to 1000m. There is an increase in area of degraded forest and dense forest and decrease in area of grass land, water body and bare land. The area of paddy fields, maize and orchard which were decreased in first case were increased in second case and in contrary to this, the area of urban and mixed agriculture which were increased in first case were decreased in second case of up scaling.

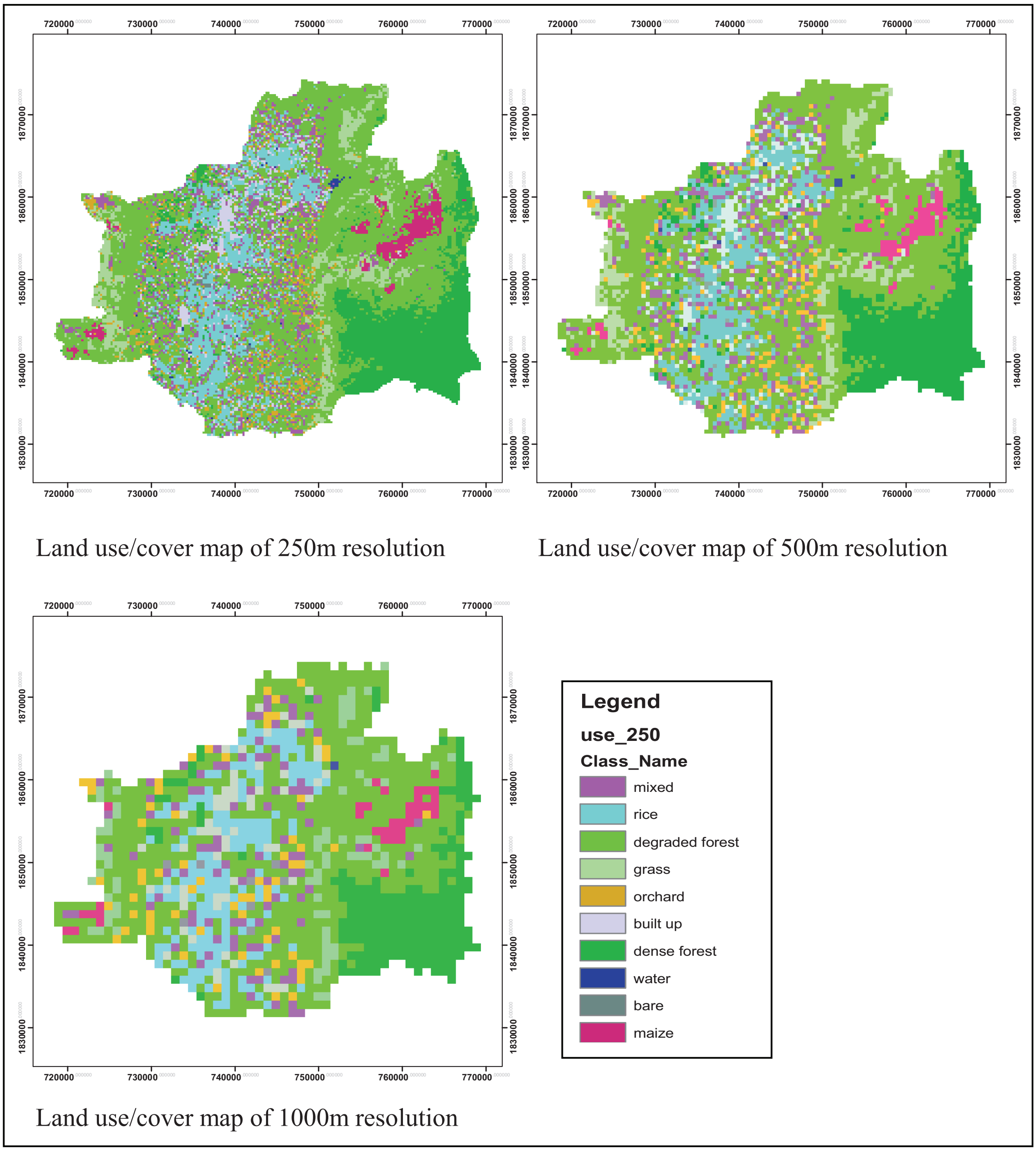

Figure 6-18: Resampled land use/land cover map

Table 6-9: Land cover wise area change due to up scaling of land cover map

Land use/land cover	Area in ha. 250m resolution map	500m resolution map	1000m resolution map
Paddy	16656.25	15975	18000
Maize	3543.75	3450	3800
Mixed agriculture	11900	12125	9900
Degraded forest	65493.75	66150	66200
Grass land	8887.5	8775	8300
Orchard	6293.75	6175	6700
Urban and residential	6200	6400	6100
Dense forest	21037.5	21225	21500
Water body	306.25	275	100
Bare land	1056.25	975	900

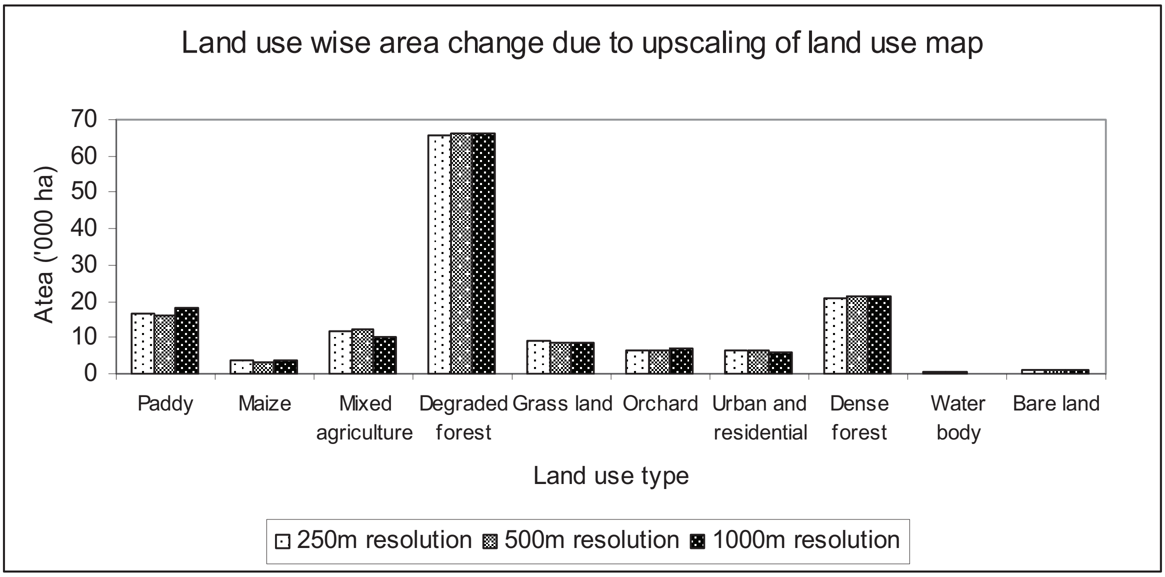

Figure 6-19: Land cover wise area change due to up scaling of land cover map

6.9.2. Upscaling effect on erosion prediction

To see the effect of the change of spatial resolution of land cover map on model prediction, model was run by using 250m, 500m and 1000m resolution input maps derived from NDVI. The model result shows that there is no difference in average annual soil erosion rates whether 250m, 500m or 100m data is used (table 6-10). Resampling land use map from 250 to 500m resolution results in to the decrease in the area of the maize and bare land which generates high rate of erosion. At the same time the degraded forest which also contributes to high erosion rate has been increased by 656 ha and grass land which has low erosion rate has been decreased by 112 ha. On the other hand the dense forest and urban and residential areas which have low erosion rate has been increased. Therefore, the resultant effect of area change in land cover types has contributed to insignificant decrease in average erosion rate in the whole area.

Table 6-10: Soil erosion rate from different resolution maps

Map scale (grid size)	Erosion rate (t/ha/year)		
	Min	Max	Mean
250m resolution	0.00	19.23	1.13
500m resolution	0.00	15.70	1.11
1000m resolution	0.00	15.18	1.10

Though, there is no difference in average soil erosion rates of the whole study area whether 250m, 500m or 100m data is used, there is significant difference in total erosion with respect to various land use classes (Table 6-11). Total soil loss from maize field predicted by the model by using 250m resolution data is 13573 ton, at 500 m resolution it is 11558 ton and at 1000 m total soil loss is 15808. Degraded forest has different trend of change in total amount of soil erosion while using different resolution data. The total soil loss from the degraded forest using 250m resolution data is 119854 ton, at 500 m resolution it increases to 129654 ton and at 1000 m it is 120484.

Table 6-11: Amount of soil erosion in different land use classes from different resolution maps

Land use class	using 250m resolution map			using 500m resolution map			using 1000m resolution map		
	Area (ha)	average erosion rate (t/ha/yr)	Total erosion (ton/yr)	Area (ha)	average erosion rate (t/ha/yr)	Total erosion (ton/yr)	Area (ha)	average erosion rate (t/ha/yr)	Total erosion (ton/yr)
Paddy	16656	0.09	1499	15975	0.06	959	18000	0.06	1044
Maize	3544	3.83	13573	3450	3.35	11558	3800	4.16	15808
Mixed agriculture	11900	0.18	2142	12125	0.21	2546	9900	0.20	1960
Degraded forest	65494	1.83	119854	66150	1.96	129654	66200	1.82	120484
Orchard	6294	0.84	5287	6175	0.77	4755	6700	0.93	6231
Dense forest	21038	0.02	337	21225	0.03	658	21500	0.03	559
Bare land	1056	2.68	2831	975	2.63	2564	900	2.58	2322
Total	**125982**		**145523**	**126075**		**152694**	**127000**		**148408**

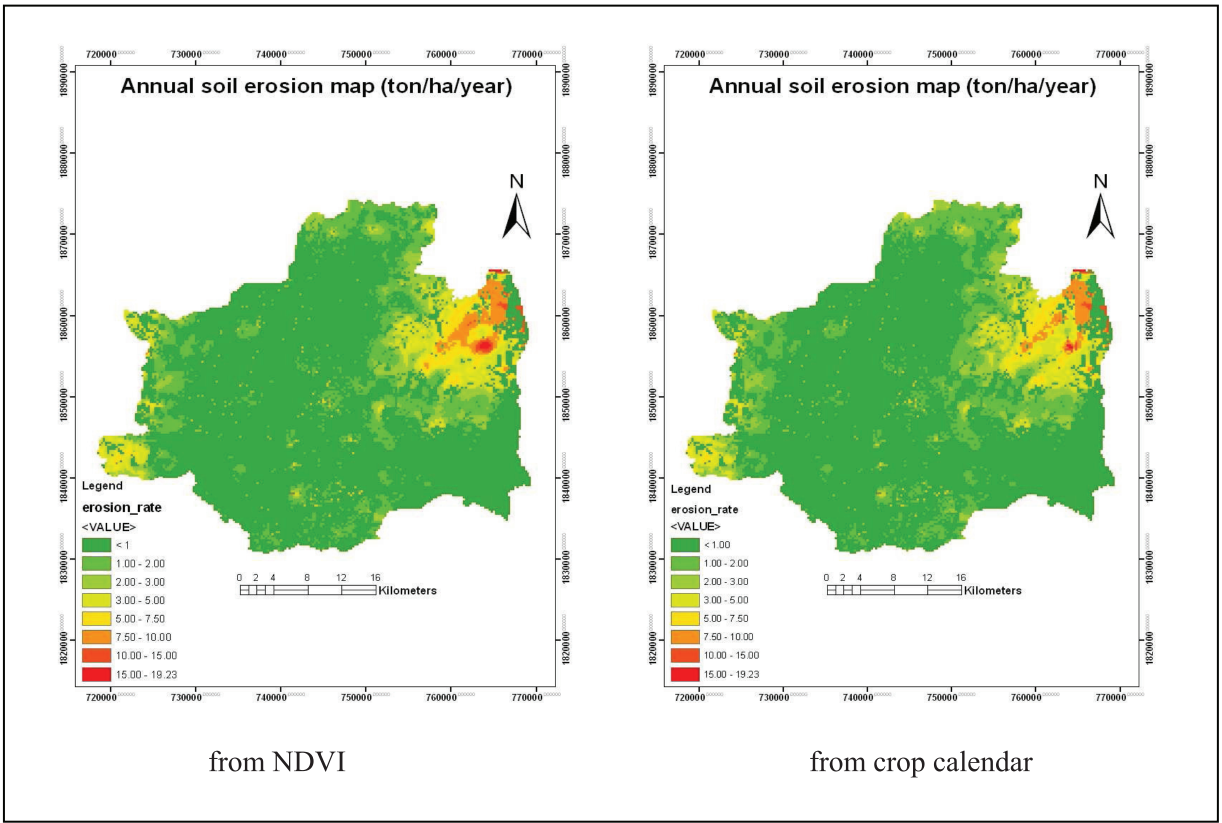

Figure 6-20: Annual soil erosion map at 250m resolution

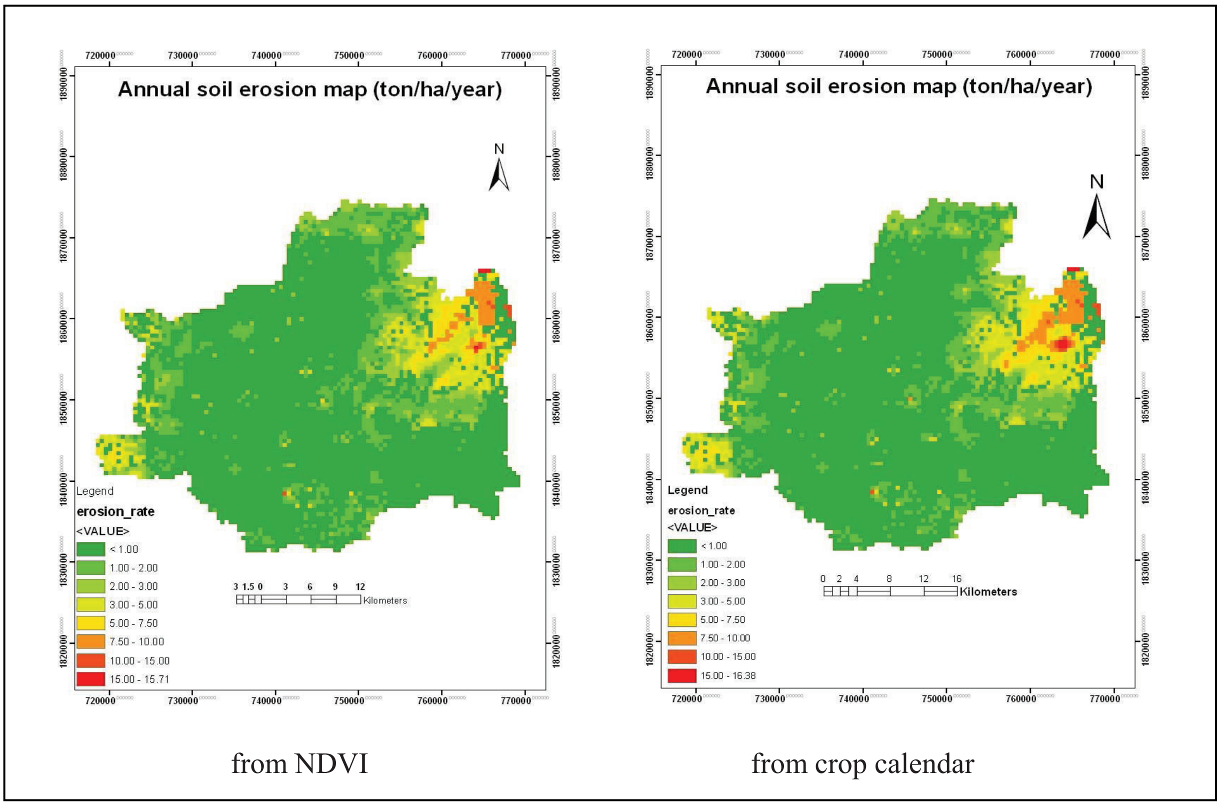

Figure 6-21: Annual soil erosion map at 500m resolution

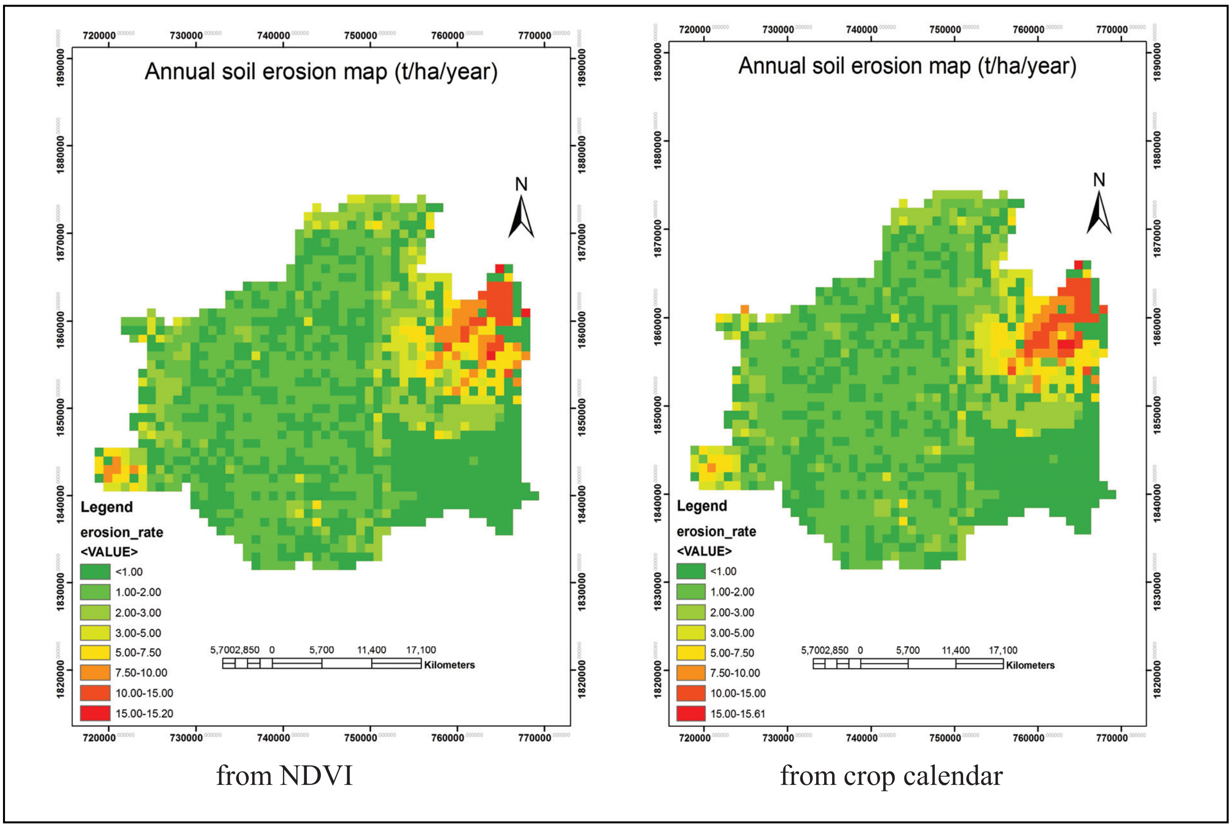

Figure 6-22: Annual soil erosion map at 1000m resolution

6.10. Erosion assessment in various land use scenarios

Scenario-1

In this case the degraded forest of existing land use/land cover system was deliberately converted to maize cultivation which results in total surface area of maize cultivation into 69038 ha. As result, the average soil erosion rate of the maize field will be increased to 5.84 ton/ha/year in changed scenario. As the surface area and average annual soil loss rate both have been increased, the total amount of soil loss from the maize field will be increased from 13573 ton/year to 402975 ton/year (Table 6-13). This indicates that if the existing degraded forest land is converted into maize field, the net increment of soil loss from the changed land use is 255974 ton/year. Because of this effect, the average annual soil erosion rate of the whole study area will be increased by 165%.

Scenario-2

In this case grassland of existing land use/land cover system of the study area was converted to maize cultivation. According to the model result, the average annual soil erosion rate of maize field will be increased from 3.83 ton/ha/year in existing situation to 8.48 ton/ha/year in changed scenario (Table 6-12). This increment in erosion rate along with the increase in surface area of maize field will result into 91862 ton/year more soil loss from the maize field than the existing maize field. The net increment of soil loss due to changed land use scenario is 90904 ton/year. Because of this effect the average annual soil erosion rate of the whole study area will be increased by 75%.

Scenario-3
In this case grass land of existing land use/land cover system of the study area was converted to orchard where the model result shows that the average annual soil erosion rate of the orchard will be increased from 0.83 ton/ha/year to 1.7 ton/ha/year (Table 6-12). Because of the increase in average soil erosion rate and the surface area of the orchard class, the total soil loss from this class will be increased from 5218 ton/year in present situation to 25732 ton/year in changed scenario (Table 6-13). This indicates that the net increment in soil loss due to changed land use scenario is 14408 ton/year.

Scenario-4
As dense forest has the least soil erosion rate (Figure 6-12), an extreme scenario of conversion of all land use classes in to dense forest was created, and the model was run. According to the model prediction the average annual soil erosion rate will be decreased by 85% i.e. from 1.18 t/ha/year in existing condition to 0.17 t/ha/year in changed scenario and thereby causing only 1979 ton /year soil loss from the whole study area (Table 6-13).

Scenario-5
As maize field has the highest soil erosion rate (Figure 6-12), an extreme scenario of conversion of all land use classes in to maize was created, and the model was run. According to the model prediction the average annual soil erosion rate of the whole area will be increased by 784% i.e. from 1.18 t/ha/year in existing condition to 8.96 t/ha/year in changed scenario (Table 6-12). In this scenario the total soil loss from the study area will be 1266720 ton/year which is 1093392 ton/year more than the soil loss in existing land use situation.

Table 6-12: Soil erosion rate in different land use change scenarios

Scenario	LU/LC class	Existing scenario			Changed scenario		
		Min	Max	Mean	Min	Max	Mean
1	Maize	0.65	17.90	3.83	0.32	65.91	5.84
2	Maize	0.65	17.90	3.83	0.32	55.24	8.48
3	Orchard	0.17	11.23	0.83	0.17	11.89	1.70
4	Dense forest	0.00	0.07	0.10	0.01	0.215	0.01
5	Maize	0.65	17.90	3.83	0.48	134.28	8.96

Table 6-13: Amount of soil loss from various land use classes in different land use scenarios

Scenario	LU/LC class	Existing scenario			Changed scenario		
		Area (ha)	Mean erosion rate (t/ha/yr)	Total erosion (t/yr)	Area (ha)	Mean erosion rate (t/ha/yr)	Total erosion (t/yr)
1	Maize	3544	3.83	13573.52	69038	5.84	402974.81
2	Maize	3544	3.83	13573.52	12432	8.48	105435.79
3	Orchard	6294	0.83	5217.73	15181	1.70	25731.80
4	Dense forest	21037	0.10	2103.70	141375	0.01	1979.25
5	Maize	3544	3.83	13573.52	141375	8.96	1266720.00

7. Conclusion and recommendation

7.1. Conclusion

The study was focussed to achieve the objective of assessing soil erosion in Lomsak district of Thailand by using PESERA model and to study the effect of upscaling of grid cells of land use/land cover on erosion prediction. Keeping with these views, this study was carried out and the results predicted by the model were discussed thoroughly. On the basis of result and discussion following conclusions were made.

- There is significant variation of soil erosion rate throughout the year. Soil erosion rate is highest in June followed by August, October and September having second, third and fourth highest soil erosion rate respectively. During January and December there is no soil erosion.

- Soil erosion rate in the beginning of the monsoon season is higher than that in the late of monsoon because of higher rainfall in the beginning of the monsoon season and no vegetation cover.

- There is significant variation in soil erosion rate according to the variation in land use/land cover types. Maize crop has the highest average soil erosion rate followed by bare land degraded forest. After these, orchard and mixed agriculture come in the order of having lesser erosion rate. Dense forest and grass land has the least soil erosion rate

- There is good correlation between the monthly runoff and monthly soil loss predicted by the model.

- There is an inverse relation between canopy cover and rate of soil erosion. Sometimes, it is difficult to see the effect of canopy cover on soil erosion because along with the canopy cover there is also variation in rainfall. However comparing the situations when other factors remaining constant, only the rainfall and canopy cover percent are decreasing but at the same time, soil erosion rate is increasing means there is effect of canopy cover on soil erosion rate.

- Soil erodibility is the most sensitive model parameter followed by the mean monthly rainfall among the tested parameters. There is an exponential increase in erosion rate due to per unit increase in erodibility value. The change in soil organic matter content has inverse but linear effect in change of soil erodibility value. Canopy cover percent is the least sensitive parameter to the model.

- The model under-predicts the rate of soil erosion and runoff generation in comparison to measured value. However this comparison has not been tested statistically due to lack of sufficient measured data.

- There is change in areas of different land use/land cover classes while up scaling the grid cells of land use/land cover map but it has very low effect on average soil erosion rate of the study area predicted by the model. However, there is significant different in total amount of erosion loss from specific land use classes.

- Land use scenario change from forest and grass land to maize cultivation will increase the soil erosion rate. Conversion of nature land to maize field will have more erosion rate than to orchard.

7.2. Limitation of the study

The major limitation of this study is availability of climatic data and detail soil map of the study area. There are only five meteorological stations inside and nearby the study area which is insufficient for interpolation of climate parameter map. Due to the time limitation for field work and inaccessibility to all part of the study area soil samples could not be taken representing enough the whole study area. The measured runoff and sediment discharge data is also insufficient for field validation of the model. Cloud free recent remotely sensed image was not available for land use classification.

7.3. Recommendation

- Climate is one of the important factors in the PESERA model and all together 96 data layers of climate factor are needed to run the model. There is only one meteorological station inside the study area and others are located nearby the study area. Data from only these five stations is insufficient to interpolate the climate parameter maps. Moreover there is an effect of altitudinal variation on climate particularly rainfall and temperature in the study area. Therefore erosion assessment by using data from more stations can give better result.

- As there is spatial variability in soil properties the more the soil data available the more would be the reliability of the result. Detail soil map of the study area could be effective for better result.

- Validation of the model result would be more realistic if sufficient measured data of runoff and sediment discharge is used.

- Use of recent remote sensing image for land use/land cover classification can improve the accuracy of classification and thereby the model prediction.

Reference

Allen, R. G.; Pereira, L. S.; Raes, D. and Smith, M. (1998). Crop evapotranspiration: Guidelines for computing crop water requirements. FAO Irrigation and drainage paper 56. R. M. a. E. Department. Rome, Food and Agriculture Organization of the United Nations.

Baize, D. (1993). Soil science analyses: a guide to current use. Chicester etc., Wiley & Sons.

Bonilla, C. A.; Norman, J. M. and Molling, C. C. (2007). Water erosion estimation in topographically complex landscapes: model description and first verifications Soil Sci Soc Am J 2007 71: 1524–1537.

Doorenbos, J.; Pruitt, W. O. and Fao (1984). Guidelines for predicting crop water requirements. Rome, FAO.

Elwell, H. A. (1981). A soil loss estimation technique for Southern Africa: In R P C Morgan (ed.), Soil Conservation: problems and prospects. Chichester Wiley.

Evans, R. (1989). Mechanics of water erosion and their spatial and temporal control: An impirical viewpoint : *In* Kirkby, M. J. and Morgan, R. P. C. (eds) Soil erosion. Chichester, Wiley & Sons. pp(110-124).

Gobin, A.; Daroussin, J. and Jones, R. (2003). PAN-EUROPEAN SOIL EROSION RISK ASSESSMENT. Contract no. QLK5-CT-1999-01323.Key Action n° 1.1.1.-5.4. DELIVERABLE 17.

Gobin, A.; Jones, R.; Kirkby, M.; Campling, P.; Govers, G.; Kosmas, C. and Gentile, A. R. (2004). Indicators for pan-European assessment and monitoring of soil erosion by water. Environmental Science & Policy 7(1): 25-38. http://eusoils.jrc.ec.europa.eu/ESDB_Archive/pesera/pesera_cd/pdf/ErosionIndsGobin.pdf. Access date: 25.12.2008

Hansakdi, E. (1998). Soil pattern analysis and the effect of soil variability on land use in the upper Pasak area Phetchabun, Thailand. Enschede, ITC**:** 139.

Hudson, N. (1986). Soil conservation. London, B.T. Batsford Limited. pp(48-87).

Irvine, B. and Kosmas, C. (2003). Pan-European Soil Erosion Risk Assessment, Contract no. QLK5-CT-1999-01323. Key Action No. 1.1.1.-5.4. DELIVERABLE 15: PESERA Users manual L. M. a. N. H. Unit, European Commission, Joint Research Centre. http://eusoils.jrc.ec.europa.eu/ESDB_Archive/pesera/pesera_cd/pdf/DL15Manual.pdf. Access date: 27.10.2008.

Jetten, V.; Govers, G. and Hessel, R. (2003). Erosion models: quality of spatial predictions. Hydrological Processes 17(5): 887-900.

Jetten, V. G. (2003). Erosion models : quality of spatial predictions. Hydrological processes : an international journal 17(5).

Jetten, V. G. and Favis-Mortlock, D. (2006). Modelling soil erosion in Europe. In Soil erosion in Europe / ed. by J. Boardman and J. Poesen. Chichester: Wiley & Sons, 2006. ISBN 978-0-470-85910-0. pp. 695-716.

Jones, R. J. A.; Grimm, M. and Montanarella, L. (2002). Soil Water Storage Capacity : Input Parameter For PESERA Soil Erosion Model: *In* Anne Gobin and Gerard Govers (eds), Pan-European Soil Erosion Risk Assessment. Contract no. QLK5-CT-1999-01323. Second Annual Report: 1 April '01 - 1 April '02. http://eusoils.jrc.ec.europa.eu/ESDB_Archive/pesera/pesera_cd/pdf/Pesera2AnnRep.pdf. Access date: 12.08.2008.

Kerle, N. e.; Janssen, L. L. F. e.; Huurneman, G. C. e.; Bakker, W. H.; Grabmaier, K. A.; Huurneman, G. C.; van der Meer, F. D.; Prakash, A.; Tempfli, K.; Gieske, A. S. M.; Hecker, C. A.; Janssen, L. L. F.; Parodi, G. N.; Reeves, C. V.; Weir, M. J. C.; Gorte, B. G. H.; Horn, J. A.; Kerle, N.; Pohl, C.; van Ruitenbeek, F. J. A. and Woldai, T. (2004). Principles of remote sensing: an introductory textbook. Enschede, ITC.

Kirkby, M.; Jones, R. J. A.; Irvine, B.; Gobin, A. G. G.; Cerdan, O.; Rompaey, J. J. v.; Le Bissonais, Y.; Daroussin, J.; King, D.; Montanarella, L.; Grimm, M.; Vieillefont, V.; Puidefabregas, J.; Boer, M.; Kosmas, C.; Yassoglou, N.; Tsara, M.; Mantel, S.; Lynden, G. W. J. v. and Huting, J. R. M. (2004). Pan-European Soil Erosion Risk Assessment for Europe: the PESERA map, version 1 October 2003. Explanation of Special Publication Ispra 2004 No. 73 (S.P.I.04.73). http://www.scientificcommons.org/1159278 . Access date: 12.08.2008

Kirkby, M. J.; Gobin, A. and Irvine, B. J. (2003). PESERA model strategy, land use and vegetation growth. PESERA (Pan-European Soil Erosion Assessment) EC Contract no. QLK5-CT-1999-01323, Deliverable 05. . 46pp. http://eusoils.jrc.ec.europa.eu/ESDB_Archive/pesera/pesera_cd/pdf/DL5ModelStrategy.pdf Access date: 15.08.2008.

Kuraji, K.; Punyatrong, K. and Suzuki, M. (2000). Altitudinal increase in rainfall in the Mae Chaem watershed, Thailand. Meteorological Society of Japan Vol.79, No. 1B, pp.353-363,2001. http://www.jstage.jst.go.jp/article/jmsj/79/1B/353/_pdf Access date: 28.12.2008.

L.P.van Reeuwijk, e. (2002). Procedures for Soil Analysis. International Soil Reference and Information Center (ISRIC), Food and Agriculture Organization (FAO).

Lal, R. (1990). Soil erosion in the tropics: principles and management. New York etc., McGraw-Hill.

Lal, R. e. (1994). Soil erosion: research methods. Delray Beach; Ankeny, St. Lucie Press; Soil and Water Conservation Society.

Morgan, R. P. C. (1995). Soil erosion and conservation. Harlow, Longman.

Morgan, R. P. C. e. a. and Davidson, D. A. (1986). Soil erosion and conservation. New York, Longman Scientific & Technical.

Nearing, M. A.; Lane, L. J. and Lopes, V. L. (1994). Modeling soil erosion: In Lal, R. (ed.) Soil erosion: research methods. Delray Beach; Ankeny, St. Lucie Press; Soil and Water Conservation Society. pp(127-135).

Nyvall, J. (2002). Soil water storage capacity and available soil moisture. Water Conservation Factsheet. Ministry of Agriculture, Food and fisheries, CANADA.

Oldeman, L. R.; Hakkeling, R. T. A. and Sombroek, W. G. (1991). World map of the status of human - induced soil degration: an explanatory note: Global Assessment of Soil Degradation GLASOD. Wageningen ; Nairobi, International Soil Reference and Information Centre (ISRIC); United Nations Environment Programme (UNEP).

Parfitt, R. L.; Roberts, A. H. C.; Thomson, N. A. and Cook, F. J. (1985). Water use, irrigation, and pasture production on Stratford silt loam. New Zealand Journal of Agricultural Research vol. 28:393-401.

Patanakanog, B.; Shrestha, D. P.; Saengthongpinit, C.; Sapet, A. and Farshad, A. (2004). Land use change and land degradation: a case study in Nam Chun subwatershed in Thailand. In ACRS 2004: Proceedings of the 25th Asian conference on remote sensing, ACRS 2004 Silver jubilee: November 22-26, 2004, Chiang Mai, Thailand. Chiang Mai: Geo-Informatics and Space Technology Development Agency (GISTDA), 2004. pp. 1384-1389.

Pimentel, D. e. (1993). World soil erosion and conservation. Cambridge, Cambridge University Press.

Prachansri, S. (2007). Analysis of soil and land cover parameters for flood hazard assessment : a case study of the Nam Chun watershed, Phetchabun, Thailand. Enschede, ITC**:** 92.

Renard, K. G. e. (1997). Predicting soil erosion by water: a guide to conservation planning with the Revised Universal Soil Loss Equation RUSLE. Washington, D.C., United States Department of Agriculture (USDA).

Romkens, M. J. M.; Youg, R. A.; Poesen, J. W. A.; McCool, D. K.; El-Swaify, S. A. and Bradford, J. M. (1997). Soil erodibility factors: *In* Renard, K. G. (ed.), Predicting soil erosion by water: a guide to conservation planning with the Revised Universal Soil Loss Equation RUSLE. Washington, D.C., United States Department of Agriculture (USDA).

Rose, C. W. (1994). Research progress on soil erosion processes and a basis for soil conservation practices: *In* Lal, R. (ed.) Soil erosion: research methods. Delray Beach; Ankeny, St. Lucie Press; Soil and Water Conservation Society. pp(172-174).

Sapkota, R. (2008). Modelling runoff and erosion in Namchun watershed, Thailand. Enschede, ITC**:** 85.

Saxton, K. E. (2005). SPAW Soil-Plant-Air-Water Field and Pond Hydrology version 6.02.75 http://hydrolab.arsusda.gov/SPAW/Index.htm . Access date: 28.10.2008.

Shrestha, D. P. (2000). Aspects of erosion and sedimentation in the Nepalese Himalaya: highland - lowland relations. ITC Dissertation;77. Enschede, ITC**:** 265.

Souksakoun, K. (2008). Soil loss assessment at regional scale for different land use - cover types: case study in Lomsak district, Phetchabun, Thailand. Enschede, ITC**:** 82.

Spiegel, M. R. and Stephens, L. J. (1999). Schaum's outline of theory and problems of statistics. New York etc., McGraw Hill.

Styczen, M. and Hogh-Schmidt, K. (1986). A new description of splash erosion in relation to raidrop sizes and vegetation: *In* Morgan R P C and Rickson R J (eds) 1988. Agriculture: erosion assessment and modelling: proceedings of a workshop held in Brussels, Belgium, on 2 and 3 December 1986. Luxembourg, Commission of the European Communities.

Suriyaprasit, M. and Shrestha, D. P. (2008). Deriving land use and canopy cover factor from remote sensing and field data in inaccessible mountainous terrain for use in soil erosion modelling. In ISPRS 2008: Proceedings of the XXI congress: Silk road for information from imagery: the International Society for Photogrammetry and Remote Sensing, 3-11 July, Beijing, China. Comm. VII, SS-7. Beijing : ISPRS, 2008. pp. 1747-1750.

Thornes, J. B. (1986). Compititive vegetation-erosion model for mediterranean conditions: *In* Morgan, R. P. C. and Rickson, R. J. (eds), Agriculture: erosion assessment and modelling: proceedings of a workshop held in Brussels, Belgium, on 2 and 3 December 1986. Luxembourg, Commission of the European Communities.

Thornes, J. B. (1989). Erosional processes of running water and their spatial and temporal controls: A theoretical viewpoint: *In* Kirkby, M. J. and Morgan, R. P. C. (eds), Soil erosion. Chichester, Wiley & Sons. pp(130-155).

Toy, T. J.; Foster, G. R. and Renard, K. G. (2002). Soil erosion: process, prediction, measurement and control., Wiley-Blackwell.

van der Knijff, J. M.; Jones, R. J. A. and Montanarella, L. (1999). Soil erosion risk assessment in Italy. European Commission, Joint Research Centre. http://eusoils.jrc.ec.europa.eu/ESDB_Archive/pesera/pesera_cd/pdf/er_it_new.pdf. Access date: 24.08.2008.

Walling, D. E. (1994). Measuring sediment yield from river basins: *In* Lal, R. (ed) Soil erosion: research methods. Delray Beach; Ankeny, St. Lucie Press; Soil and Water Conservation Society.pp (39-71).

Appendix

Appendix 1: Location and altitude of five meteorological stations

Station	X: cordinates	Y: coordinates	altitude (m)
Lomsak	740000	1857000	140
Lomkao	738000	1868000	160
Phetchabun	729000	1827700	114
Khaokhor	715000	1854000	715
Wichanburi	776634	1864165	69

Appendix 2: Location map of five meteorological stations in study area

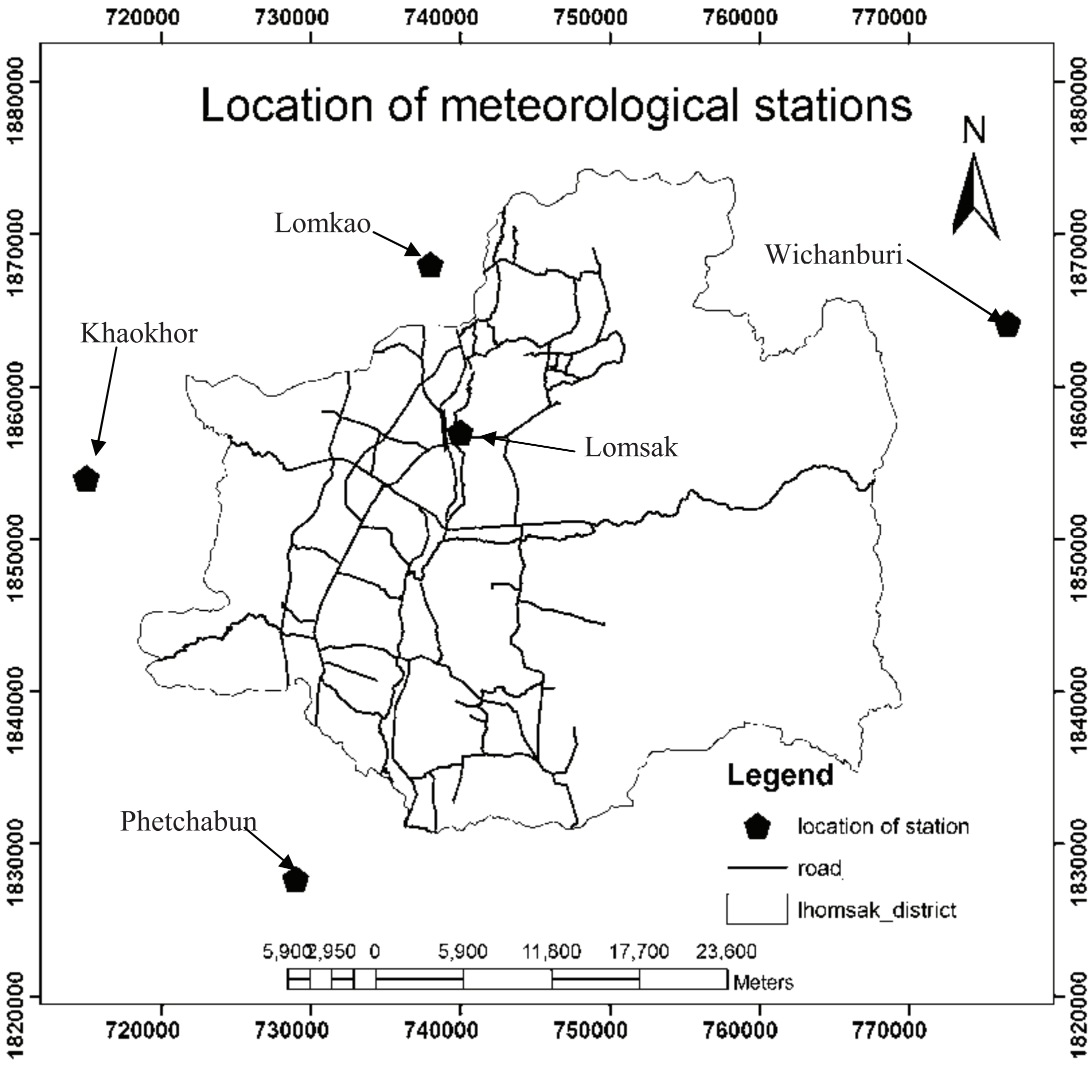

Projection: WGS84 UTM 47

Appendix 3: Mean monthly temperature (℃) of five m eteorological stations

station	Jan	Feb	Mar	Apr	May	Jun	Jul	Aug	Sep	Oct	Nov	Dec
Lomsak	23.1	24.5	28.9	30.6	30.5	29.3	28.4	27.5	26.9	26.2	24.3	25.3
Lomkao	24.2	24.7	27.5	28.3	27.4	27.2	27.5	26.5	26.4	25.4	22.4	22.1
Phetchabun	25.0	27.2	30.2	30.8	28.9	30.1	29.0	28.3	28.4	27.4	25.2	26.0
Khaokhor	22.6	24.7	27.1	27.9	26.3	27.2	26.3	25.2	26.1	25.1	23.7	23.7
Wichanburi	25.7	27.9	31.0	30.9	29.7	31.0	29.8	29.1	28.9	28.1	25.8	26.6

Appendix 4: Soil physical properties of the study area

x: cord	y: cord	sand	silt	clay	om	WAP1	WAP2	SWSC	Erodibility	S Depth	Crusting
735474	1853287	24.0	55.5	20.5	1.6	47.1	31.4	82.9	0.06	20.00	4.26
728498	1855015	21.3	65.5	13.2	2.7	56.7	37.8	98.9	0.05	20.00	4.26
727900	1846704	22.8	65.8	11.4	2.4	54.6	31.9	90.9	0.05	20.00	4.26
724554	1855828	20.8	65.5	13.6	2.4	50.1	41.8	96.3	0.06	20.00	4.26
728247	1856795	36.0	56.8	7.1	3.4	50.7	29.6	83.8	0.03	15.00	4.26
724452	1855996	20.0	70.0	9.9	2.0	56.4	0.0	60.8	0.06	20.00	4.26
725475	1855508	32.5	43.1	24.3	1.8	41.1	34.3	79.8	0.05	20.00	4.26
750329	1865099	34.0	52.8	13.2	2.3	95.4	47.7	147.5	0.04	20.00	4.26
751623	1860548	28.9	59.6	11.5	2.6	77.0	38.5	119.9	0.04	20.00	4.26
752229	1863203	23.5	50.2	26.4	2.8	42.6	24.9	71.9	0.05	20.00	4.26
755183	1852685	34.0	44.6	21.4	1.9	48.7	24.3	77.4	0.04	20.00	4.26
759832	1852011	22.6	70.2	7.2	1.0	57.0	38.0	98.5	0.06	15.00	4.26
766566	1853468	26.8	60.1	13.1	1.2	41.8	0.0	46.2	0.05	20.00	4.26
764102	1856446	19.4	70.8	9.8	1.5	56.4	42.3	103.1	0.06	20.00	4.26
749214	1851061	23.6	63.2	13.2	2.5	52.5	43.8	100.7	0.05	20.00	4.26
746335	1849708	32.1	36.0	31.8	1.8	29.5	0.0	33.9	0.05	20.00	4.26
735276	1849708	25.3	67.5	7.2	1.5	55.8	27.9	87.2	0.05	15.00	4.26
738873	1853747	21.9	67.0	11.1	1.2	54.6	27.3	86.3	0.06	20.00	4.26
748658	1844624	14.6	64.8	20.6	2.0	49.2	0.0	53.6	0.07	20.00	4.26
750285	1844765	24.9	60.6	14.5	2.1	52.2	30.5	87.1	0.05	20.00	4.26
741914	1838029	22.7	59.2	18.2	1.7	48.0	24.0	76.4	0.06	20.00	4.26
750418	1835700	30.3	58.3	11.3	1.6	49.8	41.5	95.7	0.05	20.00	4.26
749893	1837228	13.4	76.3	10.2	2.9	61.5	51.3	117.2	0.07	20.00	4.26
750609	1838193	28.0	62.8	9.1	1.8	52.2	43.5	100.1	0.05	20.00	4.26
758691	1846237	22.1	70.7	7.2	2.2	57.6	28.8	89.9	0.06	15.00	4.26
747327	1832966	24.7	66.6	8.7	2.2	89.0	44.5	137.9	0.05	20.00	4.26
740117	1831327	19.2	71.3	9.5	1.7	57.3	47.8	109.5	0.06	20.00	4.26
736162	1840191	32.5	58.6	8.8	1.2	49.8	0.0	54.2	0.04	20.00	4.26
740794	1862768	19.4	65.4	15.2	1.8	51.9	26.0	82.3	0.06	20.00	4.26
722851	1843153	23.8	64.4	11.8	2.7	55.8	41.9	102.1	0.05	20.00	4.26
731473	1856701	35.4	55.2	9.4	2.0	48.0	24.0	74.3	0.04	10.00	4.26
751004	1870673	20.5	59.5	20.0	1.7	48.9	32.6	85.9	0.06	20.00	4.26
765734	1835682	30.2	51.5	18.3	1.8	45.3	26.4	76.1	0.05	20.00	4.26
759915	1840229	24.2	69.8	6.0	2.6	58.8	73.5	135.8	0.05	15.00	4.26
736042	1858362	19.4	68.2	12.5	2.5	37.2	18.6	60.2	0.06	20.00	4.26
718072	1857719	15.6	49.2	35.2	1.9	40.2	20.1	64.7	0.07	20.00	4.26
739657	1859941	27.5	23.8	48.7	0.9	27.6	13.8	45.8	0.05	20.00	4.26

749365	1851652	11.6	70.7	17.7	1.3	52.9	35.3	91.9	0.06	15.00	4.26
747483	1856591	24.5	58.6	16.8	1.4	42.8	0.0	44.3	0.05	20.00	4.26
750723	1834154	12.6	69.3	18.1	1.4	55.2	29.5	88.4	0.05	20.00	4.26
747890	1831544	17.4	62.4	20.2	1.5	57.4	30.6	91.8	0.04	10.00	4.26
742521	1836242	28.1	58.6	13.3	1.3	51.6	34.4	89.8	0.06	15.00	4.26
752066	1835124	22.5	61.9	15.5	1.4	59.5	39.7	102.9	0.05	15.00	4.26
751952	1851652	13.7	67.1	19.3	2.5	50.5	40.4	96.2	0.04	10.00	4.26
754825	1843177	19.9	63.9	16.2	2.6	58.6	62.5	126.3	0.04	15.00	4.26
740582	1833483	22.7	57.2	20.1	1.4	55.1	36.7	95.5	0.04	10.00	4.26
755421	1838927	26.0	58.2	15.8	2.2	34.5	0.0	36.0	0.04	20.00	4.26
725817	1840865	56.6	34.0	9.4	2.5	56.8	60.6	122.6	0.04	20.00	4.26
755272	1840939	6.0	69.2	24.8	2.2	56.7	60.5	122.5	0.04	15.00	4.26
763325	1838777	8.4	70.4	21.2	2.1	58.8	62.7	126.8	0.04	10.00	4.26
752066	1841984	3.4	73.6	23.0	2.2	60.6	64.7	130.5	0.04	20.00	4.26
747890	1838703	37.3	46.8	15.9	1.4	44.9	24.0	72.6	0.04	10.00	3.40
758851	1840045	8.8	69.3	22.0	2.0	49.9	53.2	108.3	0.04	15.00	4.26
720970	1842282	4.5	71.9	23.7	1.4	31.7	16.9	52.3	0.05	10.00	4.26
763400	1842655	9.5	67.2	23.4	2.1	65.6	70.0	140.9	0.04	15.00	4.26
749530	1844146	18.9	62.4	18.7	2.2	80.6	48.3	134.2	0.04	10.00	4.26
743415	1845115	43.4	44.6	11.9	1.4	31.1	0.0	32.6	0.04	10.00	4.26
739687	1842357	11.6	70.2	18.2	1.6	32.4	0.0	33.9	0.06	20.00	4.26
752222	1864123	14.2	65.8	19.9	2.9	55.7	44.6	105.5	0.04	20.00	1.45
755943	1845638	12.8	68.4	18.8	1.9	47.5	50.7	103.4	0.05	10.00	4.26
762653	1847653	5.2	72.3	22.5	2.2	26.9	35.9	68.1	0.05	15.00	4.26
750574	1846085	22.7	61.0	16.3	1.6	47.9	51.0	104.2	0.05	15.00	4.26
729843	1847427	17.4	62.1	20.4	1.3	44.1	29.4	77.2	0.04	20.00	4.26
763241	1849417	8.3	69.6	22.0	1.7	48.1	51.4	104.8	0.04	10.00	4.26
759008	1852357	12.0	62.8	25.2	2.0	53.8	57.4	116.5	0.04	15.00	4.26
747964	1846756	46.9	44.4	8.7	1.9	82.6	49.5	137.4	0.04	10.00	4.26
733125	1843699	0.8	78.3	20.9	1.7	58.7	19.6	81.3	0.05	10.00	4.26
757008	1850240	15.2	68.2	16.6	2.4	57.2	45.8	108.2	0.05	20.00	4.26
766227	1848435	7.9	52.4	17.6	2.6	59.8	47.9	113.0	0.03	15.00	4.26
724326	1848397	7.8	75.2	16.9	1.7	53.5	28.5	85.8	0.06	10.00	4.26
767004	1857149	13.3	67.9	18.8	1.8	52.4	55.9	111.2	0.05	20.00	4.26
726936	1844519	42.5	44.5	13.0	1.8	70.2	23.4	96.6	0.04	10.00	4.26
761242	1857414	28.3	61.4	10.3	2.5	79.3	42.3	126.8	0.04	15.00	4.26
737375	1853542	3.7	77.3	18.9	1.5	43.7	0.0	45.2	0.05	15.00	4.26
757361	1853886	18.4	60.3	21.3	1.7	43.5	46.4	95.2	0.04	10.00	4.26
759242	1856356	42.5	44.5	13.0	1.6	33.8	18.1	55.7	0.04	20.00	4.26
753829	1860447	12.0	69.1	18.8	2.0	66.4	70.8	142.4	0.05	10.00	4.26
755597	1854592	22.4	55.1	22.5	0.9	41.0	27.3	72.1	0.04	20.00	4.26
763770	1857590	13.9	65.7	20.4	1.5	46.0	49.0	100.3	0.05	10.00	4.26
752774	1855062	12.3	64.4	23.3	1.2	29.6	39.4	74.2	0.04	20.00	4.26
742073	1852200	35.9	49.1	15.0	1.4	36.6	39.0	80.8	0.05	15.00	4.26
730515	1859358	6.2	72.3	21.5	2.0	56.6	60.4	122.3	0.05	10.00	4.26
727159	1857270	10.0	71.8	18.3	1.6	57.3	61.1	123.6	0.05	20.00	4.26
725370	1859582	3.0	71.1	26.0	1.9	15.2	16.2	36.6	0.05	10.00	4.26
728054	1854660	12.6	68.8	18.7	2.7	62.0	49.6	116.9	0.04	10.00	4.26
761359	1854591	22.1	60.8	17.0	1.8	47.5	50.7	103.4	0.05	15.00	4.26
748188	1853533	6.0	73.1	20.9	2.1	71.6	76.4	153.3	0.05	10.00	2.20
762300	1859060	9.4	71.5	19.1	1.9	49.6	52.9	107.7	0.05	15.00	4.26
758424	1859299	17.1	68.7	14.2	1.1	19.2	0.0	20.3	0.06	20.00	1.76

732230	1854138	7.7	71.3	21.1	1.8	49.1	26.2	79.1	0.05	15.00	4.26
755207	1862744	6.3	75.5	18.3	2.3	52.2	41.7	99.2	0.05	10.00	4.26
750384	1862514	9.0	70.1	20.8	1.2	24.4	13.0	41.1	0.05	20.00	4.26
739388	1850111	1.5	77.5	21.0	1.9	34.9	0.0	37.2	0.05	10.00	4.26
742804	1864811	26.3	58.5	15.2	1.6	62.7	41.8	108.2	0.05	15.00	4.26
752681	1867797	17.2	67.8	14.9	1.6	62.8	83.7	151.7	0.05	20.00	4.26
756585	1868945	18.7	63.7	12.9	2.7	64.9	51.9	122.0	0.04	15.00	4.26
746479	1870324	21.7	67.8	14.6	1.2	37.5	25.0	66.3	0.06	10.00	4.26
756126	1872161	17.2	69.1	14.9	1.5	52.8	56.3	114.4	0.05	15.00	3.12
748547	1868486	7.9	69.1	23.0	1.1	29.9	10.0	42.9	0.05	20.00	4.26
770873	1836349	22.0	56.0	22.0	2.5	54.9	61.2	119.9	0.03	15.00	4.26
740624	1828404	25.0	61.5	13.6	1.8	45.8	32.9	82.4	0.04	15.00	4.26
717186	1857647	27.0	54.7	18.3	1.6	43.6	14.5	61.4	0.05	20.00	4.26

Appendix 5: Calculation of measured and modeled runoff and sediment discharge

Measured runoff discharge

Date	Section area of the channel (m^2)	Velocity of the flow (m/sec)	Discharge (m^3/sec)
16.09.08	6.44	3.22	20.72
17.09.08	7.09	3.25	23.00
23.09.08	5.27	2.66	14.02
Average discharge (m^3/sec)			19.25
Discharge per day (m^3/day)			1662933.20

Modelled runoff discharge

Average runoff (mm)	17.333
Area of catchment (m^2)	65562500
Total runoff from the catchment per day (m^3/day)	1136395

Measured sediment discharge

Date	Sediment (g/litre)	Sediment (kg/m^3)	Runoff discharge (m^3/sec)	Total sediment discharge (kg/sec)
16.09.08	0.418	0.418	20.72	8.67
17.09.08	0.423	0.423	23.00	9.74
20.09.08	0.385	0.385	14.02	5.40
Average sediment discharge				7.93
Sediment discharge per month (ton/month)				20565.54

Modelled sediment discharge

Average soil erosion rate (ton/ha/month)	2.49
Area of the catchment(ha)	6556.25
Soil loss from the catchment per month (ton/month)	16331.62

Appendix 6: Scripts of PESERA Grid model

```
/*Extract/Copy input grids to d:\meteo_grids
/*create workspace d:\temp_ascii
/*open arcGRID, set workspace as d:\meteo_grids (arc w d:\meteo_grids)
/*select or create window: nrows, ncols, xll and yll must be known
/*run xgridascii103.aml (&run <path>\xgridascii103.aml)

/*&if %:PROGRAM% = ARC &then
setwindow d:\meteo_grids\erod_0702

/*TYPICAL ANALYSIS WINDOWS

Setwindow 718395.68 1830705.95 769745.69 1874455.96/* northern Thailand

&sv months = 1 2 3 4 5 6 7 8 9 10 11 12
&do mn = 1 &to 12
&sv m = [extract %mn% %months%]
   &do var &list meanpet30%m% meanrf130%m% cvrf2%m% meanrf2%m% mtrange%m%
mtmean%m% ~
   newrf130%m% newtemp%m%
      &if [exists %var% -grid] &then
      %var%o = %var% * 1
      d:\temp_ascii\%var%.dat = gridascii(%var%o)
      &if [exists %var%o -grid] &then
      kill %var%o
   &end
&end
&sv months = jan feb mar apr may jun jul aug sep oct nov dec
&do mn = 1 &to 12
&sv m = [extract %mn% %months%]
   &do var &list cov_%m%
    &if [exists %var% -grid] &then
       %var%o = %var% * 1
       d:\temp_ascii\%var%.dat = gridascii(%var%o)
       kill %var%o
   &end
&end
&do var &list rootdepth rough_red rough0 use crust_0702 erod_0702 ~
   swsc_eff_2 zm std_eudem2 ~
   itill_maize itill_crop1 itill_crop2 mitill_m mitill_1 mitill_2 ~
   maize_210c eu12crop1 eu12crop2 p1xswap1 p2xswap2

   &if [exists %var% -grid] &then
     %var%o = %var% * 1
     d:\temp_ascii\%var%.dat = gridascii(%var%o)
     kill %var%o
&end
```